Development of Natural Polymer Scaffolds with Controlled Microstructures

Shangwu Chen

Doctoral Program in Materials Science and Engineering

Submitted to the Graduate School of
Pure and Applied Sciences
in Partial Fulfillment of the Requirements
for the Degree of Doctor of Philosophy in
Engineering

at the
University of Tsukuba

Content

List of abbreviations

ANOVA	Analysis of variance
bFGF	basic fibroblast growth factor
BMSC	Bone mesenchymal stem cell
CG	Collagen-glycosaminoglycan
CH	Collagen-hyaluronic acid
CLSM	Confocal laser scanning microscopy
DMEM	Dulbecco's modified eagle medium
DNA	Deoxyribonucleic acid
ECM	Extracellular matrix
EGF	Epidermal growth factor
FBR	Foreign body reaction
FBS	Fetal bovine serum
GAG	Glycosaminoglycan
HA	Hyaluronic acid
HE	Hematoxylin and eosin
HUVEC	Human umbilical vascular endothelial cell
IGF	Insulin growth factor
MW	Molecular weight
PBS	Phosphate buffer saline
PIC	Polyion complex
PLA	Poly(lactic acid)
PLGA	Poly(lactic-co-glycolic acid)
PGA	Poly(glycolic acid)
RGD	Arginylglycylaspartic acid
RNA	Ribonucleic acid
RT-PCR	Real-time polymerase chain reaction
SD	Standard deviation
SMTE	Skeletal muscle tissue engineering
TGFβ	Transforming growth factor β
sGAG	sulfated glycosaminoglycan
VEGF	Vascular endothelial growth factor
UV	Ultraviolet

Chapter 1

General introduction

1.1 Tissue engineering

Severe disease or injury can cause malfunction or damage of tissue and organs in human body. The diseased or damaged body structures are treated with drugs, artificial prosthesis or transplantation of tissue or organs from one individual to another. However, drugs neither fully heal the tissue with major damage nor achieve its long-term recovery. Artificial prosthesis can only restore partial function of a tissue and cannot sufficiently integrate with host tissue and need to be replaced when they are worn out after 15 - 20 years. Transplantation techniques have many constraints. The major constraint is the lack of living tissue and organs for transplantation. According to the Organ Procurement and Transplantation Network (United States), the waiting list candidates for transplantation as of November 12th, 2015 are 122,719; the transplants performed during January - August 2015 are 20,705. The gap between need and supply continues to widen. In addition, the immune system produces chronic rejection of the transplanted graft over time. The reduction of activation of immune system (immunosuppression) to reduce the rejection can cause new tumor formation.

In this context, tissue engineering emerged as a new solution to these problems.[1, 2] Human cells are cultured and manipulated to form living tissue that can be transplanted to repair and restore the function of damaged tissue or organ. A small fraction of a tissue is harvested to isolate the cells, without the need of taking the whole tissue or organ as in transplantation. Living tissue can be engineered from the cells of the patient, which reduce the risk of rejection and need of immunosuppression.

1.1.1 The principle of tissue engineering

The principle of tissue engineering is depicted in Fig. 1.1. In essence, cells are isolated from a fraction of human tissue and cultured *in vitro* to expand cell number. Then the cells are harvested and cultured with bioactive molecules in a three-dimensional (3D) scaffold material *in vitro*. During the *in vitro* culture, cells grow and produce extracellular matrix (ECM) within the 3D scaffold which turn into an engineered tissue. The engineered tissue is transplanted into human body to treat the diseased body structure.

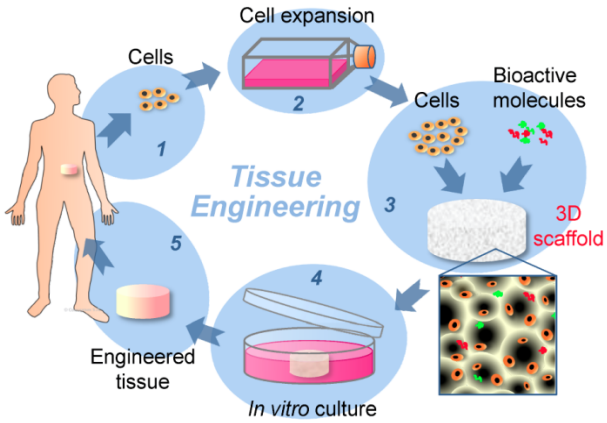

Fig. 1.1. The principle of tissue engineering.

1.1.2 Cells

The cells isolated from human tissue can be fully differentiated cells of target tissue, progenitor cells or stem cells. Fully differentiated cells such as dermal fibroblasts and articular cartilage cells (chondrocytes) can be used to engineer skin tissue or cartilage tissue, respectively. One FDA approved skin product involves the use of neonatal human dermal fibroblasts from foreskins. The fibroblasts are expanded *in vitro* and cultured in a porous poly(lactide-co-glycolide) scaffold that can be gradually degraded by hydrolysis. After the culture a dermal layer of skin can be engineered for transplantation. Progenitor cells are the cells with the capability to differentiate in to limited cell lineages. One example of progenitor cells is skeletal muscle progenitor cells (myoblasts), which can be differentiated into mature muscle fiber. Myoblasts isolated from muscle tissue can be cultured in 3D scaffolds to engineer muscle tissue to repair the muscle tissue loss. Stem cells, either from adults or from embryos, have the ability to self-renew and differentiate into many cell lineages such as bone cells (osteoblasts), chondrocytes, tendon cells, etc. Because the source of some types of differentiated cells or progenitor cells for tissue repair are very limited or hardly accessible, stem cells have been studied for tissue engineering. Stem cells can be expanded *in vitro* while keeping their undifferentiated state. To apply stem cells in tissue engineering, studies were focused on better ways to expand stem cells and differentiate them to the desired cell type.

In some culture systems one type of cell was used to engineer new tissue but other culture systems multiple types of cell were used. Culturing multiple types of cells in a 3D scaffolds mimics the complex organization of normal tissue and achieve the multiple functions of the tissue. For example, fibroblasts were cultured in collagen matrixes on which a layer of karatinocytes were cultured, which form a living dermal equivalent (ICX-SKN) for the treatment of burns and acute wounds.[3, 4] Skeletal muscle cells were cultured with vascular endothelial cells in polymer scaffolds to generate the vascularized muscle tissue to improve the viability of engineered tissue *in vivo*.[5] In some studies, skeletal muscle cells, vascular endothelial cells and fibroblasts were cultured in polymer scaffolds to engineer vascularized muscle tissue, where the fibroblasts can enhance the vascularization and stabilize the newly formed vascular network.[6]

1.1.3 Bioactive molecules

Bioactive molecules such as growth factors, cytokines and hormones were used in tissue engineering to control cell function and tissue formation. Among them growth factors are the mostly used bioactive molecules to affect cell proliferation, differentiation and morphogenesis. Growth factors are usually proteins that can act on the receptors of cell surface, which initiate the changes of cell behaviors, according to the type of growth factors. For example, bone morphogenetic proteins can affect the postnatal bone formation and are used in therapeutic treatment such as bone defects and bone fractures and osteoporosis. Transforming growth factor beta-1 is used to promote the chondrogenic differentiation of stem cells to chondrocytes and formation of cartilage tissue.[7] Fibroblast growth factor (FGF) and vascular endothelial growth factor (VEGF) are found to affect the tubule formation of vascular endothelial cells and stabilize the newly formed vascular tubules.[8] Chondrogenic induction medium containing transforming growth factor beta (TGFβ) can cause an upregulation of smooth muscle actin-alpha (α-SMA) in bone marrow stromal cells (BMSC), which lead to shrinkage of scaffolds. Addition of basic fibroblast growth factor (bFGF) in the chondrogenic induction medium can suppression the expression of α-SMA and reduce the shrinkage of engineered tissue from BMSC and improve cartilage tissue formation.[9]

Growth factors can be supplemented in the cell culture medium during in vitro culture, or incorporated into a scaffold system to affect cell behavior. For example, insulin supplemented in the differentiation medium of skeletal myoblasts can facilitate the fusion of myoblasts into mature myotubes. A porous scaffolds with tethered VEGF could induce the infiltration of vascular network after its transplantation in animal body.[10] Growth factors can be encapsulated in polymer micro-/nano-particles which were incorporated into porous scaffolds.[11, 12] The encapsulation of growth factors in polymer particles prepared from degradable polymer make it possible to control the release of growth factors. The degradation of the polymer and therefore the release profile of the encapsulated growth factor can be tailored by the chemical structure of polymer and the size of microparticles. ors in a spatiotemporally controlled manner, which is critical to manipulate the behavior of cell cultured in the scaffolds or the cell infiltration from surrounding tissue into the scaffolds. In addition, multiple kinds of growth factors can be encapsulated in different kinds of polymer microparticles in scaffolds to control the release of multiple kinds of growth factor at the same time.

1.1.4 Scaffolds

In tissue engineering, a scaffold is the 3D material that support cell adhesion, proliferation, synthesis of ECM and control the shape of engineered tissue. Scaffolds can be porous or hydrogel, both of which can accommodate cells cultured in the 3D material.

Scaffolds for tissue engineering need to meet the requirements as show below:

I. Biocompatibility

   Scaffolds should be compatible with cells cultured in them and the surrounding living tissues where they are implanted. Scaffolds should allow the attachment and proliferation of cells and maintain the specific function of cells. Scaffolds and their degradation products should not be toxic to the cells and the surrounding tissue after implantation. Implanted scaffolds should not adversely affect the function of organs or the whole body. In addition, the inflammatory response to an implant, the formation of fibrous capsule that isolate the implant with the surrounding tissue should be avoided to allow the integration of the implant with surrounding tissue.

II. Degradability

Scaffolds should be degradable through hydrolysis or enzymatic digestion. The breakdown of scaffolds need to coordinate with the growth of new tissue while maintain the structural integrity of the cell/scaffold construct during cell culture or after implantation. Finally, the implanted scaffold should be replaced by the engineered tissue.

III. Mechanical property

The mechanical property of scaffolds should be strong enough to allow surgical handling and withstand the cellular contraction and the mechanical load at the site of implantation. Many types of cells such as dermal fibroblasts, chondrocytes and muscle cells contract the scaffolds in which they are cultured, which makes it hard to control the final size or shape of engineered tissue. In addition, some tissues such as cartilage, ligament and bone are frequently subjected to mechanical load. Therefore, regeneration of these tissues necessitates a mechanically strong scaffold. It is noteworthy, however, that in some cases a too stiff scaffold might adversely affect cell behavior such as the differentiation of stem cells, which is influenced by the substrate stiffness.

IV. Pore structure

Scaffolds with proper pore structure such as open pores and controlled pore size are necessary to engineer a 3D tissue. Scaffolds with open, interconnected pore structure can enable cell infiltration into the whole space of scaffold and homogeneous distribution of cells and formation of a homogenous tissue. In contrast, a scaffold with closed pores will hinder cell infiltration into the bulk material, which leads to the cell growth and tissue formation on the peripheral region of the scaffold. On the other hand, engineering of tissues with well-ordered structure such as muscle and nerve necessitate scaffolds of well-ordered pore structure that guide the cell assembly and tissue orientation within the cell/scaffold construct.

Scaffolds are commonly used in tissue engineering because in many cases cell therapy alone cannot successfully engineer the target tissue. One example of cell therapy without scaffold material is autologous chondrocyte implantation (ACI). Chondrocytes were isolated from the non weight-bearing cartilage and cultured *in vitro* to increase their number. The expanded chondrocytes were then injected into the cartilage wound sutured with a periosteal flap taken from a lower leg bone. The injected chondrocytes will grow and form cartilage tissue in the wound. The ACI method has problems such as cell leak from the sutured wound due to the holes or tears of the fragile periosteal flap and the hypertropy of new tissue associated with the flap. As a another example, skin cells such as karatinocytes can be cultured to get epidermis for transplantation but it cannot repair the full-thickness skin wound. To solve the problems of ACI method, 3D collagen matrices are used to culture chondrocytes or load chondrocytes just prior to transplantation to repair cartilage tissue. Collagen matrices with or without dermal fibroblasts can be implanted into skin wound to regenerate the 3D dermal skin layer.

1.2 Porous scaffolds for tissue engineering

There are four major scaffolding approaches for tissue engineering: pre-made porous scaffolds, decellularized extracellular matrix, cell sheet with synthesized extracellular matrix and cell-encapsulated hydrogel (Fig. 1.2). [13] Each kind of approach has its advantages and disadvantages. Pre-made scaffolds can have tailored pore structure and mechanical property but usually cannot enable homogenous distribution of cells after cell seeding. Decellularized extracellular matrix can mimic the composition of normal tissue but they have uncontrolled pore structure, inhomogeneous distribution of cells and possibly carry pathogens or cause immunogenicity after implantation. Cell sheet with synthesized extracellular matrix have good

compatibility with the surrounding tissue after transplantation but they need numerous stacking to obtain thick tissue. Cell-encapsulated hydrogel can be injected into wounded tissue for regeneration but their mechanical property is too weak. Among the four approaches, pre-made porous scaffolds can be used to engineer soft and hard tissues. The present study focused on improving the micropore structure of pre-made porous scaffolds to enable homogenous cell distribution and tissue formation, controlled cell assembly and behavior. Therefore, pre-made porous scaffolds with detailed information are introduced below. These scaffolds are developed from biodegradable polymers, either synthetic or naturally occurring.

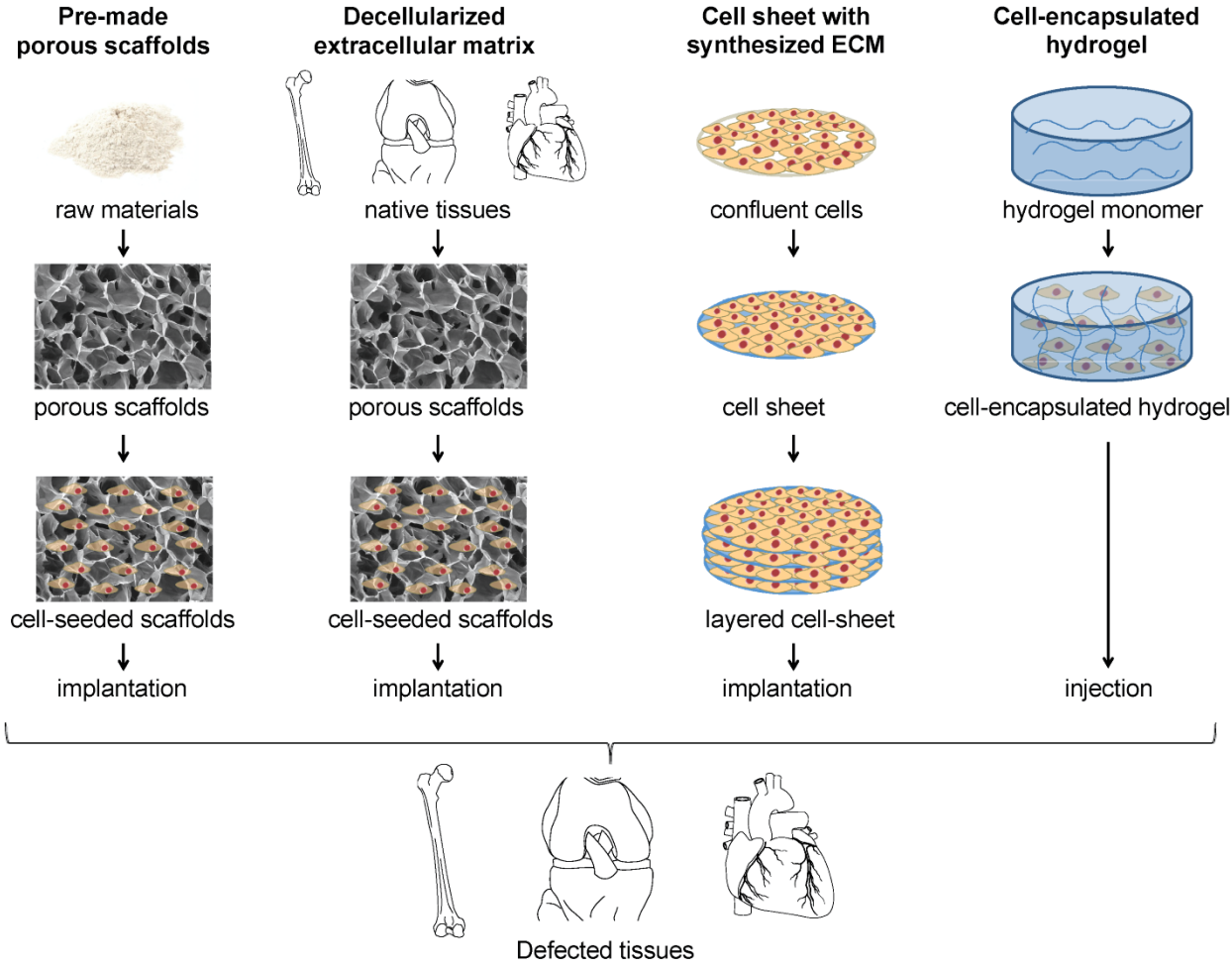

Fig. 1.2. Major scaffolding approaches for tissue engineering.

1.2.1 Synthetic polymer-based scaffolds

The most investigated biodegradable synthetic polymer for tissue engineering are aliphatic polyesters and polyurethanes. Poly(glycolic acid) (PGA), poly(lactic acid) and their copolymers poly(lactic acid-co-glycolic acid), which are aliphatic polyesters, are the most common biodegradable polymers used in medicine (Fig. 1.3). PGA is more hydrophilic than PLA and PGA is highly crystalline. PGA was used as clinical sutures and they had a crystallinity of about 46-52%.[14, 15] Because of their water uptake and hydrophilic property, the PGA based sutures usually had a degradation time of 2-4 weeks after

implantation.[14] PLA has a methyl group on the polymer backbone, which makes it more hydrophobic. The small water uptake of PLA (less than 2% for PLA films) make it harder to degrade via hydrolysis. While PGA is highly crystalline, PLGA has a reduced crystallinity due to presence of PGA in the backbone. As a rule, more PGA in PLGA results faster degradation rate. However, PLGA with 50:50 ratio of PGA and PLA has the fastest degradation.[16] In spite of their biodegradability, PGA or PLGA based resorbable pins sometimes cause a late noninflammatory response.[17] After implantation of PGA for 12 weeks or PLA for as long as 3 years, this unwanted response happened, which was suggested to be the result of acidic degradation products (glycolic acid for PGA and lactic acid for PLA).

PGA fibers have been used to develop into cylinder porous PGA scaffolds to culture chondrocytes to engineer cartilage tissue.[18-21] Porous PLA, PGA and PLGA scaffolds has been used to engineer tissues as well as their combined product with bioglass such as hydroxyapatite.[22] The combination with bioglass significantly improved the mechanical property of porous polymer scaffolds and the regeneration of bone tissue. PGA mesh scaffolds were cultured with endothelial cells and smooth muscle cells isolated from blood vessels to engineer small-diameter vessel grafts, during which the polymer degraded and ECM was synthesized[23-25]. After removal of cells in the engineered vessels, the grafts were implanted in dog model which showed no immunogenic response and maintained resisted dilation and hyperplasia.

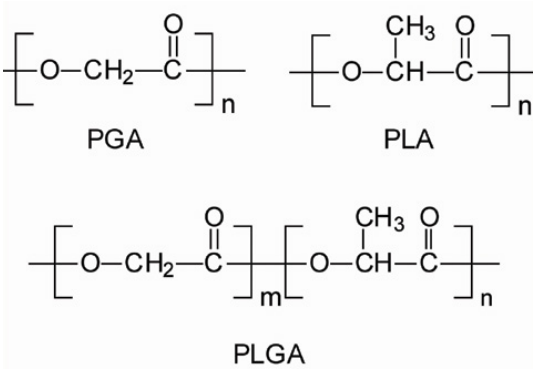

Fig. 1.3. The chemical structure of PLA, PGA and PLGA.

1.2.2 Natural polymer-based scaffolds

Natural polymers can be used to prepare porous scaffolds for tissue regeneration. Natural polymers are produced by living organisms and can be categorized as peptide and proteins, polysaccharides, polyhydroxyalkanoates, and polynucleotides. The first two categories are usually used to prepare porous scaffolds, which are usually modified or crosslinked to control their degradation to support cell culture and tissue formation. In the present study, natural proteins (collagen and gelatin) and polysaccharide (hyaluronic acid) are used to develop porous scaffolds to culture skin cells (dermal fibroblasts), cartilage cells (chondrocytes) and muscle cells (myoblasts). Therefore, their chemical structure, presence and function in living tissues and applications for tissue regeneration are summarized.

I. Collagen

Collagen is the major structural protein of extracellular matrix of normal tissue and account for about 30% of all the proteins of human body. There are about 14 types of collagens in human body and type I collagen is the major component. However, the presence of each type is dependent on the type of tissue. For example, type I collagen are the major protein in tendon, skin and bone; type II collagen are the major protein in articular cartilage. The basic unit of collagen is a polypeptide helix with the repeating sequence of

glycine-X-Y, where X and Y are frequently proline or hydroxyproline. Triple helix of such peptides assembled through hydrogen bonding into collagen fibrils, which further closely packed into collagen fibers to support the living cells and tissues. [32] For example, collagen assembled into strong aligned bundles in tendon while it randomly distributed in dermal skin.

Collagen has been developed into porous scaffolds to regenerate varied types of tissues. As a natural protein that support cells in tissue, collagen is highly compatible with cells and tissues. A porous collagen scaffolds can be implanted into skin wounded to induce the infiltration of cells from surrounding tissue into the porous material to synthesis new skin tissue.[26, 27] The pore structure and degradation time of collagen scaffolds can be controlled by using different freezing condition during freeze-drying and crosslinking density. Collagen scaffolds with proper pore size and degradation time had the optimal skin regeneration result.[27] To reduce the immunologic responses to the collagen material after implantation, type I collagen is treated with pepsin and purified to obtain atelocollagen.[28-31]

II. Gelatin

Gelatin is derived from partial acidic or alkaline hydrolysis of collagen. Gelatin is compatible with cells and tissues due to the similar chemical composition of gelatin and collagen. In addition, gelatin has low antigenicity compared to collagen.[33-35] Gelatin solution gels at a low temperature (0 - 25 ºC) and the gelation is dependent on the concentration of gelatin and temperature. The greater the concentration of gelatin, the more quickly the solution gels. Gelatin solution at a lower temperature gels more quickly. Freeze-drying gelatin solutions results in porous gelatin scaffolds. Porous gelatin scaffolds were used to engineer various kinds of tissues such as skin, cartilage and bone. For example, gelatin and glycosaminoglycans (a kind of polysaccharides) have been developed into porous scaffolds to culture articular chondrocytes to regenerate articular cartilage tissue.

III. Hyaluronic acid

Hyaluronic acid (HA), also named hyaluronan, is a linear polysaccharide with repeating disaccharides (D-glucuronic acid and D-N-acetylglucosamine) (Fig. 1.4). The number of repeating disaccharides can reach as great as about 10,000 and the molecular weight of HA can be as high as 4, 000 kDa. HA is synthesized by various types of cells such as fibroblasts and chondrocytes and HA is abundant in many types of animal tissues.

HA is the unsulfated glycosaminoglycan in ECM and can affect tissue functions and cell behaviors. HA presents in biological fluids such as the synovial fluids and the viscous fluids containing HA lubricate the surrounding articular cartilage. Cell receptors such as CD44 (cell surface glycoprotein), ICAM-1 (intracellular adhesion molecule-1) and RHAMM (receptor for HA-mediated motility) can interact with HA which affect cell behavior such as migration and differentiation. Found on the cell surface and in cytosol, RHAMM can regulate cell behavior in the presence of growth factors and affect the migration of fibroblasts and smooth cells. During the development of skeleton and limb buds and morphogensis of bone, there is a period when HA is produced followed by the destruction of HA. In addition, it has been found that the production of HA was associated with mescenchymal cell migration and the destruction of HA associated with cell differentiation. For example, chondrogenesis in the embryo limb buds and axial skeleton has a period of accumulation of mescenchymal cells and production of HA, followed by removal of HA by enzyme (hyaluronidase) and differentiation of the cells to form cartilage tissue.

Due to its chemical and biological properties, HA has been used to form porous scaffolds for tissue engineering. The hydrophilic and bioactive HA has good compatibility with cells and living tissues. Because HA is easily dissolved in water and has a high rate of turnover in animal body, HA need to be modified and

crosslinked to act as a temporal scaffold material for cell growth and tissue formation. The functional groups on the backbone of HA such as carboxylic group and hydroxyl group provide abundant modification sites. Crosslinking methods such as water-soluble carbodiimide crosslinking and modifications such as methacrylation of HA molecules, are used to stabilize HA and extend its degradation. HA based scaffolds has application in regeneration of skin and cartilage and bone. However, the effect of HA on the behavior of chondrocytes in 3D culture remain controversial. While some studies showed increasing amount of HA in 3D scaffolds resulted in higher chondrocyte proliferation or more cartilage ECM synthesis, other studies showed that a low amount of HA in 3D scaffolds favor chondrogenesis and higher amount of HA caused an inhibition of chondrogenesis.[36-38] These 3D scaffolds usually had uncontrolled pore structure and non-uniform distribution of HA, which could interfere the effects of HA on cell behavior.

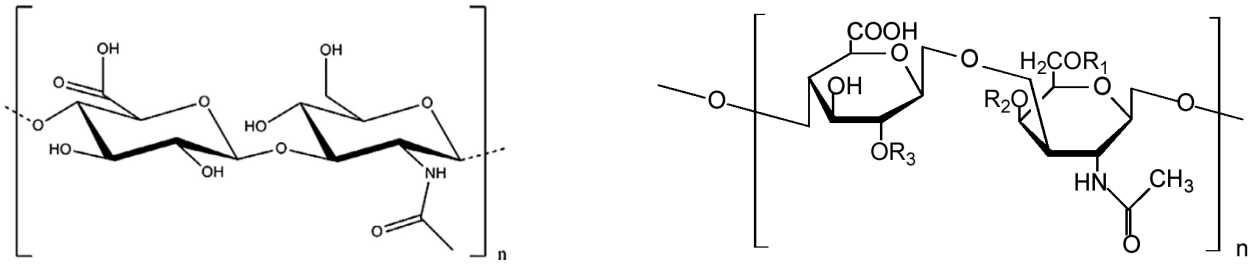

Fig. 1.4. Chemical structure of one unit in the chain of hyaluronic acid (left) or chondroitin sulfate (right). Chondroitin-4-sulfate: R1, R3 = H; R2 = SO_3H. Chondroitin-6-sulfate: R1 = SO_3H; R2, R3 = H.

IV. Chondroitin sulfate

Chondroitin sufate (CS) is a linear polysaccharide with a repeating disaccharide (N-acetylgalactosamine and glucuronic acid) (Fig. 1.4). CS is a kind of sulfated glycosaminoglycans present in many kinds of tissues such as skin and cartilage. The location of sulfate groups on the repeating disaccharide varies and each variant has its corresponding name such as chondroitin-4-sulfate and chondroitin-6-sulfate. CS variants affect cell functions differently. For example, supplement of chondroitin-6-sulfate increased the synthesis of mRNA for type II collagen in the 3D culture, while supplement of chondroitin-4-sulfate did not.[37] CS bonds to proteins to form proteoglycans such as aggrecan which is the major proteoglycan in the ECM of cartilage tissue. Aggrecan act as the structural protein in cartilage to absorb the mechanical impact and resist the compression during joint movement or load-bearing activities. Because CS were found to enhance the synthesis of cartilage ECM, supplement of CS were used to repair damaged cartilage or alleviate the symptoms of osteoarthritis.

As one kind of sulfated glycosaminoglycans (sGAG), CS is usually combined with other natural polymer to prepare porous scaffolds for tissue engineering. For example, the mixed suspension of CS and collagen were freeze-dried to prepare porous collagen/glycosaminoglycan (CG) scaffolds. Because both collagen and glycosaminoglycans are the inherent component of ECM, CG scaffolds are bio-mimetic and compatible with various types of cells and used for engineer various types of tissues such as skin, cartilage, tendon and bone. The commercialized product, Integra Dermal Regeneration Template is a porous bovine collagen crosslinked with chondroitin-6-sulfate with an upper layer of silicone, which is used to regenerate full-thickness skin wounds. Another product, Menaflex (Regenbiologics), is a bovine collagen with HA and CS for the regeneration of cartilage tissue.

V. Chitosan

Chitosan is a linear polysaccharide composed of repeating units of N-acetyl D-glucosamine and

D-glucosamine. Chitosan is derived from partial deacetylation of chitin, which is abundant in the rustacean shells or insect cuticles (Fig. 1.5). The degree of deacetylation (DD) refers to the ratio of D-glucosamine number to the sum of N-acetyl D-glucosamine and D-glucosamine numbers. Chitosan usually are the form of chitin that has 60% glucosamine (DD = 60). While chitin has limited application as a biomaterial due to its low solubility, chitosan has many good properties to make it for medical applications. Chitosan can be dissolved in acidic solution and its amine groups become protonated, which give the chitosan positive charges. Chitosan has a mucoadhesive property because the negative glycoprotein in mucin can bind to the positively charged chitosan, and the mucoadhesive ability can be improved by using chitosan with greater DD.[39] Similarly, negatively charged blood cells can interact with chitosan, a haemostatic activity to stop bleeding.[40-42]

Chitosan sponges are mainly prepared from freeze-drying method and they are mainly used as wound dressing to absorb the wound exudates and facilitate wound healing.[43] As a natural polymer with good cell interaction, chitosan are prepared into scaffolds to be used in regeneration of tissues such as bone.[44-47] Chitosan, tricalcium phosphate and collagen can be combined to prepare composite scaffolds for bone tissue engineering. Culture of rat osteoblasts in 3D chitosan/tricalcium phosphate scaffolds showed that the material could support the cell proliferation, high activity of alkaline phosphatase and synthesis of mineralized ECM.[48] Culture of rat bone marrow stromal cells on 3D chitosan/collagen scaffolds showed that the material promoted osteogenic differentiation of the cells compared with chitosan scaffolds or collagen scaffolds.[49]

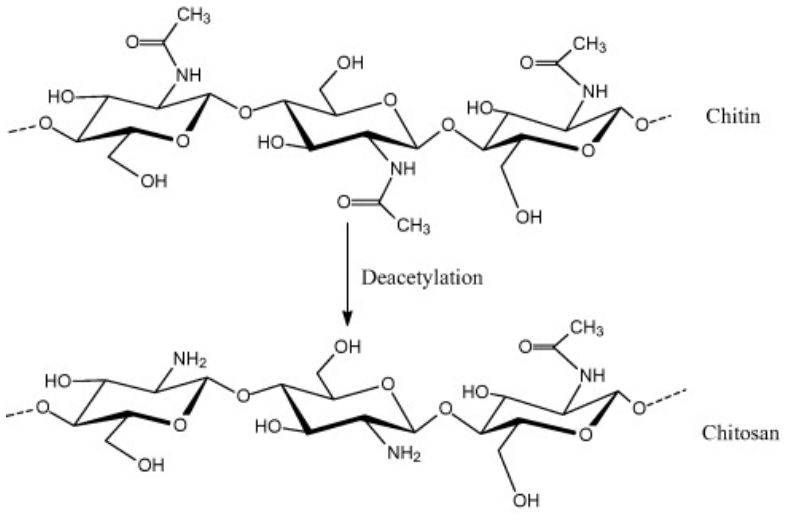

Fig. 1.5. Deacetylation of chitin to obtain chitosan.

VI. Silk fibroin

Silk fibroin is a natural polymer derived from silk produced by the silkworm *Bombyx mori* and the spider *Nephila clavipes*.[50] The mostly studied silk fibroin as biomaterial is from cocoon silk of the silkworm. Those silk has the core protein of silk fibroin, and glue-like coating of sericin protein which has been found cause adverse immune responses of silk-based material. Silk fibroin contains hydrophobic blocks with repeating amino acids that has short side chains and hydrophilic blocks with amino acids that has long side chains. Silk fibroin has strong mechanical property, good compatibility with cells and slow degradation, which make it suitable for biomedical applications. The original silk is insoluble in water, ethanol or dilute acid but it can be dissolved in the solvent of hexafluoroisopropanol (HFIP) or concentrated lithium bromide

solutions to extract silk fibroin. Silk fibroin based materials can be autoclaved or treated with 90% methanol to induce the formation of beta-sheet structure to make them insoluble in water.[51] Silk fibroin can be made into various forms such as films, coatings, hydrogels, membranes and 3D porous scaffolds.

Silk fibroin based porous scaffolds has applications in engineering of skeletal tissues such as ligament and bone and connective tissues such as skin.[52-57] Porous scaffolds prepared from synthetic polymer were coated with silk fibroin to facilitate cell adhesion. For example, polyurethane scaffolds were dipped into 4 wt.% silk fibroin solution to give a protein coating with the thickness of 200 - 600 nm. The coating on the 3D scaffolds significantly enhanced the adhesion, proliferation and synthesis of ECM of fibroblasts. In addition, inflammation-related cytokines during wound repair such as IL-1β, TNF-α, and TGF-β1 were undetected.[58] 3D porous silk fibroin scaffolds can be prepared with salt leaching method with the use of aqueous and HFIP solution of silk fibroin. Scaffolds from both kinds of solutions had the transition of silk fibroin protein structure, from random coil to β-sheet, which can strength the scaffolds and slow their degradation. Compared with the HFIP-derived scaffolds, the aqueous solution-derived scaffolds had pores with rough and hydrophilic surface and good pore interconnectivity.

The amino acid side chains of silk fibroin provide abundant modification sites to incorporate other bioactive molecules such as RGD and growth factors. RGD coupled silk fibroin fibers promoted the attachment, spreading, proliferation and differentiation of bone marrow stromal cells.[59, 60] Bone morphogenetic protein-2 (BMP-2) was chemically coupled on silk fibroin, which retained the growth factor with a higher level compared to the BMP-2 physically absorbed on silk fibroin.[61]

1.3 Fabrication methods of porous scaffolds

The fabrication methods of porous scaffolds can be categorized into (1) porogen-based methods, (2) solid freeform fabrication techniques and (3) fiber based methods.[13]

1.3.1 Porogen-based methods

In the first category, polymer suspension or solution are mixed with porogen materials which can be gases such as carbon dioxide, liquids such as water and solids such as sodium chloride particles or paraffin microspheres. After removal of the porogen in the mixture by sublimation, evaporation or dissolution of solid particles by an appropriate solvent, a porous polymer scaffolds can be obtained. Methods of the first category are particle leaching, freeze-drying and gas foaming (Fig. 1.6).

Particle leaching allows the preparation of scaffolds with controlled porosity and pore size. Polymer solution is casted in a mold with porogen particles. The porogen can be inorganic particles such as sodium chloride particles or organic particles such as saccharides, gelatin or paraffin microspheres. Evaporation of the solvent resulted in the polymer matrix embedded with porogen material. The porogen material can be dissolved in a proper solvent such as water for sodium chloride particles or aliphalic solvent for paraffin microspheres, leaving behind a polymer matrix with porous structure. The pore size and porosity of scaffolds can be controlled by using porogens with certain sizes and the ratio of porogen to the polymer solution. The advantages of this method are that no special equipment is required and the pore size and porosity can be independently controlled. However, due to the need of removing porogen embedded in polymer matrix, the scaffolds are limited to a thickness of about 2 mm. In addition, the agglomeration of porogen can hinder the formation of homogeneous pore structure. The organic solvents used during the fabrication, if not removed, can be toxic to cells or affect the efficacy of bioactive molecules.[62-64]

Freeze-drying can be used to prepare porous polymer scaffolds. The method comprises two stages,

freezing a solution and removal of the solvent. During the freezing, the polymer solution is cooled down to form ice crystals, which force the aggregation of polymer in the interstices. Then the frozen solution is put under a low pressure to sublimate the solvent. When the frozen solvent is sublimated, the unfrozen absorbed water in the polymer matrix can be removed by slightly increase the temperature of sample. The pore structure of the final porous scaffolds depends on the freezing rate, final freezing temperature and pH.[65, 66] A highly porous scaffolds can be prepared by using this method. However, this method has problems such as the random pore structure and heterogeneity of polymer matrix of scaffolds.

Supercritical fluid method generates pores in polymer by using polymer disk equilibrated with high-pressure carbon dioxide (CO_2). Polymer disk from PLA, PGA or PLGA can be prepared by using heating and compression, or by drying a polymer solution. The polymer disk is then put in a chamber with high pressure CO_2 (5MPa) and equilibrated for 72 hours at room temperature. Finally the CO_2 gas in the chamber is released in 15 seconds to reach the atmosphere pressure, during which the gas nucleate and form bubbles making the polymer material highly porous. A porosity as high as 93% could be obtained with this method. This method can prepare porous polymer scaffolds without the use of organic solvents. However, it results the closed pore structure and a skin layer on the porous scaffolds. [67, 68]

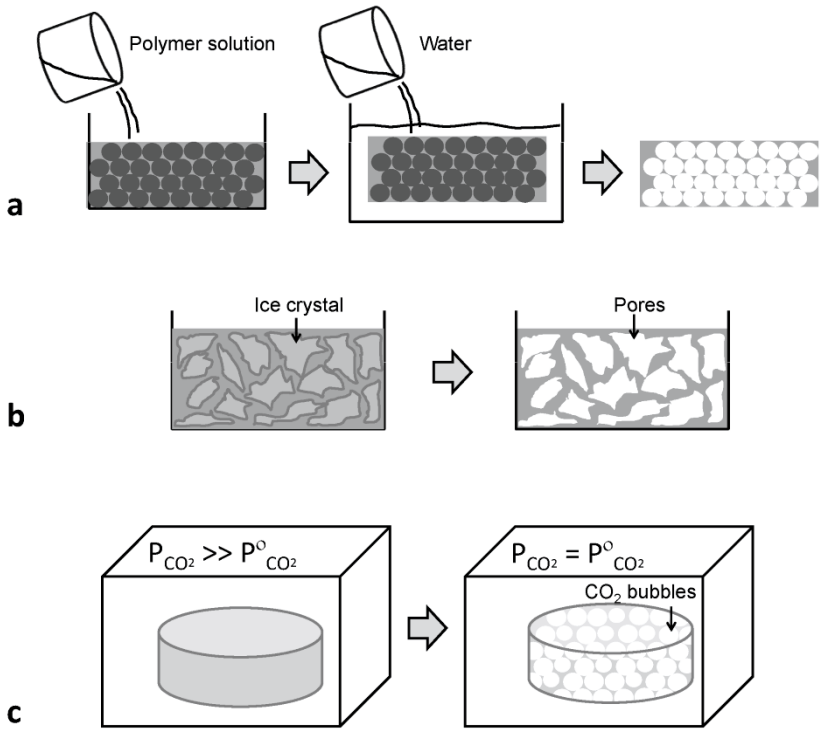

Fig. 1.6. a, Porogen leaching method. A polymer solution is casted in a molded porogen. Sublimation of the solvent and removal of the porogen results in a porous polymeric structure. b, Freeze-drying method. A polymer solution is frozen to from the ice crystals of solvent. The frozen solvent is sublimated by treating the sample in a pressure lower than the equilibrium vapor pressure of solvent, leaving behind a porous scaffolds. c, Supercritical fluid method. A polymer sample is saturated with high pressure of carbon dioxide (CO_2) and an abrupt reduction of the air pressure results in CO_2 air bubbles to form a porous scaffolds.

1.3.2 Solid freeform fabrication

Solid freeform fabrications enable fabrication of scaffolds that has the complex structure of target tissue to be repaired. Fabrication of porous scaffolds by using solid free-form methods usually depend on two types of systems. One type is laser-based system such as stereolithography which polymerizes the photopolymer solution and selective laser sintering which sinter the powered material. The other type is printing-based system such as 3D printing which deliver liquid adhesion to a moving bed of powered material and wax printing which deposit the object and support materials in sequence. [70]

Patient image date are usually used to prepare porous scaffolds of defined shape. Firstly, the target tissue to be repaired are scanned with medical imaging such as computed tomography and magnetic resonance imaging to obtain the digital information of the tissue's shape and size. The information of target tissue can be converted into a digital file that describes the slices with defined thickness (cross section of the target tissue). Secondly, with the digital information the porous scaffolds are fabricated in a layer-by-layer manner. Some methods (stereolithography, selective laser sintering) use energy such as light or heat to solidify the predetermined points of space in the soluble material bed or a powered material bed, which led to formation of porous scaffolds with hierarchical pore structure. Other methods (3D printing, wax printing) print materials from the bottom layer to the top layer to generate scaffolds of predefined shape and size.

Solid freeform techniques allow fabrication of complex, customized scaffolds, minimal manual handling, accurate and consistent pore structure and mechanical property and various kinds of processing conditions (solution, solid or powder). Shortcoming of these methods are the use of organic solvent, dependence on the expensive equipment, high temperature and limited material that can be processed and pore occlusion at the boundary of scaffolds.[69]

1.3.3 Fiber based methods

Fiber based methods such as fiber bonding or electrospinning are used to prepared porous scaffolds. Fiber bonding which involves the knitting or bonding of fibers are able to prepare a 3D fiber meshes. Fibers are prepared by wet, dry spinning methods. For example, the fibers of a PGA mesh can be bonded by a solution of PLGA or PLLA and after evaporation of solvent, a physically stable PGA mesh can be obtained. Electrospinning is another method to prepare 3D meshes (Fig. 1.7). The electrospinning device comprises a high voltage supplier, a syringe pump that supply polymer solution, and a metal collector. Polymer solution are charged by the high voltage and ejected from the capillary tube to the metal collector, during which the viscoelastic force of polymer solution stabilizes the fiber. Fibers with diameter as small as 50 nm can be collected and mounted to form a polymer mesh. The electrospinning parameters that can affect the formation of fiber are the molecular weight of polymer, viscosity and surface tension of polymer solution, voltage, the distance between the tip and the collector, ambient temperature and humidity. The disadvantages of this method are that numerous parameters need to be optimized and the tiny pore structure of electrospun scaffolds which can hinder the cell migration into the inner scaffolds. [71]

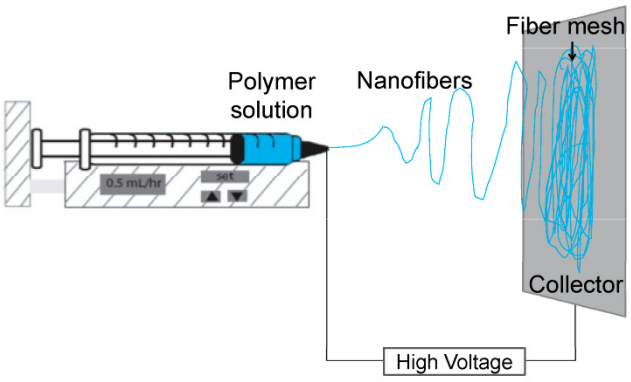

Fig. 1.7. Schematic representation of the electrospinning set-up for fabrication of porous scaffolds.

1.4 The effect of scaffold properties on cell behavior

The physical and biochemical properties of scaffolds for tissue engineering can affect behaviors of cells cultured *in vitro* or in *vivo*. Porous scaffolds with varied micro-/nanostructure, mechanical property and biochemical composition can be fabricated by using varied fabrication techniques and/or different kinds of polymers. Cell behaviors such adhesion, spreading, migration, proliferation, phenotype and assembly can be influenced by scaffold properties *in vitro*. In addition to these cell behaviors, porous scaffolds can also initiate cell responses *in vivo* such as foreign body response (FBR).

Cell adhesion and spreading are the first events since cells get in contact with scaffolds. Many types of cells need to adhere to a suitable substrate to maintain their viability. Methods to quantify cell adhesion to scaffolds vary. A simple method to quantify the cell adhesion usually involves three steps: 1) cell suspension is dispensed on a scaffold, 2) incubate the cells with the scaffold for a certain period of time, and 3) washing away the unattached cells and quantify the unattached cells or cells in the scaffolds. Cell migration in scaffolds, which is usually affected by the pore structure and composition of scaffolds, are usually based on visual observation of cell-seeded cultured for certain period of time. Cell/scaffold construct can be sectioned and stained with histological staining to check the cellular distribution in the scaffolds. In general the cells cultured in scaffolds are expected to possess a specialized phonotype. For example, hepatocytes in liver tissue have functions such as protein secretion and detoxification. Therefore the ability of hepatocytes in scaffolds to secret proteins and intracellular enzyme activity are usually analyzed. Production of tissue-specific ECM such as collagen and GAGs is required for chondrocytes, osteoblasts and fibroblasts. Cell assembly or aggregation is another behavior that can modulated by scaffold properties. One example is the assembly of vascular endothelial cells to form tubular vascular structure with the use of type I collagen.

After implantation of polymer scaffolds in animals, the scaffolds usually initiate the host cell responses such as FBR. FBR are the overlapping events that include protein adsorption, inflammatory cell (primarily neutrophils and macrophages) recruitment, foreign body giant cell formation and fibroblasts involvement. The result is the formation of a layered collagen fiber (fibrous capsule) that isolates the implant from the host tissue, which can hinder the integration of engineered tissue with host tissue and vascularization of the graft.

1.4.1 The effect of pore structure

The pore structure of scaffolds can affect the cell behaviors such as distribution, migration, assembly

and tissue formation. Cells in normal tissue are resided in a ECM with specific micro-/nanostructure. For example, tendon cells has the ECM with aligned collagen fibers. Many research studied on the effect of scaffold pore structure on cell behavior. The open-pore structure of scaffolds is the premise to enable homogeneous cell seeding and homogenous tissue formation. Some research used homogeneous scaffolds with isotropic and open pore structure can enable a homogeneous distribution of cells and formation of a homogenous tissue.[72-74] PLGA scaffolds with microtubule oriented pores facilitated formation of thick, homogeneous cartilage tissue with greater mechanical strength and higher amount of cartilage ECM.[75]

Scaffolds with anisotropic pore structure shows a great potential to engineer highly ordered tissues such as skeletal muscle. Unidirectional freeze-drying is a fabrication technique to generate oriented pores in natural polymer based scaffolds. Collagen scaffolds with parallel pores (pore width: 20-50 μm) were seeded with C2C12 skeletal myoblasts and aligned myotubes formed along the pores in these scaffolds. These cell/scaffolds constructs were implanted in the tibial muscle of immunodeficient mice and the implants integrated with the surround muscle tissue, forming functional muscle tissue from donor myoblasts and host muscle cells.[76] Another study used the similar method to develop chitosan scaffolds with unidirectional microtubule pores, which enabled formation of myotubes of about 550 μm long and 50 μm in diameter after cell culture for two weeks.[77] Micropatterned scaffolds fabricated from micropatterned templates are also potential for engineering of ordered isotropic tissue. For example, 3D scaffolds with large grooves (about 200 μm wide and 200 μm deep) facilitated the differentiation of myoblasts into myotubes, which were bigger and had more cell nuclei compared with those in narrower microgrooves.[78] Micropatterned polycaprolactone (PCL) scaffolds could guide the growth of vascular cells but the closed surface pores could limit nutrient transfer[79]. Therefore, PLGA micro/nanospheres were used as porogens to generate pores significantly smaller than the dimension of microgrooves of PCL scaffolds (48 μm grooves; 5 μm deep; 12 μm spacing). Both the porous and nonporous micropatterned scaffolds guide the organization of cells cultured on them. The porous micropatterned scaffolds had improved medium diffusion which was 6 times greater than that of non-porous PCL micropatterned scaffolds. Micropatterned porous scaffolds make it possible to engineer 3D organized tissues.

1.4.2 The effect of mechanical property

The mechanical property of scaffolds for cell culture modulates cell behavior. Tissues in human body has a wide range of mechanical properties (Table 1.1). Bone tissue as the strongest tissue in the body have a compressive strength and modulus up to 300 MPa and 1 GPa for adult femurs. In contrast, skin tissue has a soft structure with the indentation modulus of 1-2 MPa. Ideally, scaffolds should have the mechanical property similar to the normal tissue to withstand the mechanical loading after implantation. The mechanical property of tissues is an important parameter that affects cell-cell interaction and cell phenotype. Scaffolds with varied stiffness were used for cartilage tissue engineering to study the effect of scaffold stiffness on chondrogenesis. Scaffolds with varied stiffness can be prepared by varying the crosslinking density.[80, 81] Soft scaffolds contracted by chondrocytes during cell culture, which reduced the biosynthesis and proliferation of cells. Possible mechanisms that explain the reduced cell proliferation are the reduction of space for cell growth in the contracted scaffolds, and the stiffness of scaffolds which could affect the cell behavior via mechano-transductive pathways.

Scaffold stiffness could also affect the maintenance of cell phenotype or differentiation of stem cells or progenitor cells. A substrate with the stiffness similar to that of specific type of normal tissue could induce

the differentiation of stem cells into the specific phenotype of cells in that tissue.[82-84] Some studies reported that the contraction of soft scaffolds which increased the cell number density could enhance the cell-cell interaction of chondrocytes or stem cells and promote chondrogensis.[85, 86] While substrates of varied stiffness did not affect the differentiation of myoblasts into myotubes, culturing myoblasts on a substrate with the stiffness similar to the normal muscle tissue (Young's modulus, approximately 12 kPa) promoted the striation of myosin and actin which indicate greater level of differentiation of myoblasts into mature muscle cells.[87, 88]

Table 1.1 The mechanical properties and biochemical compositions of major tissue types.

Tissue type	Modulus	Major chemical constituents
Bone[89]	10 GPa (tensile)	Hydroxyapatite, Collagen I
	8.7 GPa (buckling)	
Cartilage[90-92]	400-800 kPa (compressive)	Collagen II, chondroitin sulphate
Tendon[93]	500-660 MPa (tensile)	Collagen I, elastin
Peripheral nerve[94]	1.3-2.9 Mpa (tensile)	Galatocerebroside, cholesterol
Brain[95, 96]	8-15 kPa (sheer)	
Muscle[97]	25-100 kPa (indentation)	Myosin, laminin, collagen IV
Skin[98]	1-2 MPa (indentation)	Collagen I, keratin, collagen IV

1.4.3 The effect of chemical composition

The chemical composition of scaffolds can greatly affect the behavior of cells cultured within the material. Cell adhesion and spreading are usually promoted by the use of natural polymer-based scaffolds compared with synthetic polymer-based scaffolds which usually have hydrophobic surface. Cells in normal tissue are usually surrounded with ECM which serve as a substrate to modulate cell behavior. ECM of normal tissue has multiple components such as collagen, laminin, aggrecan, hyaluronic acid, and fibronectin. Scaffolds with a chemical composition similar to that of normal tissue ECM could benefit cell growth or tissue formation.[99] However, studies also shown that scaffolds with the chemical composition that mimic the mature cartilage tissue (abundant of collagen II and aggrecan) inhibited the formation of cartilage tissue. Instead, the scaffolds with the chemical composition that mimic the early-stage of cartilage development (moderate amount of type II collagen and aggrecan) can promote chondrogenesis.[100]

Different component of ECM can have different effect on cell behavior. Type I collagen were found to promote the tubule formation of endothelial cells while laminin-1 did not.[101] Scaffolds with different components of ECM affect the engineering of skeletal muscle tissue. When type I collagen, fibrin and Matrigel (a protein mix containing collagen IV, laminin and proteoglycans; produced from culturing mouse sarcoma cells) were used to form scaffolds to engineer skeletal muscle, higher composition of fibrin and Matrigel yielded greater force generation by engineered muscle tissue and more tissue hypertrophy.[102] Collagen substrates and laminin substrates were used to culture myoblasts and the latter significantly promoted the cell replication.[103]

Although ECM components such as collagen, hyaluronic acid (HA) are normally bioactive polymers that favor cell growth or tissue formation, the effect of each component on varied types of cells can be dramatically different. HA, the polysaccharide of normal skin ECM, incorporated in collagen scaffolds promoted the proliferation of dermal fibroblasts and synthesis of collagen matrix.[104-107] However, HA incorporated into collagen scaffolds can have an inhibition effect on the chondrogenic behavior of articular chondrocytes.[37]

Almost all synthetic polymer-based scaffolds cause inflammatory responses such as FBR after their implantation into animal. The FBR results formation of a fibrous capsule (usually exceeds 100 μm) that isolate the graft from the host tissue, limit the mass transfer between the graft and the host tissue and blood vessel formation. Attempts have been made to alleviate the FBR by coating synthetic polymer scaffolds (PLGA) with natural ECM such as collagen or porcine small intestinal submucosa (SIS).[108] Implantation of these modified scaffolds inhibited the FBR *in vivo* in a short term. However, after the remodeling/degradation of natural ECM coating on the implanted scaffolds, there is still the risk of FBR.

1.5 Thesis motivation, objectives and outline

1.5.1 Motivation and objectives

Compared with synthetic polymer scaffolds, natural polymer scaffolds showed advantages such as high compatibility with various types of cells and tissues, and mimicking the microenvironment of cells in normal tissue. Synthetic polymer scaffolds lack the surface ligands that can be recognized by cells to modulate cell behavior. Moreover, synthetic polymer based implant and their degradation products usually cause adverse inflammatory responses. In contrast, natural polymers such as proteins and polysaccharides of ECM provide abundant surface ligands in favor of cell adhesion, proliferation and assembly. The degradation products of natural polymer do not cause adverse responses and can be utilized by tissues. Therefore, in this study natural polymers are chosen to develop porous scaffolds for tissue engineering.

One limitation of conventional natural polymer scaffolds prepared from common fabrication techniques is their uncontrolled and closed micropore structure, which makes it difficult to seed cells homogeneously in a 3D material, exchange of nutrients and metabolic waste and engineer a homogenous tissue. Porous scaffolds with homogeneous and open-pore structure are required to engineer 3D tissues such as skin and cartilage.

Another limitation of conventional natural polymer scaffolds is the lack of 3D topographic guidance to engineer anisotropic tissues which have aligned cells, vasculature and ECM of ordered structure. Many types of tissues such as skeletal muscle, cardiac muscle, peripheral nerve and blood vessel have highly organized tissue structure in which the muscle cells, neurons and endothelial cells are well aligned. To engineer these anisotropic tissues we need the materials with anisotropic structure to guide the adhesion, growth and assembly of cells. Current studies reported the use of 2D substrates with micropatterned natural polymer to guide cell orientation to form cell sheets. The cell sheets need to be layered to form thick tissues, which is troublesome and could reduce the cell alignment. 3D micropatterned scaffolds are necessary to engineer 3D well-ordered tissues with controlled cell orientation.

In addition, natural polymer porous scaffolds with controlled microstructure could contribute the studies of cell-material interaction and cell-cell interaction within a 3D biomimetic environment. Numerous studies have reported the effects of 2D substrates modified with natural polymer or the 2D substrates with varied

stiffness on cell behavior. However, the 2D substrates cannot provide cells the 3D microenvironment similar to that of normal tissue. 3D natural polymer scaffolds with controlled microstructure can provide a suitable platform to study the cell-material and cell-cell interactions in 3D biomimetic environment.

The limitations of conventional natural polymer scaffolds motivate the objectives of this study:

(1) To fabricate natural polymer scaffolds with controlled homogeneous micropore structure to engineer 3D homogeneous cartilage tissue;
(2) To fabricate natural polymer scaffolds with controlled anisotropic micropatterned structure to engineer 3D anisotropic skeletal muscle;
(3) To use natural polymer scaffolds with controlled microstructures to study cell-cell interactions and cell-material interactions such as cell assembly, proliferation and gene expression in 3D material environment.

1.5.2 Outline

In this study, natural polymer porous scaffolds with controlled microstructures were developed to engineer cartilage tissue and skeletal muscle and study the cell-material, cell-cell interactions in 3D culture.

Chapter 2 describes the preparation of collagen/HA scaffolds with homogeneous pore structure by using low molecular weight salts to suppress PIC formation in collagen/hyaluronic acid(HA) suspensions. The suppression of PIC formation was studied by using turbidimetry, viscosity measurement and infrared analysis. The effects of PIC formation suppression on the morphology and mechanical properties of the scaffolds were examined with scanning electron microscopy and compression tests. Collagen/HA scaffolds were used to culture human dermal fibroblasts to study the cell proliferation, tissue synthesis and gene expression.

Chapter 3 describes the preparation of homogeneous collagen/HA scaffolds with well-controlled and interconnected pore structure to study the effect of high molecular HA on chondrocyte behavior. Collagen/HA scaffolds were prepared by suppression of polyion complex formation between collagen and HA and using ice particulates as porogen. Bovine articular chondrocytes were cultured in collagen/HA scaffolds and collagen scaffolds to compare the cell proliferation, sGAG synthesis and tissue formation in the two types of scaffolds.

Chapter 4 describes the preparation of gelatin porous scaffolds with homogeneous and open pores to engineer cartilage tissue in vitro. Gelatin scaffolds were prepared by using ice particulates and freeze-drying. Varied ratios of ice particulates and varied concentrations of gelatin were used to control the micropore structure and mechanical property of gelatin scaffolds. The scaffolds were used to culture bovine articular chondrocytes to investigate the influence of micropore structure and mechanical property of gelatin porous scaffolds on the functions of chondrocytes.

Chapter 5 describes the development of 3D porous collagen scaffolds with anisotropic and concave microgrooves to engineer skeletal muscle tissue. Micropatterned ice lines were used to control the micropatterned structure of collagen scaffolds. The microgrooved collagen scaffolds were used to culture rat skeletal myoblasts to study the effect of microgroove structure on the assembly of myoblasts into muscle tissue.

Chapter 6 compares the cell behaviors of cocultured myoblasts and vascular endothelial cells in microgrooved collagen scaffolds with those in non-paterned collagen porous scaffolds and flat collagen scaffolds. The two types of cells were seeded at varied ratios and concentrations in collagen scaffolds to study the cell-assembly and formation of anisotropic vascularized muscle tissue.

Chapter 7 gives of the conclusions supported by this thesis and suggests the future work.

1.6 References

[1] Vacanti CA, Vacanti JP. The science of tissue engineering. Orthop Clin North Am. 2000;31:351-6.
[2] Langer R, Vacanti JP. Tissue engineering. Science. 1993;260:920-6.
[3] Flasza M, Kemp P, Shering D, Qiao J, Marshall D, Bokta A, Johnson PA. Development and manufacture of an investigational human living dermal equivalent (ICX-SKN). Regenerative Medicine. 2007;2:903-18.
[4] Boyd M, Flasza M, Johnson PA, Roberts JC, Kemp P. Integration and persistence of an investigational human living skin equivalent (ICX-SKN) in human surgical wounds. Regenerative Medicine. 2007;2:363-70.
[5] Takahashi H, Shimizu T, Nakayama M, Yamato M, Okano T. Anisotropic Cellular Network Formation in Engineered Muscle Tissue through the Self-Organization of Neurons and Endothelial Cells. Advanced Healthcare Materials. 2015;4.
[6] Caspi O, Lesman A, Basevitch Y, Gepstein A, Arbel G, Huber I, Habib M, Gepstein L, Levenberg S. Tissue engineering of vascularized cardiac muscle from human embryonic stem cells. Circulation Research. 2007;100:263-72.
[7] Miura Y, Fitzsimmons JS, Commisso CN, Gallay SH, Odriscoll SW. Enhancement of Periosteal Chondrogenesis in-Vitro - Dose-Response for Transforming Growth-Factor-Beta-1 (Tgf-Beta-1). Clinical Orthopaedics and Related Research. 1994:271-80.
[8] Larsen M, Willems WF, Pelzer M, Friedrich PF, Dadsetan M, Bishop AT. Fibroblast growth factor-2 and vascular endothelial growth factor mediated augmentation of angiogenesis and bone formation in vascularized bone allotransplants. Microsurgery. 2014;34:301-7.
[9] Li Q, Liu TY, Zhang L, Liu Y, Zhang WJ, Liu W, Cao YL, Zhou GD. The role of bFGF in down-regulating alpha-SMA expression of chondrogenically induced BMSCs and preventing the shrinkage of BMSC engineered cartilage. Biomaterials. 2011;32:4773-81.
[10] Kaigler D, Wang Z, Horger K, Mooney DJ, Krebsbach PH. VEGF scaffolds enhance angiogenesis and bone regeneration in irradiated osseous defects. J Bone Miner Res. 2006;21:735-44.
[11] Nanda HS, Chen S, Zhang Q, Kawazoe N, Chen G. Collagen scaffolds with controlled insulin release and controlled pore structure for cartilage tissue engineering. Biomed Res Int. 2014;2014:623805.
[12] Nanda HS, Kawazoe N, Zhang Q, Chen SW, Chen GP. Preparation of collagen porous scaffolds with controlled and sustained release of bioactive insulin. Journal of Bioactive and Compatible Polymers. 2014;29:95-109.
[13] Chan BP, Leong KW. Scaffolding in tissue engineering: general approaches and tissue-specific considerations. European Spine Journal. 2008;17:S467-S79.
[14] Reed AM, Gilding DK. Biodegradable Polymers for Use in Surgery - Poly(Glycolic)-Poly(Lactic Acid) Homo and Co-Polymers .2. Invitro Degradation. Polymer. 1981;22:494-8.
[15] Gilding DK, Reed AM. Biodegradable Polymers for Use in Surgery - Polyglycolic-Poly(Actic Acid) Homopolymers and Copolymers. Polymer. 1979;20:1459-64.
[16] Makadia HK, Siegel SJ. Poly Lactic-co-Glycolic Acid (PLGA) as Biodegradable Controlled Drug Delivery Carrier. Polymers. 2011;3:1377-97.
[17] Bostman OM. Absorbable Implants for the Fixation of Fractures. Journal of Bone and Joint Surgery-American Volume. 1991;73A:148-53.
[18] Dai WD, Yao ZJ, Dong J, Kawazoe N, Zhang C, Chen GP. Cartilage tissue engineering with controllable shape using a poly(lactic-co-glycolic acid)/collagen hybrid scaffold. Journal of Bioactive and Compatible Polymers. 2013;28:247-57.

[19] Grad S, Eglin D. The use of fibrin and poly(lactic-co-glycolic acid) hybrid scaffold for articular cartilage tissue engineering: An in vivo analysis - Discussion. European Cells & Materials. 2008;15:51-2.
[20] Kang SW, Jeon O, Kim BS. Poly(lactic-co-glycolic acid) microspheres as an injectable scaffold for cartilage tissue engineering. Tissue Engineering. 2005;11:438-47.
[21] Kang SW, Lee JS, Park JH, Kim BS. Poly(lactic-co-glycolic acid) microspheres as an injectable scaffold for cartilage tissue engineering. Tissue Engineering. 2006;12:1091-.
[22] Rezwan K, Chen QZ, Blaker JJ, Boccaccini AR. Biodegradable and bioactive porous polymer/inorganic composite scaffolds for bone tissue engineering. Biomaterials. 2006;27:3413-31.
[23] Niklason LE, Gao J, Abbott WM, Hirschi KK, Houser S, Marini R, Langer R. Functional arteries grown in vitro. Science. 1999;284:489-93.
[24] Gong ZD, Niklason LE. Small-diameter human vessel wall engineered from bone marrow-derived mesenchymal stem cells (hMSCs). Faseb Journal. 2008;22:1635-48.
[25] Dahl SLM, Kypson AP, Lawson JH, Blum JL, Strader JT, Li YL, Manson RJ, Tente WE, DiBernardo L, Hensley MT, Carter R, Williams TP, Prichard HL, Dey MS, Begelman KG, Niklason LE. Readily Available Tissue-Engineered Vascular Grafts. Science Translational Medicine. 2011;3.
[26] Murphy GF, Orgill DP, Yannas IV. Partial Dermal Regeneration Is Induced by Biodegradable Collagen-Glycosaminoglycan Grafts. Laboratory Investigation. 1990;62:305-13.
[27] Yannas IV. Tissue regeneration by use of collagen-glycosaminoglycan copolymers. Clin Mater. 1992;9:179-87.
[28] Lee KI, Moon SH, Kim H, Kwon UH, Kim HJ, Park SN, Suh H, Lee HM, Kim HS, Chun HJ, Kwon IK, Jang JW. Tissue Engineering of the Intervertebral Disc With Cultured Nucleus Pulposus Cells Using Atelocollagen Scaffold and Growth Factors. Spine. 2012;37:452-8.
[29] Yamaoka H, Tanaka Y, Nishizawa S, Asawa Y, Takato T, Hoshi K. The application of atelocollagen gel in combination with porous scaffolds for cartilage tissue engineering and its suitable conditions. Journal of Biomedical Materials Research Part A. 2010;93A:123-32.
[30] Hou LT, Liu CM, Liu BY, Chang PC, Chen MH, Ho MH, Jehng SM, Liu HC. Tissue engineering bone formation in novel recombinant human bone morphogenic protein 2-atelocollagen composite scaffolds. Journal of Periodontology. 2007;78:335-43.
[31] Sato M, Kikuchi M, Ishihara M, Ishihara M, Asazuma T, Kikuchi T, Masuoka K, Hattori H, Fujikawa K. Tissue engineering of the intervertebral disc with cultured annulus fibrosus cells using atelocollagen honeycomb-shaped scaffold with a membrane seal (ACHMS scaffold). Medical & Biological Engineering & Computing. 2003;41:365-71.
[32] Heim M, Romer L, Scheibel T. Hierarchical structures made of proteins. The complex architecture of spider webs and their constituent silk proteins. Chemical Society Reviews. 2010;39:156-64.
[33] Maurer PH. Antigenicity of Gelatin .3. The Effect of Physical and Enzymatic Treatments of Gelatin on the Subsequent Precipitin Reaction. Journal of Experimental Medicine. 1958;107:125-31.
[34] Maurer PH, Lebovitz H. Studies on the Antigenicity of Modified Fluid Gelatin. Journal of Immunology. 1956;76:335-41.
[35] Maurer PH. Antigenicity of Gelatin in Rabbits and Other Species .2. Journal of Experimental Medicine. 1954;100:515-23.
[36] Matsiko A, Levingstone TJ, O'Brien FJ, Gleeson JP. Addition of hyaluronic acid improves cellular infiltration and promotes early-stage chondrogenesis in a collagen-based scaffold for cartilage tissue engineering. Journal of the Mechanical Behavior of Biomedical Materials. 2012;11:41-52.
[37] Nishimoto S, Takagi M, Wakitani S, Nihira T, Yoshida T. Effect of chondroitin sulfate and hyaluronic acid on gene expression in a three-dimensional culture of chondrocytes. Journal of Bioscience and Bioengineering. 2005;100:123-6.

[38] Kawasaki K, Ochi M, Uchio Y, Adachi N, Matsusaki M. Hyaluronic acid enhances proliferation and chondroitin sulfate synthesis in cultured chondrocytes embedded in collagen gels. Journal of Cellular Physiology. 1999;179:142-8.
[39] He P, Davis SS, Illum L. In vitro evaluation of the mucoadhesive properties of chitosan microspheres. International Journal of Pharmaceutics. 1998;166:75-88.
[40] Park PJ, Je JY, Jung WK, Ahn CB, Kim SK. Anticoagulant activity of heterochitosans and their oligosaccharide sulfates. European Food Research and Technology. 2004;219:529-33.
[41] Rao SB, Sharma CP. Use of chitosan as a biomaterial: Studies on its safety and hemostatic potential. Journal of Biomedical Materials Research. 1997;34:21-8.
[42] Klokkevold PR, Fukayama H, Sung EC, Bertolami CN. The effect of chitosan (poly-N-acetyl glucosamine) on lingual hemostasis in heparinized rabbits. Journal of Oral and Maxillofacial Surgery. 1999;57:49-52.
[43] Jayakumar R, Prabaharan M, Kumar PTS, Nair SV, Tamura H. Biomaterials based on chitin and chitosan in wound dressing applications. Biotechnology Advances. 2011;29:322-37.
[44] Costa-Pinto AR, Reis RL, Neves NM. Scaffolds Based Bone Tissue Engineering: The Role of Chitosan. Tissue Engineering Part B-Reviews. 2011;17:331-47.
[45] Seol YJ, Lee JY, Park YJ, Lee YM, Young-Ku, Rhyu IC, Lee SJ, Han SB, Chung CP. Chitosan sponges as tissue engineering scaffolds for bone formation. Biotechnology Letters. 2004;26:1037-41.
[46] Jia S, Yang XJ, Song W, Wang L, Fang KX, Hu ZQ, Yang ZH, Shan C, Lei DL, Lu B. Incorporation of osteogenic and angiogenic small interfering RNAs into chitosan sponge for bone tissue engineering. International Journal of Nanomedicine. 2014;9:5307-16.
[47] Pallela R, Venkatesan J, Janapala VR, Kim SK. Biophysicochemical evaluation of chitosan-hydroxyapatite-marine sponge collagen composite for bone tissue engineering. Journal of Biomedical Materials Research Part A. 2012;100A:486-95.
[48] Lee YM, Park YJ, Lee SJ, Ku Y, Han SB, Choi SM, Klokkevold PR, Chung CP. Tissue engineered bone formation using chitosan/tricalcium phosphate sponges. Journal of Periodontology. 2000;71:410-7.
[49] Arpornmaeklong P, Pripatnanont P, Suwatwirote N. Properties of chitosan-collagen sponges and osteogenic differentiation of rat-bone-marrow stromal cells. International Journal of Oral and Maxillofacial Surgery. 2008;37:357-66.
[50] Wang YZ, Kim HJ, Vunjak-Novakovic G, Kaplan DL. Stem cell-based tissue engineering with silk biomaterials. Biomaterials. 2006;27:6064-82.
[51] Correia C, Bhumiratana S, Yan LP, Oliveira AL, Gimble JM, Rockwood D, Kaplan DL, Sousa RA, Reis RL, Vunjak-Novakovic G. Development of silk-based scaffolds for tissue engineering of bone from human adipose-derived stem cells. Acta Biomaterialia. 2012;8:2483-92.
[52] Fini M, Motta A, Torricelli P, Glavaresi G, Aldini NN, Tschon M, Giardino R, Migliaresi C. The healing of confined critical size cancellous defects in the presence of silk fibroin hydrogel. Biomaterials. 2005;26:3527-36.
[53] Kim KH, Jeong L, Park HN, Shin SY, Park WH, Lee SC, Kim TI, Park YJ, Seol YJ, Lee YM, Ku Y, Rhyu IC, Han SB, Chung CP. Biological efficacy of silk fibroin nanofiber membranes for guided bone regeneration. Journal of Biotechnology. 2005;120:327-39.
[54] Meinel L, Fajardo R, Hofmann S, Langer R, Chen J, Snyder B, Vunjak-Novakovic G, Kaplan D. Silk implants for the healing of critical size bone defects. Bone. 2005;37:688-98.
[55] Meinel L, Karageorgiou V, Fajardo R, Snyder B, Shinde-Patil V, Zichner L, Kaplan D, Langer R, Vunjak-Novakovic G. Bone tissue engineering using human mesenchymal stem cells: Effects of scaffold material and medium flow. Annals of Biomedical Engineering. 2004;32:112-22.
[56] Meinel L, Karageorgiou V, Hofmann S, Fajardo R, Snyder B, Li CM, Zichner L, Langer R,

Vunjak-Novakovic G, Kaplan DL. Engineering bone-like tissue in vitro using human bone marrow stem cells and silk scaffolds. Journal of Biomedical Materials Research Part A. 2004;71A:25-34.
[57] Kim HJ, Kim UJ, Vunjak-Novakovic G, Min BH, Kaplan DL. Influence of macroporous protein scaffolds on bone tissue engineering from bone marrow stem cells. Biomaterials. 2005;26:4442-52.
[58] Dal Pra I, Petrini P, Charini A, Bozzini S, Fare S, Armato U. Silk fibroin-coated three-dimensional polyurethane scaffolds for tissue engineering: Interactions with normal human fibroblasts. Tissue Engineering. 2003;9:1113-21.
[59] Sofia S, McCarthy MB, Gronowicz G, Kaplan DL. Functionalized silk-based biomaterials for bone formation. Journal of Biomedical Materials Research. 2001;54:139-48.
[60] Chen JS, Altman GH, Karageorgiou V, Horan R, Collette A, Volloch V, Colabro T, Kaplan DL. Human bone marrow stromal cell and ligament fibroblast responses on RGD-modified silk fibers. Journal of Biomedical Materials Research Part A. 2003;67A:559-70.
[61] Karageorgiou V, Meinel L, Hofmann S, Malhotra A, Volloch V, Kaplan D. Bone morphogenetic protein-2 decorated silk fibroin films induce osteogenic differentiation of human bone marrow stromal cells. Journal of Biomedical Materials Research Part A. 2004;71A:528-37.
[62] Hutmacher DW. Scaffolds in tissue engineering bone and cartilage. Biomaterials. 2000;21:2529-43.
[63] Sachlos E, Czernuszka JT. Making tissue engineering scaffolds work. Review: the application of solid freeform fabrication technology to the production of tissue engineering scaffolds. Eur Cell Mater. 2003;5:29-39; discussion -40.
[64] Yang SF, Leong KF, Du ZH, Chua CK. The design of scaffolds for use in tissue engineering. Part II. Rapid prototyping techniques. Tissue Engineering. 2002;8:1-11.
[65] Dagalakis N, Flink J, Stasikelis P, Burke JF, Yannas IV. Design of an artificial skin. Part III. Control of pore structure. Journal of Biomedical Materials Research. 1980;14:511-28.
[66] Doillon CJ, Whyne CF, Brandwein S, Silver FH. Collagen-Based Wound Dressings - Control of the Pore Structure and Morphology. Journal of Biomedical Materials Research. 1986;20:1219-28.
[67] Mooney DJ, Baldwin DF, Suh NP, Vacanti JP, Langer R. Novel approach to fabricate porous sponges of poly(D,L-lactic-co-glycolic acid) without the use of organic solvents. Biomaterials. 1996;17:1417-22.
[68] Puppi D, Chiellini F, Piras AM, Chiellini E. Polymeric materials for bone and cartilage repair. Progress in Polymer Science. 2010;35:403-40.
[69] Leong KF, Cheah CM, Chua CK. Solid freeform fabrication of three-dimensional scaffolds for engineering replacement tissues and organs. Biomaterials. 2003;24:2363-78.
[70] Hollister SJ. Porous scaffold design for tissue engineering. Nature Materials. 2005;4:518-24.
[71] Croisier F, Jerome C. Chitosan-based biomaterials for tissue engineering. European Polymer Journal. 2013;49:780-92.
[72] Zhang Q, Lu HX, Kawazoe N, Chen GP. Pore size effect of collagen scaffolds on cartilage regeneration. Acta Biomaterialia. 2014;10:2005-13.
[73] Zhang Q, Lu HX, Kawazoe N, Chen GP. Preparation of collagen porous scaffolds with a gradient pore size structure using ice particulates. Materials Letters. 2013;107:280-3.
[74] Zhang Q, Lu HX, Kawazoe N, Chen GP. Preparation of collagen scaffolds with controlled pore structures and improved mechanical property for cartilage tissue engineering. Journal of Bioactive and Compatible Polymers. 2013;28:426-38.
[75] Zhang YY, Yang F, Liu K, Shen H, Zhu YD, Zhang WJ, Liu W, Wang SG, Cao YL, Zhou GD. The impact of PLGA scaffold orientation on in vitro cartilage regeneration. Biomaterials. 2012;33:2926-35.
[76] Kroehne V, Heschel I, Schugner F, Lasrich D, Bartsch JW, Jockusch H. Use of a novel collagen matrix with oriented pore structure for muscle cell differentiation in cell culture and in grafts. Journal of Cellular and Molecular Medicine. 2008;12:1640-8.

[77] Jana S, Cooper A, Zhang MQ. Chitosan Scaffolds with Unidirectional Microtubular Pores for Large Skeletal Myotube Generation. Advanced Healthcare Materials. 2013;2:557-61.
[78] Hume SL, Hoyt SM, Walker JS, Sridhar BV, Ashley JF, Bowman CN, Bryant SJ. Alignment of multi-layered muscle cells within three-dimensional hydrogel macrochannels. Acta Biomaterialia. 2012;8:2193-202.
[79] Sarkar S, Lee GY, Wong JY, Desai TA. Development and characterization of a porous micro-patterned scaffold for vascular tissue engineering applications. Biomaterials. 2006;27:4775-82.
[80] Lee CR, Grodzinsky AJ, Spector M. The effects of cross-linking of collagen-glycosaminoglycan scaffolds on compressive stiffness, chondrocyte-mediated contraction, proliferation and biosynthesis. Biomaterials. 2001;22:3145-54.
[81] Haugh MG, Murphy CM, McKiernan RC, Altenbuchner C, O'Brien FJ. Crosslinking and Mechanical Properties Significantly Influence Cell Attachment, Proliferation, and Migration Within Collagen Glycosaminoglycan Scaffolds. Tissue Engineering Part A. 2011;17:1201-8.
[82] Guvendiren M, Burdick JA. Stiffening hydrogels to probe short- and long-term cellular responses to dynamic mechanics. Nature Communications. 2012;3.
[83] Discher DE, Sweeney L, Sen S, Engler A. Matrix elasticity directs stem cell lineage specification. Biophysical Journal. 2007:32a-a.
[84] Engler AJ, Sen S, Sweeney HL, Discher DE. Matrix elasticity directs stem cell lineage specification. Cell. 2006;126:677-89.
[85] Vickers SM, Squitieri LS, Spector M. Effects of cross-linking type II collagen-GAG scaffolds on chondrogenesis in vitro: Dynamic pore reduction promotes cartilage formation. Tissue Engineering. 2006;12:1345-55.
[86] Vickers SM, Gotterbarm T, Spector M. Cross-Linking Affects Cellular Condensation and Chondrogenesis in Type II Collagen-GAG Scaffolds Seeded with Bone Marrow-Derived Mesenchymal Stem Cells. Journal of Orthopaedic Research. 2010;28:1184-92.
[87] Engler AJ, Griffin MA, Sen S, Bonnetnann CG, Sweeney HL, Discher DE. Myotubes differentiate optimally on substrates with tissue-like stiffness: pathological implications for soft or stiff microenvironments. Journal of Cell Biology. 2004;166:877-87.
[88] Webber MJ, Khan OF, Sydlik SA, Tang BC, Langer R. A Perspective on the Clinical Translation of Scaffolds for Tissue Engineering. Annals of Biomedical Engineering. 2015;43:641-56.
[89] Rho JY, Kuhn-Spearing L, Zioupos P. Mechanical properties and the hierarchical structure of bone. Medical Engineering & Physics. 1998;20:92-102.
[90] Anthanasiou KA, E. M. Darling, and J. C. Hu. Articular Cartilage Tissue Engineering.: Morgan and Claypool Publishers; 2010.
[91] Athanasiou KA, Agarwal A, Dzida FJ. Comparative-Study of the Intrinsic Mechanical-Properties of the Human Acetabular and Femoral-Head Cartilage. Journal of Orthopaedic Research. 1994;12:340-9.
[92] Jurvelin JS, Buschmann MD, Hunziker EB. Optical and mechanical determination of Poisson's ratio of adult bovine humeral articular cartilage. Journal of Biomechanics. 1997;30:235-41.
[93] Wang JHC. Mechanobiology of tendon. Journal of Biomechanics. 2006;39:1563-82.
[94] Singh A, Lu Y, Chen C, Cavanaugh JM. Mechanical properties of spinal different nerve roots subjected to tension at strain rates. Journal of Biomechanics. 2006;39:1669-76.
[95] Ommaya AK. Mechanical properties of tissues of the nervous system. Journal of Biomechanics. 1968;1:127-38.
[96] Saher G, Brugger B, Lappe-Siefke C, Mobius W, Tozawa R, Wehr MC, Wieland F, Ishibashi S, Nave KA. High cholesterol level is essential for myelin membrane growth. Nature Neuroscience. 2005;8:468-75.
[97] Mathur AB, Collinsworth AM, Reichert WM, Kraus WE, Truskey GA. Endothelial, cardiac muscle and

skeletal muscle exhibit different viscous and elastic properties as determined by atomic force microscopy. Journal of Biomechanics. 2001;34:1545-53.
[98] Geerligs M, van Breemen L, Peters G, Ackermans P, Baaijens F, Oomens C. In vitro indentation to determine the mechanical properties of epidermis. Journal of Biomechanics. 2011;44:1176-81.
[99] Benders KEM, van Weeren PR, Badylak SF, Saris DBF, Dhert WJA, Malda J. Extracellular matrix scaffolds for cartilage and bone regeneration. Trends in Biotechnology. 2013;31:169-76.
[100] Cai R, Nakamoto T, Kawazoe N, Chen GP. Influence of stepwise chondrogenesis-mimicking 3D extracellular matrix on chondrogenic differentiation of mesenchymal stem cells. Biomaterials. 2015;52:199-207.
[101] Liu YQ, Senger DR. Matrix-specific activation of Src and Rho initiates capillary morphogenesis of endothelial cells. Faseb Journal. 2004;18:457-68.
[102] Hinds S, Bian WN, Dennis RG, Bursac N. The role of extracellular matrix composition in structure and function of bioengineered skeletal muscle. Biomaterials. 2011;32:3575-83.
[103] Foster RF, Thompson JM, Kaufman SJ. A Laminin Substrate Promotes Myogenesis in Rat Skeletal-Muscle Cultures - Analysis of Replication and Development Using Antidesmin and Anti-Brdurd Monoclonal-Antibodies. Developmental Biology. 1987;122:11-20.
[104] Park SN, Lee HJ, Lee KH, Suh H. Biological characterization of EDC-crosslinked collagen-hyaluronic acid matrix in dermal tissue restoration. Biomaterials. 2003;24:1631-41.
[105] Kutty JK, Cho E, Lee JS, Vyavahare NR, Webb K. The effect of hyaluronic acid incorporation on fibroblast spreading and proliferation within PEG-diacrylate based semi-interpenetrating networks. Biomaterials. 2007;28:4928-38.
[106] Suh H, Lee JE. Behavior of fibroblasts on a porous hyaluronic acid incorporated collagen matrix. Yonsei Medical Journal. 2002;43:193-202.
[107] Chen SW, Zhang Q, Nakamoto T, Kawazoe N, Chen GP. Highly active porous scaffolds of collagen and hyaluronic acid prepared by suppression of polyion complex formation. Journal of Materials Chemistry B. 2014;2:5612-9.
[108] Kim MS, Ahn HH, Shin YN, Cho MH, Khang G, Lee HB. An in vivo study of the host tissue response to subcutaneous implantation of PLGA- and/or porcine small intestinal submucosa-based scaffolds. Biomaterials. 2007;28:5137-43.

Chapter 2

Preparation of highly active porous scaffolds of collagen and hyaluronic acid by suppression of polyion complex formation

2.1 Summary

Collagen-hyaluronic acid scaffolds with high bioactivity, good mechanical property and homogeneous pore structures are desirable for their applications in tissue engineering. However, in aqueous condition collagen and hyaluronic acid form polyion complexes (PIC), which results in heterogeneous structures and poor mechanical properties of the scaffolds. In this study, we used low molecular weight salts to suppress PIC formation in collagen-hyaluronic acid suspensions during scaffold preparation. The suppression of PIC formation was studied by using turbidimetry, viscosity measurement and infrared analysis. The effects of PIC formation suppression on the morphology and mechanical properties of the scaffolds were examined with scanning electron microscopy and compression tests. PIC formation was found to be dependent on the ionic strength of the suspension. The secondary structure of collagen was partially altered by its strong electrostatic interactions with hyaluronic acid. The suppression of PIC formation resulted in collagen-hyaluronic acid scaffolds with homogeneous pore structures and remarkably enhanced mechanical properties. Collagen-hyaluronic acid scaffolds prepared under suppression of PIC formation promoted proliferation of fibroblasts and upregulated the expression of genes encoding EGF, VEGF and IGF-1. Using low molecular weight salts to suppress PIC formation could aid in the design of collagen-glycosaminoglycan scaffolds for tissue engineering.

2.2 Introduction

Three-dimensional porous scaffolds used in tissue engineering act as temporary templates to guide cell ingrowth and tissue regeneration. Apart from the requirements of good biocompatibility and nontoxicity, scaffolds should have an appropriate pore structure to facilitate cell infiltration and metabolite exchange and robust mechanical properties that allow them to endure cell-mediated contraction[1] during cell culture and mechanical load at the transplantation site. Ideally, porous scaffolds should mimic the chemical composition of native tissue and provide suitable mechanical, structural and biological signals to enhance cell activity and tissue regeneration.

Collagen-glycosaminoglycan (CG) scaffolds, whose components are the major structural proteins and polysaccharides found in a natural extracellular matrix, are widely used in tissue engineering due to their good biocompatibility and non-toxic degradation products. Improvements in the biofunctionality and regeneration capacity of collagen-derived scaffolds can be achieved through the incorporation of glycosaminoglycan[2, 3] and CG scaffolds have been used for the regeneration of various tissues such as skin, tendon, nerve, conjunctiva, cartilage and bone[4-8]. However, CG scaffolds prepared by freeze-drying CG slurries have inadequate mechanical properties[9, 10] and uneven matrix distribution, which may limit their practical use, particularly for applications in load-bearing tissues such as cartilage and bone. Attempts to improve the mechanical properties of CG scaffolds have been made by increasing the concentrations of collagen and glycosaminoglycan in the CG slurry. However, high CG concentrations result in a heterogeneous microstructure[10, 11] due to the heterogeneity of the CG suspension. New methods to prepare CG scaffolds with high bioactivity, good mechanical properties and homogeneous pore structures are necessary.

In this study, we used low molecular weight (MW) salts to prepare homogeneous collagen-hyaluronic acid (CH) suspensions for scaffold fabrication. The formation of polyion complex (PIC) between positively charged collagen and negatively charged hyaluronic acid was suppressed by the salts in the CH suspensions[12], making these CH suspensions homogeneous. We hypothesize that PIC suppression in CH suspensions will improve the pore structure, mechanical properties and bioactivity of CH scaffolds. Therefore, the objective of this research is to study PIC formation in CH suspensions with different concentrations of salts and the effects of PIC suppression on the pore structure, mechanical property and bioactivity of CH scaffolds.

2.3 Materials and methods

2.3.1 Preparation of CH suspensions

An aqueous solution (pH = 3.0) of type I collagen (1 wt.%) isolated from porcine skin (Nippon Meat Packers, Inc.) and an aqueous solution of hyaluronic acid (HA) (1 wt.%) isolated from rooster comb (Wako Pure Industries, Ltd.) were used to prepare aqueous suspensions of collagen-hyaluronic acid (CH) mixture. Before the two solutions were mixed, sodium chloride (NaCl) granules were added to the collagen and HA aqueous solutions, and the solutions were gently stirred at 4 ºC for 12 h. The collagen and HA aqueous solutions were then mixed at a volume ratio of 9:1 (collagen:HA) and gently stirred at 4 ºC for 24 h. The mixed aqueous suspensions and subsequently freeze-dried samples were designated as CHx, with x representing the NaCl concentration (x = 0.000-0.200 M). To study the relationship between ionic strength and PIC formation by turbidimetry, we also prepared CH suspensions with a divalent salt (sodium sulfate, Na_2SO_4) at various concentrations. The ionic strength was adjusted to be equivalent to that of NaCl.

2.3.2 Turbidimetry and viscosity measurements

The transmittance of the CH mixture aqueous suspensions at 500 nm with different concentrations of NaCl and Na_2SO_4 was measured using an UV-Vis spectrophotometer (V-660, JASCO, Inc.). The sheer viscosity of the CH suspensions (within the sheer-speed range of 1-1000 s^{-1}) was recorded at 4 ºC by a MCR301 Rheometer and RheoPlus software (Anton Paar Co.). To observe the gross appearance of PIC, CH suspensions were centrifuged at a speed of 15,000 rpm at 4 ºC for 30 min to precipitate the PIC in these

suspensions.

2.3.3 Preparation of CH scaffolds

CH porous scaffolds were prepared by freeze-drying. First, a CH suspension was poured into a silicone frame on a copper plate wrapped with perfluoroalkoxy (PFA) film (Universal Co., Ltd). Copper plates were chosen as substrates to facilitate heat conduction and PFA film was used to ensure the easy detachment of frozen suspensions. A silicone frame (60 mm × 40 mm × 5 mm) on the copper plate was used to confine the suspension to the copper plate and control the thickness. The surface of the suspension was flattened by covering the silicon frame with a glass plate wrapped in PFA film. The entire construct was then frozen at -30 ºC for 9 h. After glass plate and copper plate were removed from the construct, the frozen construct was freeze-dried under a vacuum of less than 5 Pa with a freeze dryer (FDU-2200, Tokyo Rikakikai Co., Ltd.) for 24 h. All samples were frozen and freeze-dried under the same conditions. The non-crosslinked CH scaffolds were used for infrared spectrum measurements, while crosslinked CH scaffolds were used for other experiments.

1-ethyl-3-(3-dimethylaminopropyl) carbodiimide (EDC, Peptide Institute, Inc.) and N-hydroxysuccinimide (NHS, Wako Pure Chemical Industries, Ltd.) were used as crosslinking agents. EDC and NHS were dissolved in an ethanol/water (80/20, v/v) mixture, which was used to protect the CH scaffolds from dissolution during crosslinking. A crosslinking solution containing 50 mM EDC and 20 mM NHS was prepared. CH scaffolds were kept in the crosslinking solution at room temperature for 8 h. The crosslinked scaffolds were washed with MilliQ water for five times. The scaffolds were then soaked in MilliQ water, frozen and freeze-dried again under the same previous conditions. The CH porous scaffolds prepared with 0.000, 0.025, 0.050, 0.075, 0.100, 0.125, 0.150 and 0.200 M NaCl were referred as CH0, CH0.025, CH0.050, CH0.075, CH0.100, CH0.125, CH0.150 and CH0.200, respectively.

2.3.4 Infrared analysis

The infrared spectra of non-crosslinked CH0, CH0.050, CH0.100 and CH0.150 scaffolds were obtained using a Fourier transformed infrared spectrometer (FTIR-8400S, Shimadzu Corp.) at a resolution of 4 cm-1. For each scaffold, spectra from six different locations were recorded and averaged. Two-dimensional infrared correlation spectroscopy (2D-IR) was used to study the changes in molecular conformation. Using correlation analysis, 2D-IR can enhance the resolution of an IR spectrum by spreading overlapped IR peaks along two dimensions[13] and 2D-IR has been used to analyze the secondary structures and denaturation of proteins[14-16]. Under an external perturbation of a system (chemical, electrical, thermal, mechanical stimulation, etc.), a sequential set of dynamic IR spectra can be collected and transformed into a 2D correlation map to reveal any spectral changes induced by the perturbation. The 2D-IR map, on which correlation intensity is plotted as a function of two independent wavenumbers, shows peaks corresponding to the structural change caused by the perturbation. Before two-dimensional correlation analysis, the baselines of averaged spectra of different CH scaffolds were corrected. These spectra were then analyzed using a 2D Pocha software provided by Daisuke Adachi (Kwansei Gakuin University) to generate 2D-IR maps for interpretation.

2.3.5 Scanning electron microscopy (SEM) and compression tests

Crosslinked CH scaffolds were cut with a blade and their cross sections were sputter-coated with platinum. The cross sections were observed at 10 kV with a scanning electron microscope (JSM-5610, JEOL, Ltd.). For compression testing, crosslinked CH scaffolds were cut into disks with a diameter of 8 mm and a height of 4 mm using a biopsy punch. The dry disk samples were compressed at a rate of 0.1 mm/s to generate stress-strain curves with a texture analyzer (TA.XTPlus, Texture Technologies Corp.). The Young's modulus was calculated from the initial linear region of the stress-strain curve and sample dimension. A minimum of six samples were tested for each type of scaffold.

2.3.6 Culture of dermal fibroblasts in CH scaffolds

The CH0 and CH0.150 scaffolds were used for culture for human dermal fibroblasts. Collagen porous scaffolds prepared by the same procedure as that of CH0 scaffolds were used as a control. The three types of scaffolds were punched into disks with a diameter of 12 mm and cut to a thickness of 2 mm. The discs were sterilized with 70% ethanol for 30 minutes, rinsed three times with sterile Milli-Q water and conditioned with culture medium. Neonatal human dermal fibroblasts (NHDF, Cascade Biologics, Inc.) were subcultured in 75-cm^2 tissue culture flasks in Medium 106 (Life Technologies Corporation) supplemented with low serum growth supplement kit (Life Technologies Corporation) in an incubator equilibrated with 5% CO_2 at 37°C. The adjusted medium was referred as serum medium. The fibroblasts in confluence were rinsed with N-2-hydroxyethylpiperazine-N'-2-ethanesulfonic acid (HEPES) buffer, detached from the culture flasks using 0.025% (w/v) trypsin and 0.01% (w/v) ethylenediaminetetraacetic acid (EDTA), and neutralized by HEPES solution containing 10% FBS (Kurabo Industries, Ltd.). The collected cell suspension was centrifuged and suspended in the serum medium to a concentration of 5.0×10^6 cells/ml. The cells were then seeded in the three types of scaffolds placed in the wells of 12-well cell culture plates by dropping 200 µl of cell suspension solution onto the top surface of each scaffold and cultured in an incubator equilibrated with 5% CO_2 at 37°C. After 3 h incubation to allow cell attachment, 10 mL serum medium was added to each well of the plates and cultured for 14 days with the serum medium in an incubator equilibrated with 5% CO_2 at 37°C. The medium was exchanged every two days.

2.3.7 Analysis of cell distribution and viability

After 24 hours, 7 days or 14 days of culture, the scaffolds were washed three times with PBS and fixed with 2.5% glutaraldehyde aqueous solution at room temperature for 1 hour. The scaffolds were then washed three times with pure water, frozen at -30 ºC and freeze-dried for 2 days. The cross sections of the freeze-dried samples were coated with platinum for SEM observation to examine cell distribution in the scaffolds.

Live/dead staining was performed to evaluate cell viability using calcein-AM (live: green) and propidium iodide (dead: red) staining reagents (Cellstain Double Staining Kit, Dojindo Laboratories). After two weeks of culture, the cell/scaffold constructs were washed with HEPES buffer and incubated in 2 µM calcein-AM and 4 µM propidium iodide solution in HEPES buffer for 30 minutes. After being rinsed with HEPES buffer, the submerged specimens were observed with a fluorescence microscope.

2.3.8 Cell proliferation assay and real-time PCR analysis

The cell proliferation in the scaffolds was evaluated by quantifying the DNA amount. After being cultured for 1, 3, 7, or 14 days, the cell/scaffold constructs were washed with pure water, freeze-dried and then digested with papain solution. Papain (Sigma-Aldrich, St Louis, Missouri, USA) was dissolved at 400 μg/ml in 0.1 M phosphate buffer (pH 6.0), with 5 mM cysteine hydrochloride and 5 mM ethylenediaminetetraaceticacid (EDTA). An aliquot of papain digests was used to measure the DNA content with Hoechst 33258 dye (Sigma-Aldrich) and an FP-6500 spectrofluorometer (JASCO, Tokyo, Japan) at an excitation wavelength of 360 nm and emission wavelength of 460 nm. Four samples were used to calculate the average and standard deviation.

For analysis of gene expression, the cell/scaffold constructs (3 samples for each type of scaffolds) after the 14-day culture were rinsed with PBS buffer, immersed in 1 ml Sepasol-RNA I Super G solution (Nacalai Tesque, Inc.) and frozen at -80 ºC. The frozen constructs were crushed into powder by an electric crusher and transferred back into the Sepasol solution to isolate the RNA from the cells. Total RNA (1.0 μg) was used as a first strand reaction that included random hexamer primers and murine leukemia virus reverse transcriptase (Applied Biosystems, Foster City, CA). Real-time PCR was amplified for 18 S rRNA, glyceraldehyde 3 phosphate dehydrogenase (GAPDH), epidermal growth factor (EGF), vascular endothelial growth factor (VEGF) and insulin-like growth factor-1 (IGF-1). The reaction was performed with 10 ng of cDNA, 90 nM PCR primers, 25 nM PCR probe, and FastStart TaqMan Probe Master (Roche Diagnostics Japan, Tokyo, Japan). The expression levels of 18 S rRNA were used as an endogenous control, and gene expression levels relative to GAPDH were calculated using the comparative Ct method. The sequences of primers and probes are listed in Table 1. The primers and probes were obtained from Applied Biosystems and Hokkaido System Science (Sapporo, Japan).

Table 1. Primers and probes for real-time PCR analysis.

mRNA	Oligonucleotide
18 S rRNA	Hs99999901_s1
GAPDH	Hs99999905_m1
VEGF	Hs00900054_m1
EGF	Hs00153181_m1
IGF-1	Hs00153126_m1

2.3.9 Statistical analysis

A one-way analysis of variance followed by pairwise multiple comparison (Tukey Test) was used to compare groups of data. Paired t-tests were used to compare individual sets of data. Significant differences were considered when $p < 0.05$.

2.4 Results and discussion

2.4.1 PIC formation and turbidity of CH suspensions

Collagen and HA aqueous solutions were mixed with or without salts to prepare the CH aqueous suspensions. Two kinds of low molecular weight salts, NaCl and Na_2SO_4, were used to prepare the CH suspensions for the study of the relationship between ionic strength and PIC formation. By gross observation, the CH suspensions prepared without salt (CH0) were opaque. CH suspensions prepared with 0.100 M NaCl (CH0.100) were semitransparent, while CH suspensions prepared with 0.200 M NaCl (CH0.200) were clear (Fig. 2.1a). The CH0, CH0.100 and CH0.200 suspensions were centrifuged to further reveal the PIC formation in different CH suspensions. After centrifugation, the PIC in CH0 settled at the bottom of tube and was white and compact in appearance. The PIC in CH0.100 was watery and loose, while no obvious PIC sediment was observed in CH0.200 (Fig. 2.1b). The transmittance of the CH suspensions was measured after the suspensions were prepared at ionic strengths of 0.000 to 0.200 M (Fig. 2.1c, d). Despite the different salts used, the transmittance of CH suspensions remained approximately zero at low ionic strengths, increased gradually as the ionic strength increased and increased rapidly when the ionic strength changed from a 0.100 M to 0.150 M, after which the maximum transmittance was maintained.

With the presence of salts in the CH suspensions, PIC formation between collagen and HA was suppressed due to the ability of cations and anions from low MW salt to screen the charges along the polymer chains. The suppression of PIC formation by different concentrations of salts resulted in the different transparencies observed in the CH suspensions. When CH suspensions were prepared without salts or with a low concentration of salt, PIC formed and the suspension was opaque, resulting in low transmittance. When high concentrations of salts were used, PIC formation was suppressed and the CH suspensions were clear, resulting in high transmittance. The similarity between the two transmittance curves of CH suspensions prepared with monovalent salts (NaCl) or divalent salts (Na_2SO_4) indicates that PIC formation was dependent on the ionic strength of the CH suspensions rather than the type of salt used, which is consistent with previous studies on PIC formation and ionic strength[17-19]. Therefore, only NaCl was used for the following experiments.

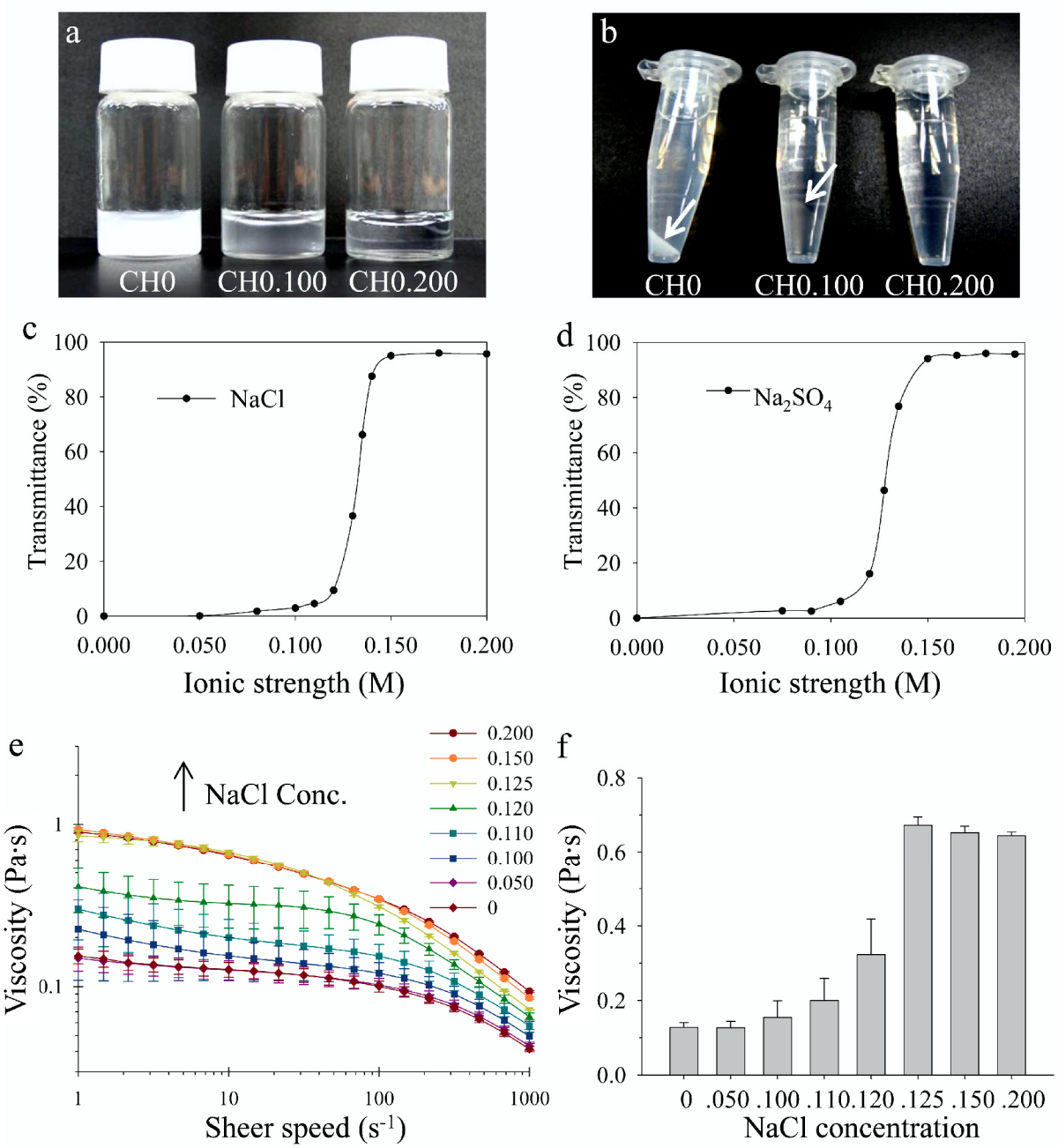

Fig. 2.1. Formation of polyion complex in CH suspensions. Gross appearance of (a) CH suspensions with different concentrations of NaCl (0, 0.100 or 0.200 M NaCl) and (b) CH suspensions after centrifugation. Arrows mark the boundary between the precipitated PIC and supernatant. Transmittance at 500 nm of CH suspensions prepared with different concentrations of (c) monovalent NaCl or (d) divalent Na_2SO_4.The ionic strength (M) was calculated from molar concentrations of salt ions. (e) Sheer viscosity-sheer speed relationship of CH suspensions prepared with different concentrations of NaCl (0 - 0.200 M). (f) Viscosities of CH suspensions measured at a sheer speed of 10 s^{-1}. Means ± SD, N = 3.

2.4.2 Viscosity of CH suspensions

The sheer viscosity of CH suspensions prepared with different NaCl concentrations was measured, as

shown in Fig. 2.1e, f. All CH suspensions were sheer-thinning: their viscosity decreased with increasing sheer speed. The viscosities of the CH suspensions prepared without NaCl or with 0.050 M NaCl were the lowest of those measured. The viscosity increased when the NaCl concentration increased from 0.050 M to 0.120 M, and remained unchanged after the NaCl concentration reached 0.125 M.

The observed variations in viscosity can be explained by the electrostatic interactions between collagen and HA molecules in suspension. When the positively charged collagen and negatively charged HA interacted, they formed PIC. The binding affinity between collagen and HA molecules was weakened by the presence of Na^+ and Cl^- ions in the suspensions. With no NaCl or low concentrations of NaCl (< 0.100 M), ionic strength was too low to shield the charges on collagen and HA polymer chains and to weaken their strong binding affinity, resulting in the formation of compact PIC. The formation of compact PIC resulted in decrease of soluble polymer molecules in the suspension and therefore a low viscosity. At intermediate NaCl concentrations (0.100 – 0.125 M), the collagen and HA polyions were partially shielded by Na^+ and Cl^- ions, weakening the binding affinity between the polyions. A weak binding affinity resulted in loose PIC that was not completely separated from the suspension and therefore viscosity of median values. The viscosity increased with NaCl concentration and peaked at high NaCl concentrations (≥ 0.150 M), where the polyions were completely shielded by their counterions and PIC formation was suppressed. Therefore, viscosity reached a stable maximum.

2.4.3 Infrared analysis

To examine the effects of the addition of salt on the molecular structures of collagen and HA, we analyzed the infrared spectra of non-crosslinked CH sponges prepared from CH suspensions with different NaCl concentrations (Fig. 2.2a). Non-crosslinked CH sponges, prepared by freeze-drying CH suspensions, were used for IR analysis to eliminate any effects from the crosslinking reagent. No obvious differences among these spectra were observed because of the same functional groups of collagen and HA in all of the sponges.

The 2D-IR map was used to elucidate the structural change of collagen and HA molecules in CH scaffolds caused by the addition of varying amounts of NaCl. A sequential set of spectra of non-crosslinked CH sponges (CH0, CH0.050, CH0.100, CH0.150) was used for 2D-IR analysis to generate the synchronous 2D-IR maps (Fig. 2.2b, c). The autopeak (autopeaks: peaks located on the diagonal line) at 1655 cm^{-1} denoted a shift of the amide I band, indicating that collagen had a partially unordered structure at low NaCl concentrations while maintained its α helical structure at high NaCl concentrations. This suggests that the strong electrostatic interactions between collagen and HA molecules in suspensions without NaCl or with low NaCl concentrations could disturb the triple helical structure of collagen. The autopeaks at 3346 cm^{-1} and 1552 cm^{-1} demonstrated that N—H stretching and N—H bending were stronger at higher NaCl concentrations. The more intense stretching and bending vibrations of the amine groups suggested that collagen and HA molecules were less complexed at higher NaCl concentrations. The loss of α helical structure or the increase of unordered structure in proteins interacting with polyions has also been reported in previous works [20-22].

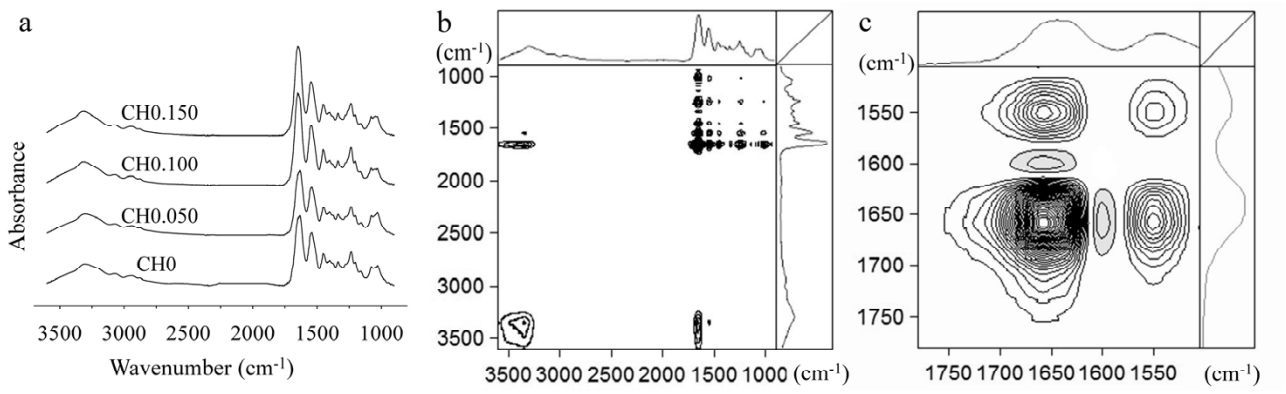

Fig. 2.2. (a) IR spectra of non-crosslinked CH sponges prepared from CH suspensions with different NaCl concentrations (0, 0.050, 0.100 or 0.150 M NaCl). (b and c) Synchronous 2D-IR maps of non-crosslinked CH sponges prepared from CH suspensions with different NaCl concentrations. The upper right zone (1500-1775 cm^{-1}) of (b) is magnified and shown in (c). The one-dimensional spectra on the top and right columns of the maps are the average spectra used in the correlation analysis.

2.4.4 Scaffold morphology

Fig. 2.3 displays the SEM images of the microstructures of the crosslinked CH scaffolds. Crosslinked CH sponges exhibited flake-like microstructures. There were some matrix blocks indicated by arrows and fibers indicated by arrowheads in the images of CH0, CH0.025, CH0.050 and CH0.075 CH scaffolds. The blocks were polymer matrix-rich regions with a high polymer density, while the fibers were polymer matrix-poor regions with a low polymer density. When NaCl concentrations were lower than 0.075 M, CH scaffolds exhibited heterogeneous pore structures with an unevenly distributed polymer matrix. Scaffolds prepared at intermediate or high NaCl concentrations (≥ 0.100 M) showed well-ordered micropore structures and an even distribution of polymer matrix.

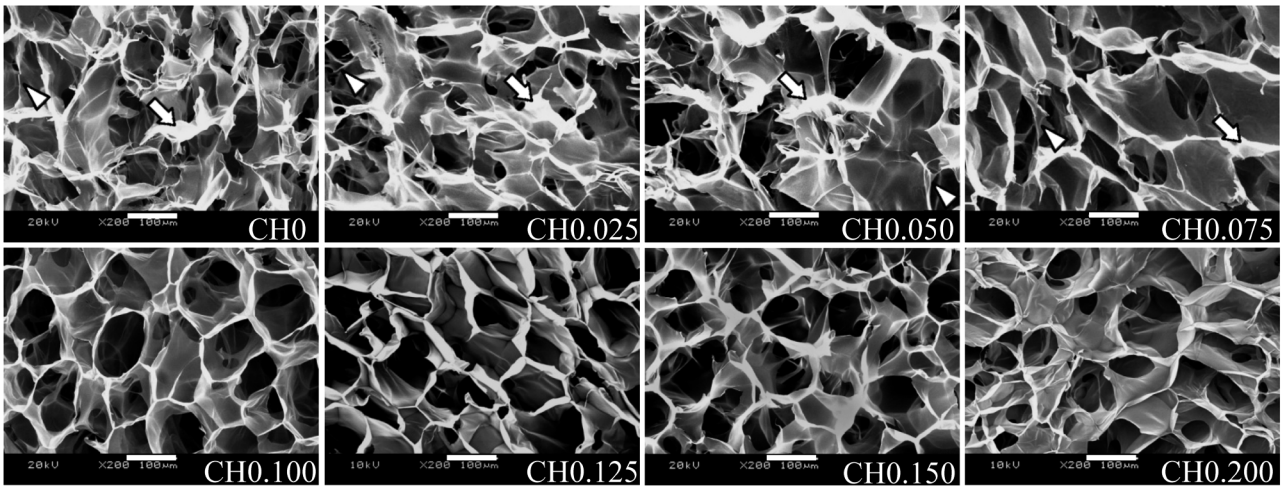

Fig. 2.3. SEM images of cross sections of crosslinked CH scaffolds prepared with different concentrations of NaCl (0 - 0.200 M). The arrows indicate the regions of high polymer density, and the arrowheads indicate the regions of low polymer density. Scale bar = 100 μm.

The scaffold morphology was consistent with PIC formation as examined in previous parts. The

compact PIC that formed without NaCl or at low NaCl concentrations resulted in the local condensation of the polymer matrix and a heterogeneous pore structure. The blocks CH0, CH0.025, CH0.050 and CH0.075 CH scaffolds should be due to the PIC in the CH suspensions which resulted in generation of polymer matrix-rich and poor regions. However, at higher NaCl concentrations, either PIC became loose or no PIC formed. The CH suspensions without PIC or with loose PIC avoided the local condensation of polymer matrix, resulting in the even distribution of polymer matrix and a homogeneous pore structure.

Previous studies by Harley et al.[10] and Davidenko et al.[11] reported that a high concentration (≥ 1 wt.%) of collagen and GAG suspension for scaffold preparation would result in heterogeneous CG scaffolds. This was confirmed by the heterogeneous morphology of CH0 scaffolds in our study. With the addition of NaCl to suppress PIC formation, a homogenous distribution of polymer matrix could be achieved. Apart from NaCl, other low molecular weight salts such as KCl and Na_2SO_4 can be used. Therefore, the difficulty in preparing homogeneous CG scaffolds from highly concentrated suspensions can be overcome by suppressing the PIC formation using low MW salts.

2.4.5 Mechanical property

The compressive Young's modulus of the crosslinked CH scaffolds prepared with different concentrations of NaCl was measured through compression tests and the results are shown in Fig. 2.4. The compressive modulus increased with NaCl concentration and reached a plateau when the NaCl concentration was higher than 0.100 M. The modulus of a CH scaffold prepared with 0.100 M NaCl was approximately 5-fold higher than that of a CH0 scaffold. The higher mechanical properties of CH scaffolds prepared with high concentrations of NaCl (0.100 - 0.200 M) might result from the homogeneous pore structure of these scaffolds. In contrast, the CH scaffolds prepared without NaCl or low NaCl concentrations showed heterogeneous pore structures and had lower mechanical strength. The correlation between improved mechanical property and a well-defined pore structure in porous scaffolds has also been previously reported[23-25].

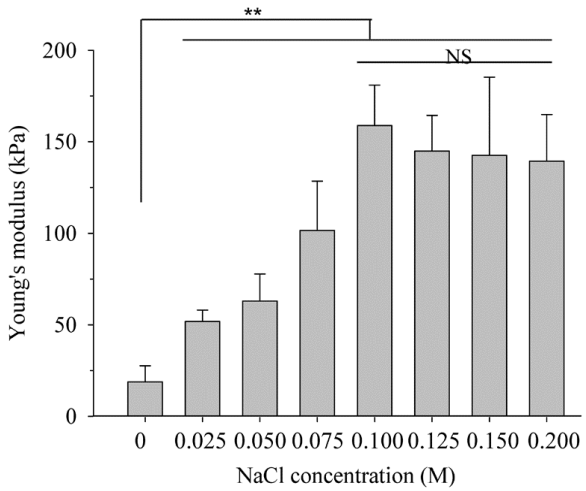

Fig. 2.4. Compression moduli of crosslinked CH scaffolds prepared with different concentrations of NaCl (0 - 0.200 M). Mean ± SD, N =6; **, $p<0.01$; NS, no significant difference.

After examining the PIC formation in CH suspensions and the properties of scaffolds from these suspensions, we proposed a mechanism to explain the formation of PIC at different ionic strengths and its

effects on the morphology and mechanical properties of scaffolds. The interactions between the polyions (collagen and HA) and the different states of PIC formed under different ionic strengths are illustrated in Fig. 2.5. Because the binding affinity of collagen and HA molecules was determined by the ionic strength of the aqueous environment, polyions of opposite charges are compactly complexed at a low ionic strength (Fig. 2.5a), or become loosely complexed at an intermediate ionic strength (Fig. 2.5b) but no complexes are formed at high ionic strengths (Fig. 2.5c). Compact PIC in CH suspensions interferes with the polymer diffusion during the solidification of the CH suspensions at a low temperature, which renders the network of polymer solids heterogeneous. CH suspensions with loose PIC or no PIC are able to undergo even polymer diffusion that results in a homogeneous polymer matrix network. The homogeneous micropore structure and the uniform distribution of collagen and HA within the matrix may account for the improved mechanical properties of CH scaffolds.

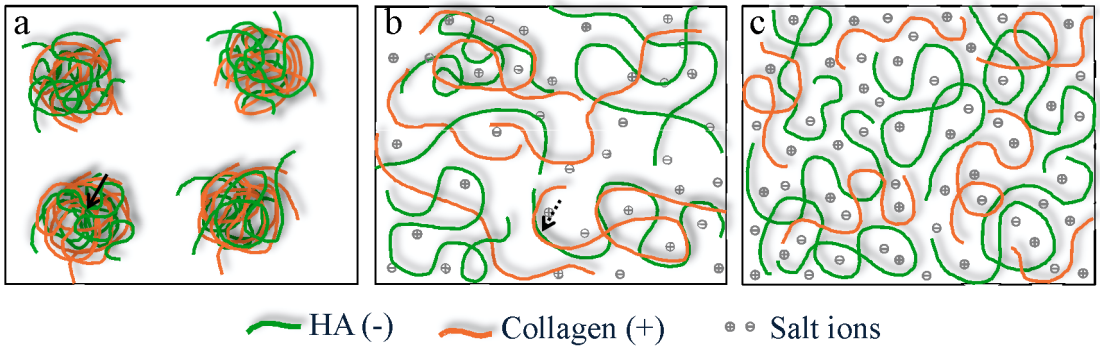

Fig. 2.5. Speculated schema of (a) compact PIC, (b) loose PIC and (c) no PIC formation in CH suspensions at different concentrations of salt. The solid arrows indicate complete complexation of collagen and HA, and the dashed arrows indicate partial complexation of collagen and HA.

2.4.6 Cell adhesion and proliferation in CH scaffolds

Adhesion of fibroblasts in the scaffolds after culture for 24 hour was observed by using SEM. Fibroblasts adhered to all the three types of scaffolds and showed better spread in the CH0.150 than did in CH0 and Col scaffolds (Fig. 2.6a). The cell proliferated with culture time and filled the spaces in the scaffolds (Fig. 2.6b-d). Most of the cells were alive and few dead cells were detected (Fig. 2.6e). DNA Quantification (Fig. 2.7) showed that the DNA content in the three types of scaffolds was almost the same after one day culture and increased with culture time. The increase of DNA content in the three scaffolds with culture time was in the increasing order of Col<CH0<CH0.15. DNA content in the CH0.15 scaffold after 14 days culture was significantly higher than that in the Col and CH0 scaffolds. The results indicated that CH0.15 scaffold had a higher promotive effect on the proliferation of fibroblasts compared to Col and CH0 scaffolds.

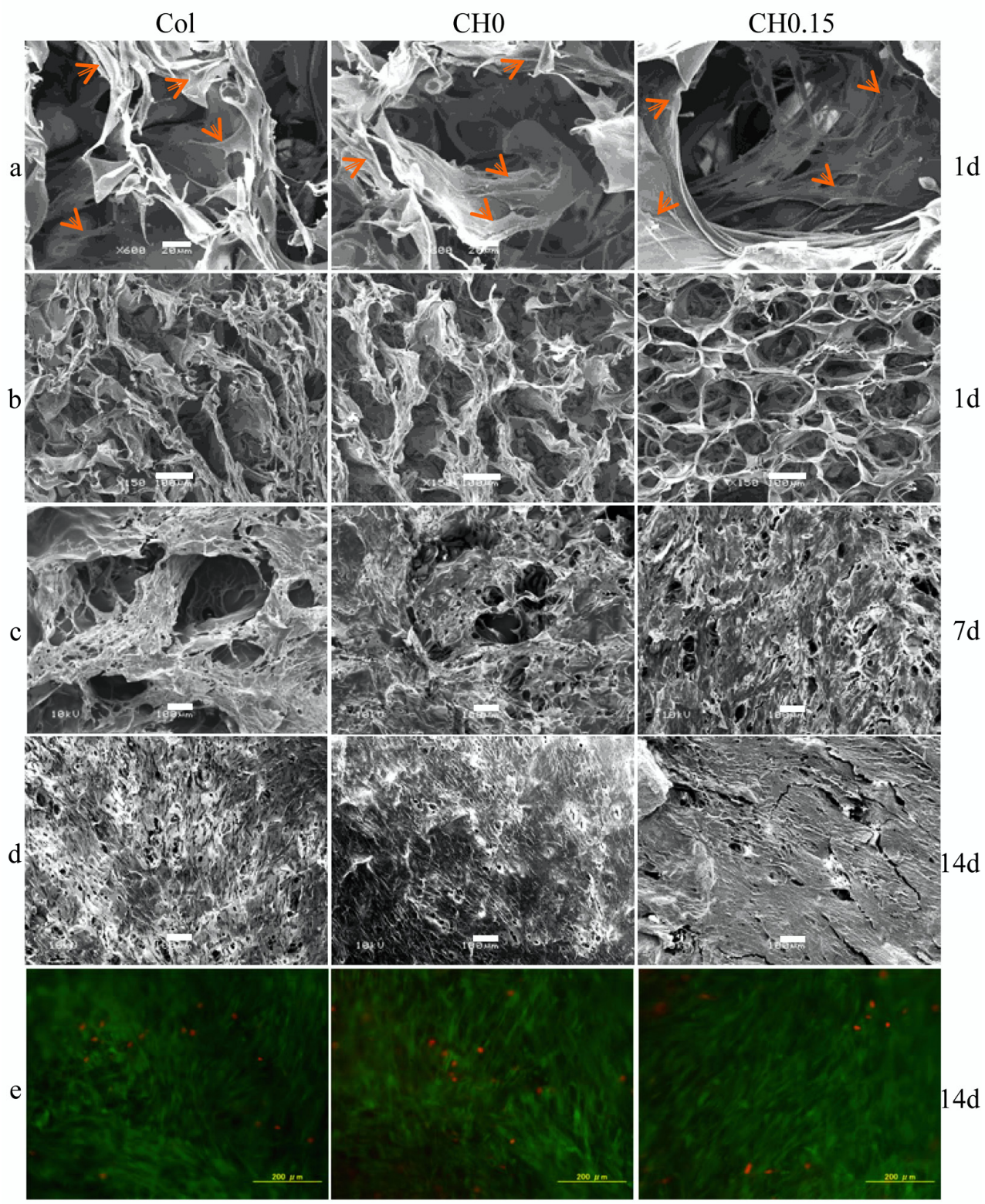

Fig. 2.6. (a) Adhesion of NHDFs in Col, CH0, and CH0.15 scaffolds after culture for 24 hours. Arrows mark some of the fibroblasts adhered on the walls of scaffolds. (b-d) SEM images showing proliferation of NHDFs and production of ECM during the 14 days culture. (e) Live/dead staining of NHDFs in collagen (Col), CH0, and CH0.15 scaffolds after culture for the 14 days. Green: live cells; red: dead cells. Scale bars, a: 20 μm; b-d: 100 μm; e: 200 μm.

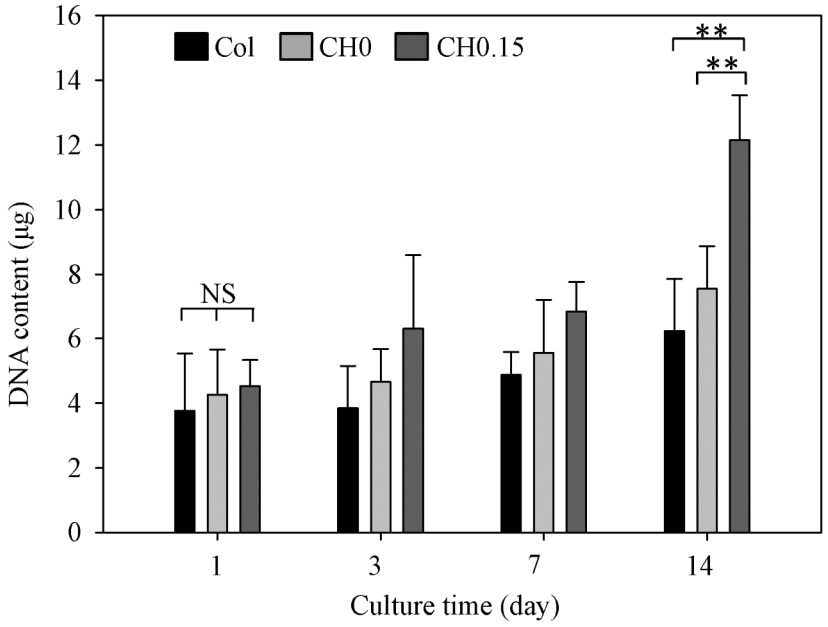

Fig. 2.7. Proliferation of NHDFs in Col, CH0, and CH0.15 scaffolds during the 14 days culture, as determined by DNA quantification. Mean ± SD, N = 4; **, p<0.01; NS, no significant difference.

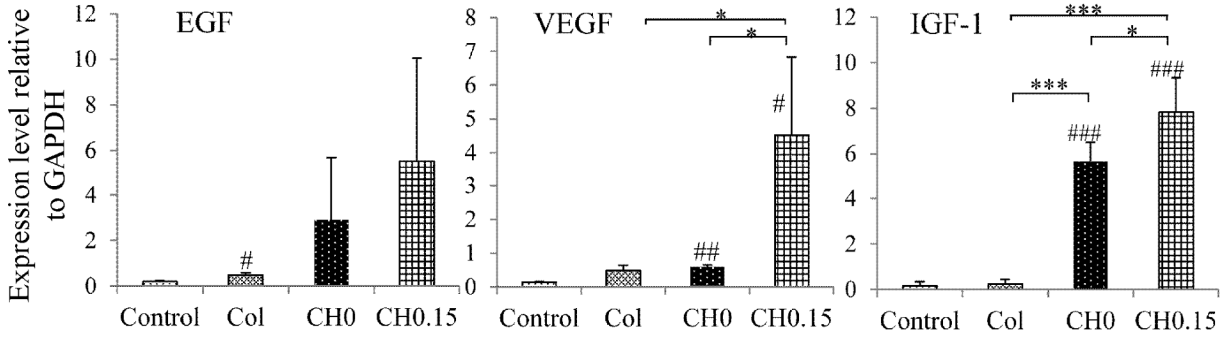

Fig. 2.8. Gene expression levels of NHDFs cultured in Col, CH0, and CH0.15 scaffolds for 14 days; the NHDFs used for cell seeding at day 1 were used as control group. EGF: epidermal growth factor; VEGF: vascular endothelial growth factor; IGF-1: insulin-like growth factor 1. Mean ± SD, N =3; *, p<0.05; ***, p<0.001; #, p<0.05, compared to Control; ##, p<0.01, compared to Control; ###, p<0.001, compared to Control.

The expression of genes encoding EGF, VEGF and IGF-1 was analyzed after 14 days culture (Fig. 2.8). Fibroblasts cultured in the CH0.15 scaffold showed the highest expression of these genes. The cells cultured in the CH0 scaffold showed higher expression level of these genes than did in the Col scaffold. These results indicated that the CH scaffolds promoted cell proliferation and expression of the genes encoding EGF, VEGF and IGF-1. The results were in good agreement with previous reports that show that CH scaffolds have a promotive effect on cell proliferation [11, 26]. Cell proliferation was further promoted and the expression of EGF, VEGF and IGF-1 was upregulated when fibroblasts were cultured in the CH0.15 scaffold. Suppression of PIC formation during the scaffolds preparation could make the homogeneous distribution of HA in collagen matrix and maintain collagen's secondary structure, which therefore stimulated cell proliferation in the porous matrices at the highest level. High expression of EGF, VEGF and IGF-1 should

have some effects on the promotion of cell proliferation because these genes have been reported to be concerned with proliferation of fibroblasts [27-29]. On the other hand, cells may sense the mechanical property of their substrate via the integrin-actin coupling at focal adhesion complexes[30] and adapt their behaviors such as adhesion and proliferation to different scaffold stiffness[31, 32]. Therefore, the high mechanical property of CH0.15 scaffold might also have promoted the proliferation of fibroblast through mechano-transduction pathways.

2.5 Conclusions

The interactions between collagen and hyaluronic acid in suspensions of various ionic strengths were examined with turbidimetry and viscosity measurements. Gross appearance observations and turbidimetry showed that PIC formation between collagen and HA was dependent on the ionic strength of their suspension. Viscosity measurements further confirmed the different states of PIC formed under various ionic strengths. The strong binding affinity of collagen and HA can partially induce a change in collagen's secondary structure, as indicated by infrared analysis. The effects of PIC suppression by low molecular weight salts on the morphology and mechanical properties of CH scaffolds were examined with SEM and compression tests. CH suspensions with no PIC or loose PIC resulted in scaffolds with homogeneous micropore structures and markedly improved compressive moduli, compared with those fabricated from CH suspensions with compact PIC. CH scaffolds prepared with no PIC promoted proliferation of fibroblasts and expression of EGF, VEGF and IGF-1 genes. Using low molecular weight salts to suppress PIC in CG suspensions used to prepare scaffolds should aid in the design of highly active CG scaffolds with homogeneous pore structures and good mechanical properties for tissue engineering.

2.6 References

[1] Corin KA, Gibson LJ. Cell contraction forces in scaffolds with varying pore size and cell density. Biomaterials. 2010;31:4835-45.
[2] Tierney CM, Jaasma MJ, O'Brien FJ. Osteoblast activity on collagen-GAG scaffolds is affected by collagen and GAG concentrations. Journal of Biomedical Materials Research Part A. 2009;91A:92-101.
[3] Callahan LAS, Ganios AM, McBurney DL, Dilisio MF, Weiner SD, Horton WE, Becker ML. ECM Production of Primary Human and Bovine Chondrocytes in Hybrid PEG Hydrogels Containing Type I Collagen and Hyaluronic Acid. Biomacromolecules. 2012;13:1625-31.
[4] Yannas IV, Burke JF. Design of an Artificial Skin .1. Basic Design Principles. Journal of Biomedical Materials Research. 1980;14:65-81.
[5] Louie LK, Yannas IV, Hsu HP, Spector M. Healing of tendon defects implanted with a porous collagen-GAG matrix: Histological evaluation. Tissue Engineering. 1997;3:187-95.
[6] Hsu WC, Spilker MH, Yannas IV, Rubin PAD. Inhibition of conjunctival scarring and contraction by a porous collagen-glycosaminoglycan implant. Investigative Ophthalmology & Visual Science. 2000;41:2404-11.
[7] Farrell E, O'Brien FJ, Doyle P, Fischer J, Yannas I, Harley BA, O'Connell B, Prendergast PJ, Campbell VA. A collagen-glycosaminoglycan scaffold supports adult rat mesenchymal stem cell differentiation along osteogenic and chondrogenic routes. Tissue Engineering. 2006;12:459-68.
[8] Douglas T, Heinemann S, Mietrach C, Hempel U, Bierbaum S, Scharnweber D, Worch H. Interactions of collagen types I and II with chondroitin sulfates A-C and their effect on osteoblast adhesion.

Biomacromolecules. 2007;8:1085-92.
[9] Kanungo BP, Gibson LJ. Density-property relationships in collagen-glycosaminoglycan scaffolds. Acta Biomaterialia. 2010;6:344-53.
[10] Harley BA, Leung JH, Silva ECCM, Gibson LJ. Mechanical characterization of collagen-glycosaminoglycan scaffolds. Acta Biomaterialia. 2007;3:463-74.
[11] Davidenko N, Campbell JJ, Thian ES, Watson CJ, Cameron RE. Collagen-hyaluronic acid scaffolds for adipose tissue engineering. Acta Biomaterialia. 2010;6:3957-68.
[12] Taguchi T, Ikoma T, Tanaka J. An improved method to prepare hyaluronic acid and type II collagen composite matrices. Journal of Biomedical Materials Research. 2002;61:330-6.
[13] Noda I. Two-Dimensional Infrared (2D IR) Spectroscopy: Theory and Applications Applied Spectroscopy. 1990:550-61.
[14] Ozaki Y, Murayama K, Wu Y, Czarnik-Matusewicz B. Two-dimensional infrared correlation spectroscopy studies on secondary structures and hydrogen bondings of side chains of proteins. Spectroscopy-an International Journal. 2003;17:79-100.
[15] Demirdoven N, Cheatum CM, Chung HS, Khalil M, Knoester J, Tokmakoff A. Two-dimensional infrared spectroscopy of antiparallel beta-sheet secondary structure. Journal of the American Chemical Society. 2004;126:7981-90.
[16] Filosa A, Wang Y, Ismail A, English AM. Two-dimensional infrared correlation spectroscopy as a probe of sequential events in the thermal unfolding of cytochromes c. Biochemistry. 2001;40:8256-63.
[17] Xu YS, Mazzawi M, Chen KM, Sun LH, Dubin PL. Protein Purification by Polyelectrolyte Coacervation: Influence of Protein Charge Anisotropy on Selectivity. Biomacromolecules. 2011;12:1512-22.
[18] Kim B, Lam CN, Olsen BD. Nanopatterned Protein Films Directed by Ionic Complexation with Water-Soluble Diblock Copolymers. Macromolecules. 2012;45:4572-80.
[19] Wu ZL, Kurokawa T, Liang SM, Gong JP. Dual Network Formation in Polyelectrolyte Hydrogel via Viscoelastic Phase Separation: Role of Ionic Strength and Polymerization Kinetics. Macromolecules. 2010;43:8202-8.
[20] Henzler K, Wittemann A, Breininger E, Ballauff M, Rosenfeldt S. Adsorption of bovine hemoglobin onto spherical polyelectrolyte brushes monitored by small-angle x-ray scattering and Fourier transform infrared Spectroscopy. Biomacromolecules. 2007;8:3674-81.
[21] Schwinte P, Ball V, Szalontai B, Haikel Y, Voegel JC, Schaaf P. Secondary structure of proteins adsorbed onto or embedded in polyelectrolyte multilayers. Biomacromolecules. 2002;3:1135-43.
[22] Gilde F, Maniti O, Guillot R, Mano JF, Delphine Logeart-Avramoglou D, Sailhan F, Picart C. Secondary Structure of rhBMP-2 in a Protective Biopolymeric Carrier Material. Biomacromolecules. 2012.
[23] Zhou QL, Gong YH, Gao CY. Microstructure and mechanical properties of poly(L-lactide) scaffolds fabricated by gelatin particle leaching method. Journal of Applied Polymer Science. 2005;98:1373-9.
[24] Hollister SJ, Maddox RD, Taboas JM. Optimal design and fabrication of scaffolds to mimic tissue properties and satisfy biological constraints. Biomaterials. 2002;23:4095-103.
[25] Draghi L, Resta S, Pirozzolo MG, Tanzi MC. Microspheres leaching for scaffold porosity control. Journal of Materials Science-Materials in Medicine. 2005;16:1093-7.
[26] Park SN, Lee HJ, Lee KH, Suh H. Biological characterization of EDC-crosslinked collagen-hyaluronic acid matrix in dermal tissue restoration. Biomaterials. 2003;24:1631-41.
[27] Harley BA, Hastings AZ, Yannas IV, Sannino A. Fabricating tubular scaffolds with a radial pore size gradient by a spinning technique. Biomaterials. 2006;27:866-74.
[28] Harley BA, Spilker MH, Wu JW, Asano K, Hsu HP, Spector M, Yannas IV. Optimal degradation rate for collagen chambers used for regeneration of peripheral nerves over long gaps. Cells Tissues Organs. 2004;176:153-65.

[29] Marinucci L, Lilli C, Guerra M, Belcastro S, Becchetti E, Stabellini G, Calvi EM, Locci P. Biocompatibility of collagen membranes crosslinked with glutaraldehyde or diphenylphosphoryl azide: An in vitro study. Journal of Biomedical Materials Research Part A. 2003;67A:504-9.
[30] Ingber DE. Tensegrity: The architectural basis of cellular mechanotransduction. Annual Review of Physiology. 1997;59:575-99.
[31] Haugh MG, Murphy CM, McKiernan RC, Altenbuchner C, O'Brien FJ. Crosslinking and Mechanical Properties Significantly Influence Cell Attachment, Proliferation, and Migration Within Collagen Glycosaminoglycan Scaffolds. Tissue Engineering Part A. 2011;17:1201-8.
[32] Lee CR, Grodzinsky AJ, Spector M. The effects of cross-linking of collagen-glycosaminoglycan scaffolds on compressive stiffness, chondrocyte-mediated contraction, proliferation and biosynthesis. Biomaterials. 2001;22:3145-54.

Chapter 3

Effect of high molecular weight hyaluronic acid on chondrocytes cultured in collagen/hyaluronic acid porous scaffolds

3.1 Summary

Engineering cartilage tissue by culturing chondrocytes in porous scaffolds is one promising method to repair or restore the functions of diseased cartilage. Hyaluronic aid (HA) was used in porous scaffolds or hydrogels to promote the proliferation of chondrocytes and synthesis of cartilage extracellular matrix (ECM). However, whether HA in scaffolds has a beneficial effect on chondrocytes remains uncertain, possibly due to the uncontrolled pore structure and inhomogeneous HA in scaffolds. In this study, homogeneous collagen/HA scaffolds with well-controlled and interconnected pore structure were prepared by suppression of polyion complex formation between collagen and HA and using ice particulates as porogen. The pore structure and mechanical property of collagen/HA scaffolds and collagen scaffolds could be well controlled. High molecular weight HA in collagen/HA scaffolds inhibited the cellular proliferation, synthesis of sulfated glycosaminoglycan and cartilage ECM, compared with the results of collagen scaffolds. This study should provide additional information on the effects of HA in porous scaffolds on the chondrocyte behavior in 3D culture.

3.2 Introduction

Human articular cartilage has limited self-repair because of the avascular nature, low rate of chondrocyte proliferation and matrix turnover [1-3]. Tissue engineering has been developed to engineer cartilage tissue to repair and restore the function of diseased cartilage. In cartilage tissue engineering, chondrocytes from the non-load bearing parts of cartilage are isolated, expanded *in vitro*, seeded in a three-dimensional (3D) scaffolds and cultured to engineer cartilage tissue. 3D porous scaffolds can provide the space for the adhesion and proliferation of chondrocytes and formation of extracellular matrix of cartilage [4-6].

Porous collagen scaffolds have been widely used to engineer various types of tissues such as skin, muscle and cartilage [7-12]. Collagen scaffolds with a high porosity and good interconnectivity are required to enable the homogeneous seeding of chondrocytes in the whole scaffolds and nutrient/oxygen transfer

during cell culture. Porous collagen scaffolds can be prepared by using freeze-drying a collagen aqueous solution and cross-linking treatment. To enable good interconnectivity of collagen scaffolds, ice particulates have been used as porogen which can also initiate ice crystallization during freezing of collagen solution for the formation of interconnected pore structure after freeze-drying [13, 14].

Hyaluronic acid (HA) is abundant in the synovial fluid which functions to lubricate the surface of articular cartilage of joints. HA is also contained in cartilage and low concentrations of HA has important biological effects [15, 16]. HA has been used to maintain the phenotype, promote the proliferation of chondrocytes and synthesis of cartilage ECM. For example, chondrocytes have been cultured in hydrogels that contained HA of different concentrations and the concentration of HA affected the cell proliferation and synthesis of aggrecan or chondroitin sulfate[17, 18]. HA has also been supplemented in culture medium to culture chondrocytes in hydrogels or porous scaffolds, and HA in the medium affected cell proliferation and ECM synthesis in a dose-dependent manner [19, 20]. However, the effects of HA in collagen scaffolds or hydrogels remains controversial. While some studies have shown high molecular weight (MW) HA can promote the proliferation of chondrocytes and the synthesis of sulfated glycosaminoglycan (sGAG), some other studies have shown that high MW HA suppresses the expression of chondrogenesis-related genes such as the genes for collagen type II and aggrecan [21-23]. The inhomogeneous HA in scaffolds due to formation of polyion complex (PIC) between collagen and HA and uncontrolled pore structure from normal freeze-drying might confound the effect of HA on chondrocytes.

In this study, homogeneous collagen/HA scaffolds were prepared to study the effect of high MW HA on the proliferation and ECM synthesis of chondrocytes in 3D culture. Firstly, a homogeneous suspension of collagen/HA was prepared by suppression of PIC formation between collagen and HA. Secondly, the homogeneous collagen/HA suspension was used in combination with ice particulates to prepare collagen/HA scaffolds with well-controlled and interconnected pore structure. Finally, the porous scaffolds were used to culture bovine articular chondrocytes and the cell proliferation, ECM synthesis and tissue formation were examined to study the effect of high MW HA in collagen scaffolds for cartilage tissue engineering.

3.3 Materials and methods

3.3.1 Preparation of porous collagen/HA scaffolds

An aqueous solution (pH = 3.0) of type I collagen (2 wt.%) from porcine skin (Nippon Meat Packers, Inc.) and an aqueous solution of high MW hyaluronic acid (HA) (2 wt.%) from rooster comb (MW, ~ 1×10^6 Da; Wako Pure Industries, Ltd.) were used to prepare aqueous suspensions of collagen/HA mixture. 10 v.% of ethanol was used to dissolve collagen and HA. Before the two solutions were mixed, sodium chloride (NaCl) granules were added separately to the collagen and HA aqueous solutions, and the solutions were gently stirred at 4 °C for 12 h. The collagen and HA aqueous solutions were then mixed at a ratio of 9 : 1 (collagen : HA, v/v) and gently stirred at 4 °C for 24 h. Type I collagen (2 wt.%) solution without NaCl addition was used to prepare collagen scaffolds. The transmittance of the collagen/HA suspensions at 500 nm with different concentrations of NaCl was measured using an UV-Vis spectrophotometer (V-660, JASCO, Inc.).

Collagen/HA scaffolds and collagen scaffolds were prepared by using ice particulates and freeze-drying [11]. Briefly, ice particulates were prepared by spraying pure water into liquid nitrogen and sieving to control their diameter to 150 - 250 μm. Images of the ice particulates were imported into ImageJ software to measure the diameter of ice particulates. Collagen/HA suspension (NaCl concentration: 0.2 M) and collagen

solution were cooled and mixed with pre-prepared ice particulates at the ratio of 1:1 (volume of liquid (ml): weight of ice particulates (g)) at -5 °C. The mixtures were transferred into a silicone mold (60 mm × 40 mm × 5 mm) on a copper plate wrapped with perfluoroalkoxy (PFA) film (Universal Co., Ltd). The mixture in the mold was flattened by covering the silicon frame with a glass plate wrapped with PFA film. The entire construct was frozen at -80 ºC for 9 h. After glass plate and copper plate were removed from the construct, the frozen constructs were freeze-dried under a vacuum of less than 5 Pa for 24 h by using a freeze dryer (FDU-2200, Tokyo Rikakikai Co., Ltd.) to obtain porous scaffolds. The porous scaffolds were crosslinked using a solution of 50 mM 1-ethyl-3-(3-dimethylaminopropyl) carbodiimide (EDC, Peptide Institute, Inc.) and 20 mM N-hydroxysuccinimide (NHS, Wako Pure Chemical Industries, Ltd.) in an ethanol/water mixture (80/20, v/v) for 8 h as reported previously [24]. The crosslinked scaffolds were washed with MilliQ water for six times, soaked in MilliQ water, frozen and freeze-dried again under the same conditions.

3.3.2 Scanning electron microscopy and compression test

Crosslinked scaffolds were cut with a blade and their cross sections were sputter-coated with platinum. The cross sections were observed at 10 kV with a scanning electron microscope (SEM) (JSM-5610, JEOL, Ltd.). SEM images were imported in ImageJ software to measure the pore size of scaffolds. Three images of each type of scaffolds were imported and at least 60 pores per image were measured. For unconfined compression test, crosslinked scaffolds were cut into disks with a diameter of 6 mm and a height of 3 mm using a biopsy punch. Mechanical property of scaffolds in dry state and hydrated state were tested. The dry scaffolds were immersed in phosphate buffered saline (PBS) for 2 hours at room temperature to get hydrated scaffolds. Each sample was placed on the testing platform (Heavy Duty Platform, Stable Micro System) of a texture analyzer (TA.XTPlus, Texture Technologies Corp.) and compressed with a 20-mm diameter cylinder probe (P/20, Stable Micro System). The compression test started with a trigger force of 0.1 g. Samples were compressed at the rate of 0.1 mm/s until reaching 80% strain. Stress and strain values were acquired at the sampling frequency of 50 Hz by using a TA.XTPlus software to generate stress-strain curves. Young's modulus was calculated from the initial linear region of the stress-strain curve and sample dimension. A minimum of four samples were tested for each type of scaffold.

3.3.3 Culture of cells in scaffolds

Bovine articular chondrocytes (BACs) were isolated from the articular cartilage of the knees of 9-week old female calves from a local slaughterhouse as reported previously [11]. Cell culture medium was prepared from high-glucose Dulbecco's Modified Eagle's Medium (D6546, Sigma-Aldrich Co.) supplemented with 10% fetal bovine serum, 4 mM glutamine, 100 U/ml penicillin, 100 μg/ml streptomycin, 0.1 mM nonessential amino acids, 0.4 mM proline, 1 mM sodium pyruvate and 50 μg/ml ascorbic acid. The primary BACs were subcultured in tissue culture flasks with the culture medium. P2 chondrocytes were harvested and suspended in the culture medium to get the suspension of BACs (3.33×10^7 cells/ml) for cell seeding.

Porous scaffolds were punched into disks (6 mm in diameter and 3 mm in thickness), sterilized with 70(v/v)% ethanol aqueous solution, washed with PBS for 6 times and conditioned with culture medium at 37 °C for 2 hours. After the culture medium in the scaffold disks was absorbed away using sterilized Kimwipe paper, 60 μl of the chondrocyte suspension was pipetted onto each scaffold disk and incubated at 37 °C. After 3 hours of incubation, the scaffolds were turned upside down and the medium inside was absorbed away. Another 60 μl chondrocyte suspension was pipetted onto each scaffold disk and incubated at 37 °C for 3 hours and culture medium was added. After 1 day culture, all the cell/scaffold constructs were

transferred to 25-cm^2 tissue culture flasks and cultured in the medium under shaking (60 rpm) for 4 weeks.

3.3.4 Live/dead staining

Live/dead staining was performed to evaluate cell viability using calcein-AM and propidium iodide staining reagents (Cellstain Double Staining Kit, Dojindo Laboratories). After culture for 1 day, 1 week, 2 weeks or 4 weeks, the cell/scaffold constructs were washed with PBS and incubated in PBS-diluted calcein-AM (2 μM) and propidium iodide (4 μM) for 30 minutes. After being rinsed with PBS, the constructs were observed with a fluorescence microscope.

3.3.5 Quantification of DNA and sGAG and compression test of cultured constructs

Proliferation of the chondrocytes in scaffolds was evaluated by quantifying the DNA amount as described previously [24]. Briefly, cell/scaffold constructs cultured for 1 week, 2 weeks, 3 weeks or 4 weeks were harvested, freeze-dried and digested with papain solution. Aliquots of the papain digests were used to measure the DNA and sGAG amount of each sample. The DNA amount was quantified by using Hoechst 33258 dye (Sigma-Aldrich) and an FP-6500 spectrofluorometer (JASCO, Tokyo, Japan). The sGAG content was quantified by using Blyscan™ Glycosaminoglycan Assay (Biocolor Ltd., UK) according to the manufacturer's instructions.

Cell/scaffold constructs cultured for 1 week, 2 weeks or 4 weeks were harvested and kept in culture medium before compression test. The compressive modulus of cell/scaffold constructs was determined by using the compressive test described above. Four samples were used to calculate the average and standard deviation.

3.3.6 Histological staining

Cell/scaffold constructs cultured for 4 weeks were washed in PBS and fixed in 10% neutral buffered formalin for 2 days at room temperature. The constructs were dehydrated in ethanol series, embedded in paraffin and sectioned to get the vertical cross sections of constructs (8-μm thick). The cross sections were deparaffinized and stained with hematoxylin/eosin staining or safranin O/light green staining as described in previous work [11] .

3.3.7 Statistical analysis

Student-t test was used to compare two groups of data. Significant differences were considered when $p < 0.05$.

3.4 Results and discussion

3.4.1 Suppression of PIC

Collagen/HA scaffolds were prepared by suppressing formation of polyion complex (PIC) between collagen and HA and using ice particulates as porogen. Before collagen and HA solutions were mixed, sodium choloride (NaCl) was added into each solution to increase their ionic strength so that the formation of PIC in collagen/HA suspension could be suppressed. Formation of PIC was dependent on the ionic strength of collagen/HA suspensions (Fig. 3.1). Collagen/HA suspension without NaCl treatment was opaque due to the formation of PIC and the inhomogeneous suspension made it difficult to prepare a homogeneous scaffold. Collagen/HA suspensions with a high NaCl concentration (0.20 - 0.30 M) were transparent due to the suppression of PIC formation. Sodium and chloride ions in these suspensions shielded the electronic interaction of oppositely charged collagen and HA molecules and suppressed the formation of PIC. A homogeneous collagen/HA suspension (NaCl concentration = 0.2 M) was chosen to prepare collagen/HA scaffolds. Collagen solution without HA was used to prepare collagen scaffolds as the control group.

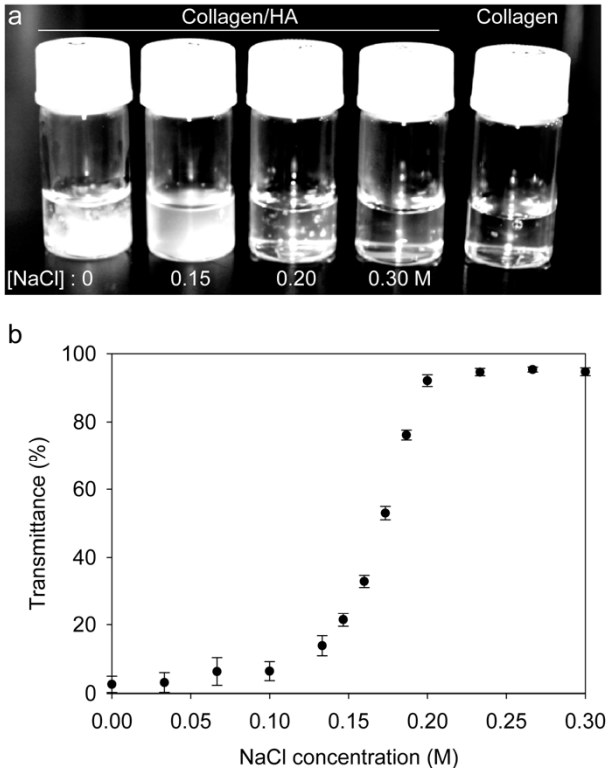

Fig. 3.1. Suppression of polyion complex formation in collagen/HA suspension by adding NaCl. (a) Collagen solution and collagen/HA suspensions with different concentration of NaCl ([NaCl] = 0 - 0.3 M). (b) Transmittance at 500 nm of collagen/HA suspensions with different concentration of NaCl. Means ± SD, N = 3.

3.4.2 Pore structure and mechanical property

Collagen scaffolds and collagen/HA scaffolds had homogeneous, interconnected pore structure which were well controlled by using ice particulates and freeze-drying (Fig. 3.2). The ice particulates used to prepare scaffolds had the diameter of 179 ± 33 μm. The macropores of collagen scaffolds and collagen/HA had the diameter of 172 ± 38 μm and 187 ± 45 μm, respectively, which were controlled by the size of ice particulates (Fig. 3.3 and Fig. 3.4). The macropores were interconnected by the micropores due to the ice crystallization between neighbouring ice particulates [13]. The mechanical property of these scaffolds in dry state or hydrated state was quantified using a compression test. The two types of scaffolds in dry state or hydrated state had similar compressive moduli (Fig. 3.5). The dry scaffolds had higher compressive moduli than hydrated scaffolds. The two types of scaffolds had the same scaffold density (both prepared from 2 wt.% polymer solution). Collagen scaffolds were prepared from 2 wt.% collagen solution and collagen/HA scaffolds were prepared from the solution with 1.8 wt.% collagen and 0.2 wt.% HA. The polymer mass of the solutions used to prepare two types of scaffolds was the same. In addition, the two types of scaffolds had similar pore structure which was controlled by using ice particulates as porogen. The similarity in scaffold density and pore structure might explain the similar compressive modulus of two types of scaffolds. These results showed that the pore structure and mechanical property of two types of scaffolds were controlled by using ice particulates as porogen.

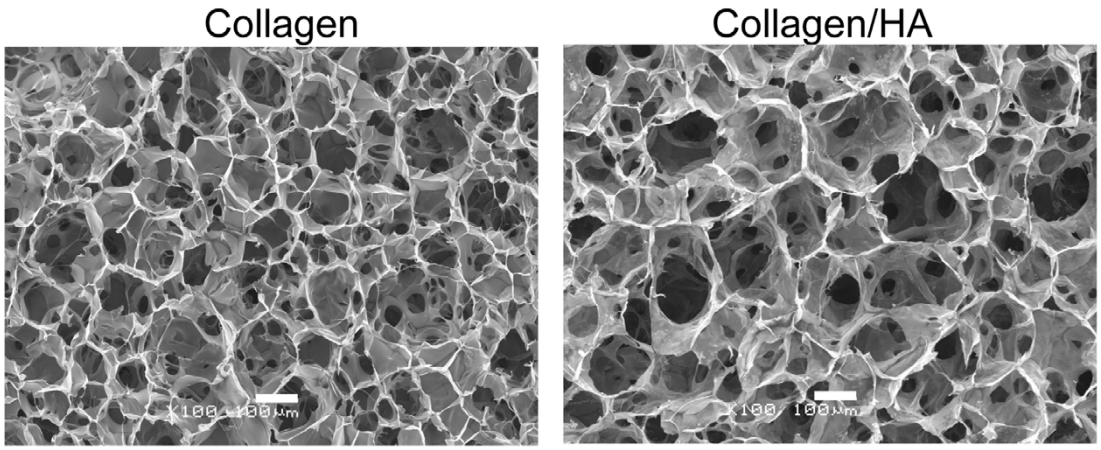

Fig. 3.2. SEM images of cross sections of collagen and collagen/HA scaffolds after crosslinking. Scale bar = 100 μm.

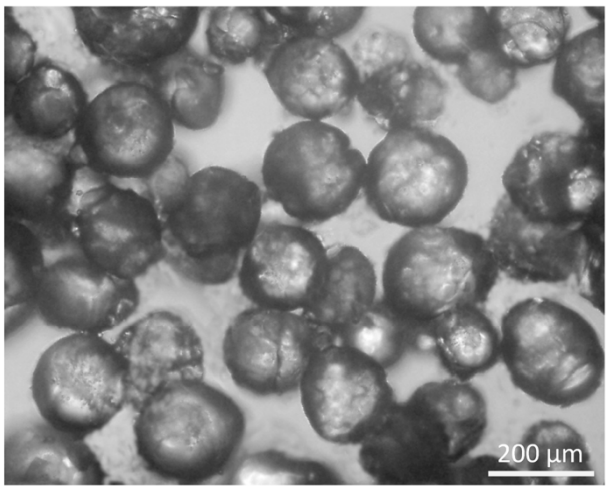

Fig. 3.3. Ice particulates with the diameter of 150-250 μm.

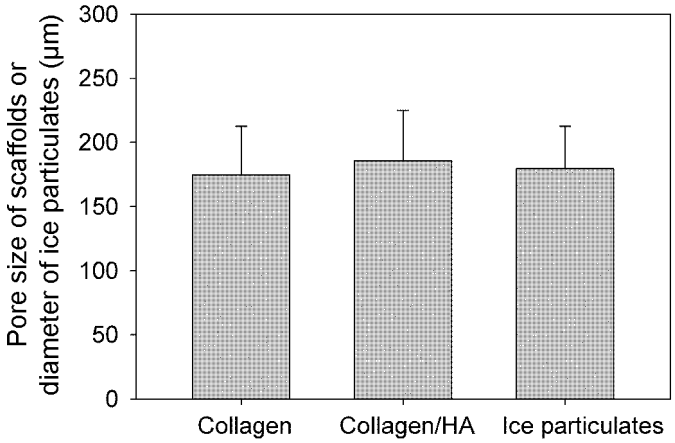

Fig. 3.4. The pore size of collagen scaffolds or collagen/HA scaffolds, and the diameter of ice particulates used for scaffold preparation (μm). Means ± SD, N ≥ 60. There was no significant statistical difference among the data of three groups.

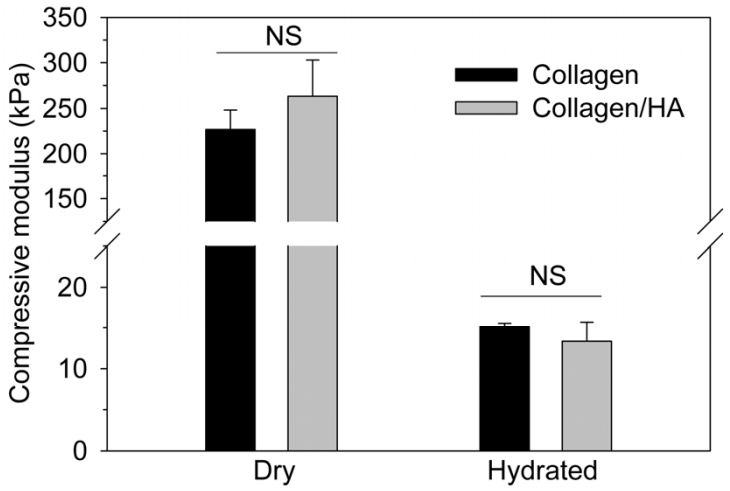

Fig. 3.5. Compressive modulus of crosslinked collagen and collagen/HA scaffolds in dry state or hydrated state. Means ± SD, N = 4. NS, no significant difference.

3.4.3 Cell viability

Bovine articular chondrocytes were seeded in the porous scaffolds to study the effects of high MW HA in porous collagen scaffolds on the functions of chondrocytes. Live/dead staining of the cells cultured in the collagen and collagen/HA porous scaffolds showed that cell proliferated and maintained a high viability during the 4-week culture (Fig. 3.6).

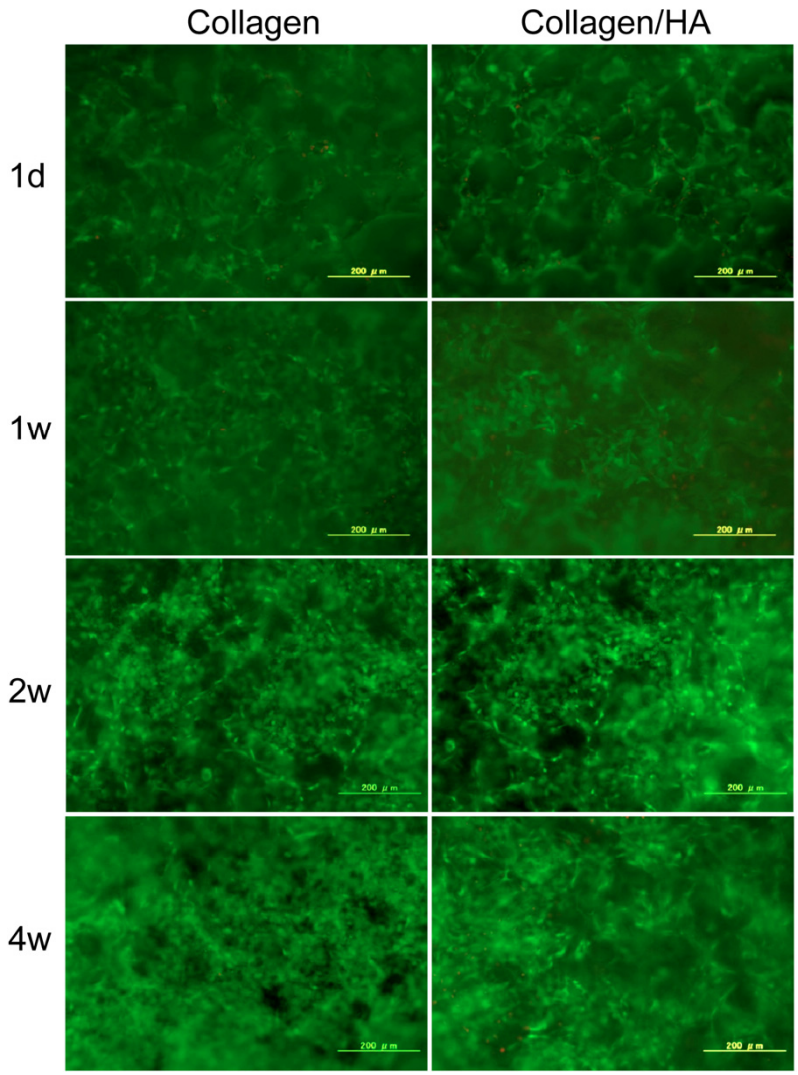

Fig. 3.6. Live/dead staining of chondrocytes cultured in collagen and collagen/HA scaffolds for 1 day (1d), 1 week (1w), 2 weeks (2w) and 4 weeks (4w). Green: live cells; red: dead cells. Scale bar = 200 μm.

3.4.4 Proliferation, sGAG synthesis of cells and mechanical property of tissue

The proliferation of chondrocytes in the porous scaffolds was measured using DNA quantification (Fig. 3.7a). The cells proliferated in the two types of porous scaffolds during the 4-week culture, with a greater proliferation rate in collagen scaffolds than that in collagen/HA scaffolds. The DNA amount in collagen scaffolds was significantly higher than that in collagen/HA scaffolds after 2-week culture. Synthesis of sGAG by chondrocytes in the porous scaffolds were also measured (Fig. 3.7b). The chondrocytes cultured in collagen scaffolds synthesized significantly higher amount of sGAG than those in collagen/HA scaffolds. The compressive modulus of cell/scaffold constructs was measured after cell culture for different time (Fig. 3.7c). The compressive modulus of cell/scaffold constructs increased with culture time. Cell/scaffold constructs from collagen scaffolds had significantly higher compressive modulus than the constructs from collagen/HA scaffolds.

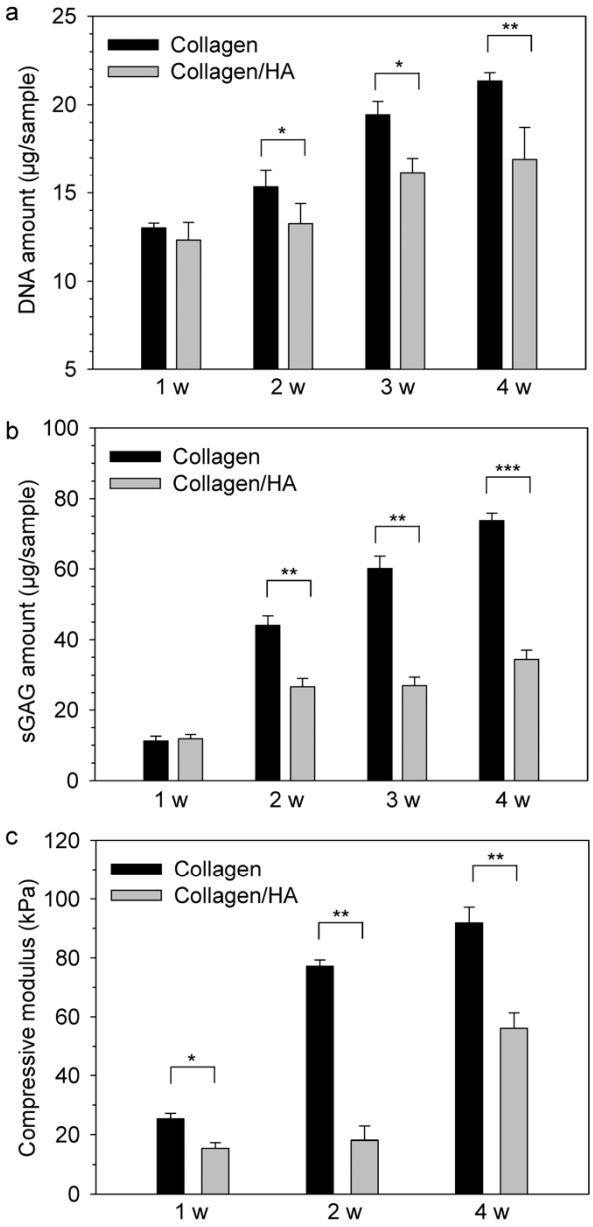

Fig. 3.7. The proliferation, synthesis of sGAG by chondrocytes and the mechanical property of cultured constructs. (a, b) The amount of DNA and sGAG in cell/scaffold constructs cultured for 1 week (1w), 2 weeks (2w), 3 weeks or 4 weeks (4w). (c) The compressive modulus of cell/scaffolds constructs cultured for 1 week, 2 weeks or 4 weeks. Means ± SD, N = 4. *, $p < 0.05$; **, $p < 0.01$; ***, $p < 0.001$.

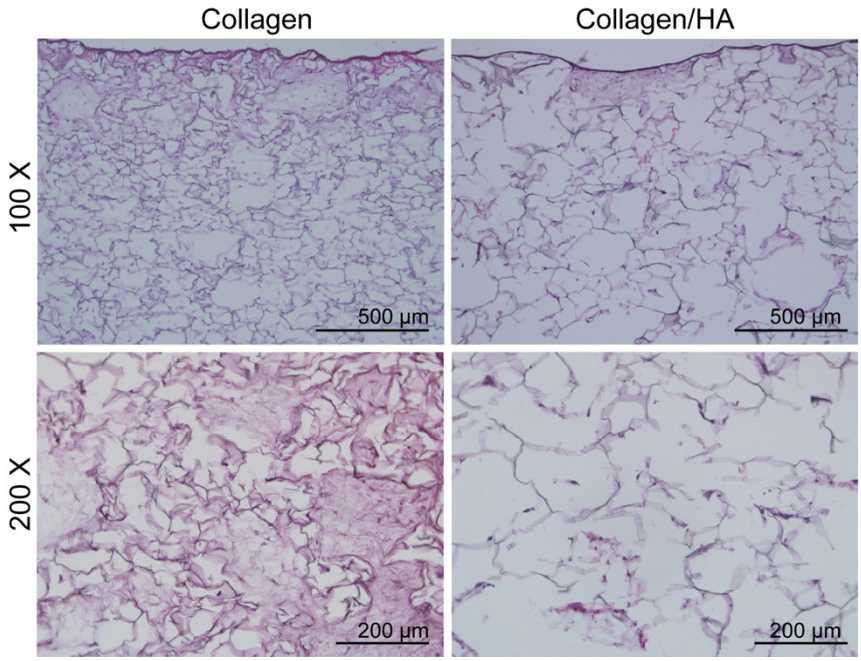

Fig. 3.8. HE staining of cell/scaffolds constructs cultured for 4 weeks *in vitro*. Images were taken at low and high magnifications.

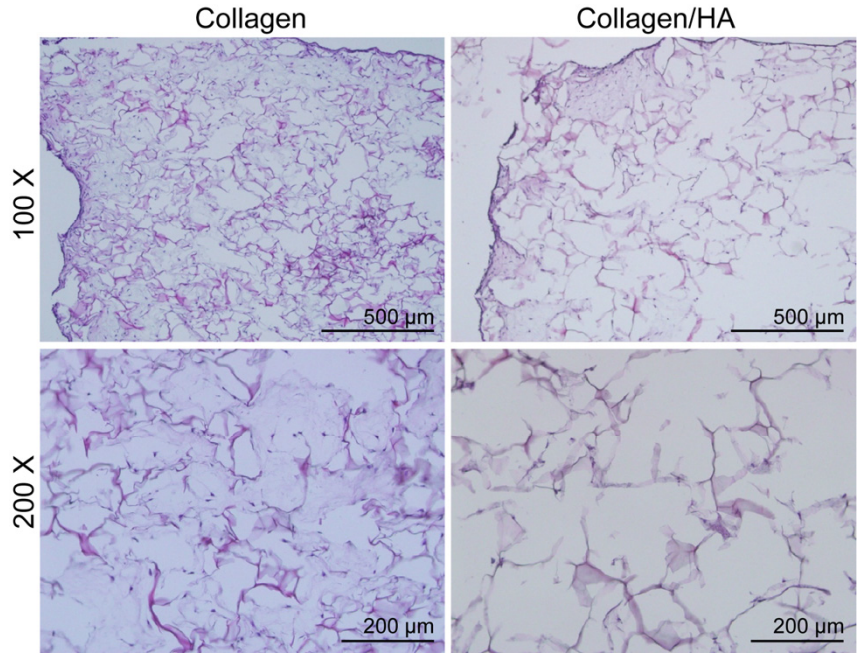

Fig. 3.9. Safranin O staining of cell/scaffolds constructs cultured for 4 weeks *in vitro*. Images were taken at low and high magnifications.

3.4.5 Synthesis of cartilage tissue

The formation of cartilage tissue in cell/scaffold constructs were examined using HE staining and safranin O staining. HE staining of the cell/scaffold constructs cultured for 4 weeks showed that the chondrocytes cultured in collagen scaffolds synthesized ECM that filled the pores of collagen scaffolds (Fig.

3.8). In contrast, the chondrocytes cultured in collagen/HA scaffolds synthesized less ECM, most of which were synthesized in the peripheral region of porous scaffolds. Similarly, the safranin O staining of cell/scaffold constructs from collagen scaffolds showed more intense staining of sGAG compared with those from collagen/HA scaffolds (Fig. 3.9). These results showed that the chondrocytes cultured in collagen scaffolds synthesized more cartilage tissue than those cultured in collagen/HA scaffolds.

Whether addition of high MW HA in hydrogel or porous scaffolds has a beneficial effect on chondrocytes is controversial. For example, when high MW HA was added in the culture medium to culture chondrocytes-seeded gelatin sponge, the DNA amount and sGAG synthesis increased with the concentration of HA [22]. When high MW HA was used to prepare collagen/HA scaffolds or hydrogel for chondrocyte culture, lower amount of HA (2%, 5%) promoted the synthesis of sGAG or mRNA of type II collagen and aggrecan but a greater amount of HA (10%, 14%) inhibited the synthesis of sGAG and cartilage ECM [18, 21]. It was found that increasing amount of HA in collagen/HA scaffolds led to reduction of pore size of porousscaffolds which could impede the migration, proliferation and function of chondrocytes [21]. For high concentrations of HA in hydrogels, HA molecules would overlap with each other forming entanglements and hydrophobic patches. These physical properties of HA were suggested to inhibit the synthesis of cartilage ECM [18]. However, other studies pointed out that HA affected chondrocyte behaviour through its chemical properties rather than its physical properties. For example, Toole et al. found that very low concentrations of HA in culture medium (as low as 1 ng/ml) inhibited chondrogenesis on chondrocytes [16]. Solursh et al. found that not only HA in culture medium inhibited chondrogenesis, the oligosaccharides derived from HA by using hyaluronidase caused more potent inhibition effect [25]. It is noteworthy that the uncontrolled pore structure of porous scaffolds and inhomogeneous distribution of HA in porous scaffolds or hydrogel could confound the effects of HA on the proliferation and ECM synthesis of chondrocytes.

In the present study, homogeneous collagen/HA mixture suspension were prepared by suppression of PIC formation between collagen and HA. In addition, ice particulates were used as porogen to control the pore structure of collagen/HA scaffolds. The effects of high MW HA on chondrocytes were examined using the 3D collagen/HA scaffolds with well-controlled pore structure and homogeneous HA. We hypothesized that these collagen/HA scaffolds wound favour the chondrogenic behaviour of chondrocytes. However, the results showed that high MW HA in the porous scaffolds inhibited the cellular proliferation, synthesis of sGAG and formation of cartilage ECM from chondrocytes. Due to the inhibition of ECM formation within collagen/HA scaffolds, the mechanical property of cultured tissue from collagen/HA scaffolds were significantly lower than those from collagen scaffolds. It was also found that a lower amount of high MW HA (2%, 5%) in collagen/HA scaffolds prepared using ice particulates and suppression of PIC formation also caused inhibition effect on chondrocytes, with a trend of higher amount of HA causing greater inhibition (Fig. 3.10). Our results were in agreement with previous studies that used high MW HA in the medium for two-dimensional culture of chondrocytes [25-28]. Different concentrations of high MW HA (from 1×10^{-4} μg/ml to 100 μg/ml) was applied homogenously into culture medium, which inhibited the sGAG synthesis and accumulation of synthesized proteoglycan in the chondrocyte layer, with higher concentration of HA caused greater inhibition effect. By excluding the interfering factors such as uncontrolled pore structure and PIC formation in porous scaffolds, we also found that the homogenous HA in collagen/HA scaffolds inhibited the chondrogenesis in a similar dose-dependent manner. This inhibition effect from HA were found to be specific to chondrocytes but not to skin fibroblasts [26], which is in agreement of our previous study that showed collagen/HA scaffolds promoted the proliferation of skin fibroblasts [24].

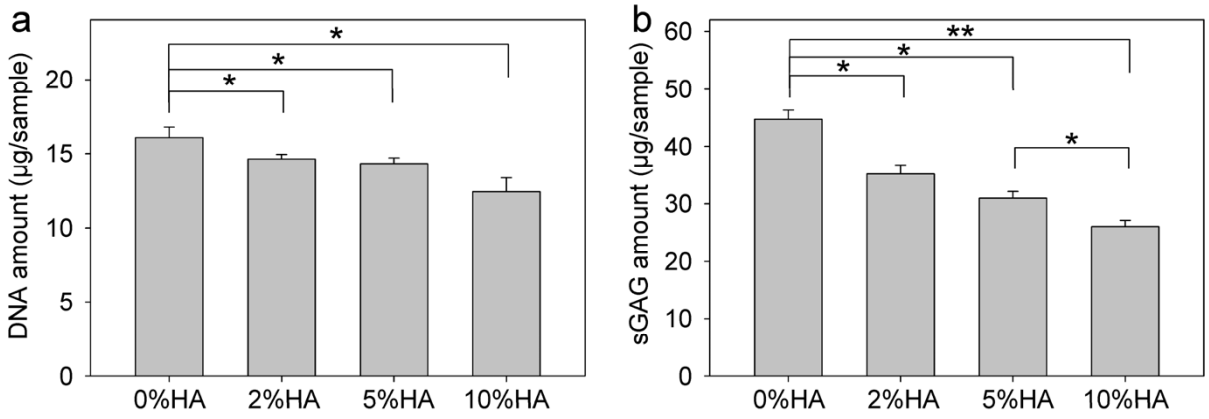

Fig. 3.10. The DNA amount (a) and sGAG amount (b) of cell/scaffold constructs from collagen/HA scaffolds that had different ratios of HA (0%, 2%, 5% or 10%). Bovine articular chondrocytes were cultured on these scaffolds for 2 weeks before the analysis. Means ± SD, N = 4. *, $p < 0.05$; **, $p < 0.01$.

3.5 Conclusions

Collagen/HA scaffolds with well-controlled pore structure and homogenous HA were prepared by using ice particulates as porogen and suppression of polyion complex formation. The homogeneous mixture suspension of collagen and HA were achieved by using NaCl to suppress the formation of polyion complex. The pore structure and mechanical property of collagen and collagen/HA scaffolds could be controlled by using ice particulates. Compared with collagen scaffolds, high MW HA in the porous collagen/HA scaffolds inhibited the proliferation, synthesis of sGAG and formation of cartilage ECM from chondrocytes. This study should provide additional information on the effects of high MW HA in porous scaffolds on the behaviour of chondrocytes in 3D culture.

3.6 References

[1] Hannouche D. Tissue engineering for the repair of cartilage defects. Revue De Chirurgie Orthopedique Et Reparatrice De L Appareil Moteur. 2008;94:S383-S93.
[2] Johnstone B, Alini M, Cucchiarini M, Dodge GR, Eglin D, Guilak F, Madry H, Mata A, Mauck RL, Semino CE, Stoddart MJ. Tissue Engineering for Articular Cartilage Repair - the State of the Art. European Cells & Materials. 2013;25:248-67.
[3] Ochi M, Uchio Y, Tobita M, Kuriwaka M. Current concepts in tissue engineering technique for repair of cartilage defect. Artificial Organs. 2001;25:172-9.
[4] Chen GP, Ushida T, Tateishi T. Development of biodegradable porous scaffolds for tissue engineering. Materials Science & Engineering C-Biomimetic and Supramolecular Systems. 2001;17:63-9.
[5] Chen GP, Ushida T, Tateishi T. Scaffold design for tissue engineering. Macromolecular Bioscience. 2002;2:67-77.
[6] Zhang Q, Lu HX, Kawazoe N, Chen GP. Preparation of collagen porous scaffolds with a gradient pore size structure using ice particulates. Materials Letters. 2013;107:280-3.
[7] Da Silva LFA, Micol L, Tiemenssen D, Oosterwijk E, Van Kuppevelt TH, Geutjes P, Frey P, Feitz W. Tubular collagen-based and collagen-PCL scaffolds with seeded smooth muscle cell for urethra repair in

rabbits. Bju International. 2014;113:101-2.
[8] Kawazoe N, Lin XT, Tateishi T, Chen GP. Three-dimensional Cultures of Rat Pancreatic RIN-5F Cells in Porous PLGA-collagen Hybrid Scaffolds. Journal of Bioactive and Compatible Polymers. 2009;24:25-42.
[9] Nanda HS, Kawazoe N, Zhang Q, Chen SW, Chen GP. Preparation of collagen porous scaffolds with controlled and sustained release of bioactive insulin. Journal of Bioactive and Compatible Polymers. 2014;29:95-109.
[10] Oh HH, Ko YG, Lu HX, Kawazoe N, Chen GP. Preparation of Porous Collagen Scaffolds with Micropatterned Structures. Advanced Materials. 2012;24:4311-6.
[11] Zhang Q, Lu HX, Kawazoe N, Chen GP. Pore size effect of collagen scaffolds on cartilage regeneration. Acta Biomaterialia. 2014;10:2005-13.
[12] Chen S, Nakamoto T, Kawazoe N, Chen G. Engineering multi-layered skeletal muscle tissue by using 3D microgrooved collagen scaffolds. Biomaterials. 2015;73:23-31.
[13] Zhang Q, Lu HX, Kawazoe N, Chen GP. Preparation of collagen scaffolds with controlled pore structures and improved mechanical property for cartilage tissue engineering. Journal of Bioactive and Compatible Polymers. 2013;28:426-38.
[14] Zhang Q, Nakamoto T, Chen SW, Kawazoe N, Lin KL, Chang J, Chen GP. Collagen/Wollastonite Nanowire Hybrid Scaffolds Promoting Osteogenic Differentiation and Angiogenic Factor Expression of Mesenchymal Stem Cells. Journal of Nanoscience and Nanotechnology. 2014;14:3221-7.
[15] Hardingh.Te, Muir H. Binding of Oligosaccharides of Hyaluronic-Acid to Proteglycans. Biochemical Journal. 1973;135:905-8.
[16] Toole BP, Jackson G, Gross J. Hyaluronate in Morphogenesis - Inhibition of Chondrogenesis in-Vitro. Proceedings of the National Academy of Sciences of the United States of America. 1972;69:1384-6.
[17] Akmal M, Singh A, Anand A, Kesani A, Aslam N, Goodship A, Bentley G. The effects of hyaluronic acid on articular chondrocytes. Journal of Bone and Joint Surgery-British Volume. 2005;87B:1143-9.
[18] Liao E, Yaszemski M, Krebsbach P, Hollister S. Tissue-engineered cartilage constructs using composite hyaluronic acid/collagen I hydrogels and designed poly(propylene fumarate) scaffolds. Tissue Engineering. 2007;13:537-50.
[19] Ehlers EM, Behrens P, Wunsch L, Kuhnel W, Russlies M. Effects of hyaluronic acid on the morphology and proliferation of human chondrocytes in primary cell culture. Annals of Anatomy-Anatomischer Anzeiger. 2001;183:13-7.
[20] Kawasaki K, Ochi M, Uchio Y, Adachi N, Matsusaki M. Hyaluronic acid enhances proliferation and chondroitin sulfate synthesis in cultured chondrocytes embedded in collagen gels. Journal of Cellular Physiology. 1999;179:142-8.
[21] Allemann M, Mizuno S, Eid K, Yates KE, Zaleske D, Glowacki J. Effects of hyaluronan on engineered articular cartilage extracellular matrix gene expression in 3-dimensional collagen scaffolds. Journal of Biomedical Materials Research. 2001;55:13-9.
[22] Goodstone NJ, Cartwright A, Ashton B. Effects of high molecular weight hyaluronan on chondrocytes cultured within a resorbable gelatin sponge. Tissue Engineering. 2004;10:621-31.
[23] Nishimoto S, Takagi M, Wakitani S, Nihira T, Yoshida T. Effect of chondroitin sulfate and hyaluronic acid on gene expression in a three-dimensional culture of chondrocytes. Journal of Bioscience and Bioengineering. 2005;100:123-6.
[24] Chen SW, Zhang Q, Nakamoto T, Kawazoe N, Chen GP. Highly active porous scaffolds of collagen and hyaluronic acid prepared by suppression of polyion complex formation. Journal of Materials Chemistry B. 2014;2:5612-9.
[25] Solursh M, Vaerewyck SA, Reiter RS. Depression by Hyaluronic-Acid of Glycosaminoglycan Synthesis by Cultured Chick-Embryo Chondrocytes. Developmental Biology. 1974;41:233-44.

[26] Wiebkin OW, Muir H. The inhibition of sulphate incorporation in isolated adult chondrocytes by hyaluronic acid. FEBS Lett. 1973;37:42-6.
[27] Toole BP. Hyaluronate Inhibition of Chondrogenesis - Antagonism of Thyroxine, Growth-Hormone, and Calcitonin. Science. 1973;180:302-3.
[28] Toole BP. Hyaluronate Turnover during Chondrogenesis in Developing Chick Limb and Axial Skeleton. Developmental Biology. 1972;29:321-9.

Chapter 4

Gelatin scaffolds with controlled pore structure and mechanical property for cartilage tissue engineering

4.1 Summary

Engineering of cartilage tissue *in vitro* using porous scaffolds and chondrocytes provides a promising approach for cartilage repair. However, nonuniform cell distribution and heterogeneous tissue formation together with weak mechanical property of *in vitro* engineered cartilage limit their clinical application. In this study, gelatin porous scaffolds with homogeneous and open pores were prepared using ice particulates and freeze-drying. The scaffolds were used to culture bovine articular chondrocytes to engineer cartilage tissue *in vitro*. The pore structure and mechanical property of gelatin scaffolds could be well controlled by using different ratios of ice particulates to gelatin solution and different concentrations of gelatin. Gelatin scaffolds prepared from ≥70% ice particulates enabled homogeneous seeding of bovine articular chondrocytes throughout the scaffolds and formation of homogeneous cartilage ECM. While soft scaffolds underwent cellular contraction, stiff scaffolds resisted cellular contraction and had significantly higher cell proliferation and synthesis of sulfated glycosaminoglycan. Compared with the gelatin scaffolds prepared without ice particulates, the gelatin scaffolds prepared with ice particulates facilitated formation of homogeneous cartilage tissue with significantly higher compressive modulus. The gelatin scaffolds with highly open-pore structure and good mechanical property can be used to improve *in vitro* tissue-engineered cartilage.

4.2 Introduction

The self-repair of articular cartilage is difficult due to the avascular nature of cartilage tissue, low rate of chondrocyte proliferation and matrix turnover. Tissue engineering of articular cartilage *in vitro* is a promising approach for cartilage repair. Porous scaffolds are used to support cell adhesion and proliferation and to guide formation of cartilage tissue. The engineered tissue can be implanted to repair a cartilage defect. However, *in vitro* engineered cartilage often has thickness limitation,[1-4] heterogeneous cartilage extracellular matrix (ECM) and weak mechanical property which limit their clinical application.[5-8] One of the reasons of the problems is due to the scaffold structure. Heterogeneous structure and closed pores of scaffolds may hinder seeding and delivery of cells into the central parts of scaffolds, which leads to

formation of heterogeneous cartilage ECM, void cores accompanying with the poor mechanical property of engineered cartilage.[5, 9] In addition, cellular contraction of porous scaffolds is common during the engineering of cartilage tissue, which makes it hard to control the final size and shape of engineered tissue.[10-15] Therefore porous scaffolds with homogeneous, interconnected pores for homogeneous tissue formation and good mechanical property to withstand cellular contraction are necessary for successful engineering of cartilage *in vitro*.

Polymer scaffolds prepared from direct freeze-drying of a polymer solution usually have few interconnected pores, which is more obvious when polymer concentration is increased to enhance the mechanical property of scaffolds.[16-18] By using ice particulate templates and freeze-drying, porous scaffolds with controlled open-pore structure and good mechanical property can be prepared.[19, 20] During the freeze-drying process, the ice particulate templates act as porogen to form macropores, while the ice crystallization initiated by the templates can generate open-pore structure by forming micropores interconnecting those macropores.

Gelatin is derived from collagen by hydrolysis and has the chemical composition similar to collagen but lack antigenicity and immunogenicity.[21-25] It has been used to engineer many kinds of tissues such as cartilage, bone and nerve tissues.[26-29] In this study, gelatin porous scaffolds were prepared using ice particulates and freeze-drying and were used to culture bovine articular chondrocytes to engineer cartilage tissue *in vitro*. The pore structure and mechanical property of gelatin scaffolds could be well controlled by using different ratios of ice particulates to gelatin solution and different concentrations of gelatin. Bovine articular chondrocytes could be homogeneously seeded and distributed throughout the gelatin scaffolds, which led to formation of homogeneous cartilage tissue. Cellular contraction, proliferation, synthesis of cartilage ECM and the mechanical property of engineered tissue were analyzed to study the gelatin scaffolds with different properties for cartilage tissue engineering. The gelatin scaffolds with highly open pore structure and controlled mechanical property showed great promise to improve *in vitro* engineered cartilage.

4.3 Materials and methods

4.3.1 Preparation of porous gelatin scaffolds

Gelatin porous scaffolds were prepared with ice particulates and freeze-drying (Fig. 4.1). 30 (v/v)% acetic acid was used as the solvent for gelatin to suppress the gelation of gelatin solutions at low temperature. 2, 4, 6 and 8 (wt/v) % gelatin aqueous solutions were prepared by adding different amount of gelatin granules (porcine derived gelatin, Nitta Gelatin, Inc) into the 30 (v/v)% acetic acid and stirring at 45 ºC for 2 hours and at room temperature for 4 hours. The gelatin solutions were stirred at -5 ºC for 20 minutes for temperature balance.

The ice particulates were prepared by spraying pure water into liquid nitrogen. One sieve with mesh-hole size of 500 μm and another sieve with mesh-hole size of 425 μm were cooled and used to sieve the ice particulates in a low temperature chamber at -15 ºC. The obtained ice particulates with diameters in a range of 425-500 μm were transferred into a cooled glass bottle in the low temperature chamber and kept at -5 ºC for 2 hours for temperature balance before mixing with gelatin aqueous solution. The ice particulates were put into cooled gelatin aqueous solution and mixed at -5 ºC. To control the dimension of scaffolds, a silicone frame mold with an inner open dimension of 36.5 × 66.5 ×5.0 mm was placed on a copper plate wrapped with a perfluoroalkoxy (PFA) film (USL PFA film, Universal Co., Ltd) and was cooled at -5 ºC for 2 hours. The gelatin solution/ice mixtures were poured into the cooled frame mold, firmly packed and

covered with a cooled glass plate wrapped with PFA film. The whole construct was transferred into a -80 ºC freezer and kept there for 12 hours. And then the frozen mixture was detached from the mold and freeze-dried at a vacuum of less than 5 Pa for 48 hours to obtain gelatin porous scaffolds.

Two sets of gelatin scaffolds were prepared. One set of scaffolds was prepared from 4 (wt/v)% gelatin aqueous solution and the mixing ratio of the volume of gelatin solution to the weight of ice particulates at 20/80, 25/75, 30/70, 40/60 and 50/50 (ml/g), which were designated as G20, G25, G30, G40 and G50 scaffolds, respectively. The other set was prepared from 2, 4, 6 and 8 (wt/v)% gelatin solutions and a fixed mixing ratio of the volume of gelatin solution to the weight of ice particulates at 30/70, which were designated as 2%G, 4%G, 6%G and 8%G scaffolds, respectively. Control samples were prepared from 4 (wt/v)% gelatin solution without using ice particulates.

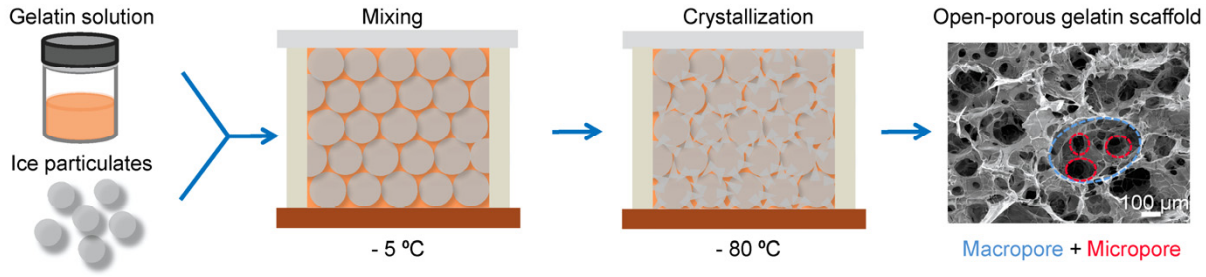

Fig. 4.1. Preparation of open-porous gelatin scaffolds by using ice particulates and freeze-drying.

4.3.2 Crosslinking of gelatin scaffold

Three solvents of decreasing ethanol concentrations (ethanol/water = 95/5, 90/10, or 85/15, v/v) were used to prepare crosslinking solutions that contained 50 mM 1-ethyl-3-(3-dimethylaminopropyl) carbodiimide (EDC, Peptide Institute, Inc.), 20 mM N-hydroxysuccinimide (NHS, Wako Pure Chemical Industries, Ltd.) and 0.1 (wt/v)% 2-(N-morpholino) ethanesulfonic acid (MES).[18] Gelatin scaffolds were crosslinked sequentially in the three crosslinking solutions of decreasing ethanol fraction (from 95/5 to 90/10 to 85/15). Each scaffold was kept in the first crosslinking solution (ethanol/water, 95/5, 30 ml) for 8 hours, followed by the second solution (ethanol/water, 90/10, 30 ml) for 8 hours and the third solution (ethanol/water, 85/15, 30 ml) for another 8 hours. The crosslinked scaffolds were rinsed with MilliQ water for 10 times at room temperature and freeze-dried again at a vacuum of less than 5 Pa for 48 hours to obtain the final scaffolds.

4.3.3 Scanning electron microscopy and compressive test

Crosslinked gelatin scaffolds were cut with a blade and their cross sections were sputter-coated with platinum. The cross sections were observed at 10 kV with a scanning electron microscope (JSM-5610, JEOL, Ltd.). Pore size was analyzed by measuring the diameters of pores (≥40 pores per image) on four SEM images of each type of scaffolds with the ImageJ software(ImageJ2, NIH). For compressive test, the crosslinked gelatin scaffolds were cut into disks (diameter = 6 mm) with a biopsy punch and the disks were cut into 3-mm-thick using two blades spaced 3 mm apart. Some samples were hydrated by degassing the scaffold disks in phosphate buffered saline (PBS) and soaking in PBS for 2 hours. Scaffold disks in dry and

hydrated states were used for the compressive test. The scaffold disks were compressed at a rate of 0.1 mm/s to generate stress-strain curves with a texture analyzer (TA.XTPlus, Texture Technologies Corp.). To study the mechanical isotropy of gelatin scaffolds, the control scaffolds and G30 were cut into cubes (5 × 5 × 5 mm) and compressed in three directions (X, Y and Z axis of samples) using the same machine setting as the above. The Young's modulus was calculated from the initial linear region of the stress-strain curve and sample dimension. Four samples of each type of scaffold were used to calculate the average and standard deviation.

4.3.4 Culture of chondrocytes in scaffolds

Bovine articular chondrocytes were isolated from articular cartilage of the knees of a 9-week old female calf from a local slaughterhouse. Cartilage tissue was minced into 1-2 mm pieces and digested using a 0.2% w/v collagenase type II (Worthington Biochemical, Lakewood, NJ) solution overnight at 37°C under shaking. Isolated chondrocytes were collected and cultured with culture medium in 175-cm^2 tissue culture flasks. The culture medium was prepared from high-glucose Dulbecco's Modified Eagle's Medium (D6546, Sigma-Aldrich Co.) supplemented with 10% fetal bovine serum, 4 mM glutamine, 100 U/ml penicillin, 100 μg/ml streptomycin, 0.1 mM nonessential amino acids, 0.4 mM proline, 1 mM sodium pyruvate and 50 μg/ml ascorbic acid. Culture medium was refreshed every 3 days. The chondrocytes reaching confluence were treated with a trypsin/EDTA solution, harvested and re-plated in 175-cm^2 tissue culture flasks. The chondrocytes reaching confluence were harvested (P2 chondrocytes) and suspended in culture medium to get a cell suspension of 6.67×10^7 cells/ml for cell seeding.

Porous gelatin scaffolds were punched into disks (6 mm in diameter and 3 mm in thickness) as above described, sterilized with 70(v/v)% ethanol aqueous solution, washed with PBS for 6 times and conditioned with culture medium at 37 °C for 2 hours. After absorbing away the culture medium from the scaffold disks using sterilized Kimwipe, 60 μl of the chondrocyte suspension was pipetted onto the scaffold and incubated at 37°C. After 3 hours of incubation, the scaffolds were turned up-side down and the medium inside was absorbed away. Another 60 μl chondrocyte suspension was pipetted onto the scaffold disks and incubated at 37°C for 3 hours. Seeded scaffolds were transferred to new 6-well plates and culture medium was added. The leaked cells in 6-well plates were tripsinized and counted to calculate the efficiency of seeding cells in gelatin scaffolds (seeding efficiency = (1-number of unseeded cells / total number of cells for seeding) × 100%). Four sampes per group were counted for the calculation. After 1 day culture, all the cell/scaffold constructs were transferred to 25-cm^2 tissue culture flasks and cultured in the medium under shaking (60 rpm) for 8 weeks.

4.3.5 Cell distribution in seeded scaffolds

Cell/scaffold constructs cultured for 1 day were washed with PBS and fixed in 10% neutral buffered formalin for 2 days. The constructs were dehydrated, embedded in paraffin and sectioned to get the vertical cross sections of constructs (8 μm thick). Cell nuclei in the sections were stained with 2 μg/ml 4',6-diamidino-2-phenylindole, dihydrochloride (DAPI, Dojindo Molecular Technologies, Inc.) and observed under a fluorescence microscope (Olympus, Tokyo, Japan). The images of nuclei staining were imported into ImageJ software to analyze the integrated fluorescence intensities of three regions of interest (ROI: 500 × 1000 μm rectangle), the upper zone, the center and the lower zone of cross section.[30] The integrated intensity of each ROI was divided by the area of ROI to obtain the average intensity. The average intensity of each ROI was subtracted from the average intensity of background (Fig. S1). Four images of each kind of

scaffold were used for the analysis.

4.3.6 Biochemical quantification and compressive test of engineered constructs

Proliferation of the chondrocytes in scaffolds was evaluated by quantifying the DNA amount as described previously.[18] Briefly, cell/scaffold constructs cultured for 8 weeks were harvested, freeze-dried and digested with papain solution. An aliquot of the papain digests was used to measure the DNA content with Hoechst 33258 dye (Sigma-Aldrich) and an FP-6500 spectrofluorometer (JASCO, Tokyo, Japan). Sulfated glycosaminoglycan (sGAG) content was analyzed using Blyscan™ Glycosaminoglycan Assay (Biocolor Ltd., UK) from the above papain digests according to the manufacturer's instructions. The compressive modulus of cell/scaffold constructs after 8 weeks culture was determined by using the compressive test described above. Four samples were used to calculate the average and standard deviation.

4.3.7 Histological and immunological staining

Cell/scaffold constructs cultured for 8 weeks were washed with PBS and fixed in 10% neutral buffered formalin for 2 days at room temperature. The constructs were dehydrated, embedded in paraffin and sectioned to get the vertical cross sections of constructs (8 μm thick). The cross sections were deparaffinized and stained with Safranin O and light green staining. The cross sections were also immunologically stained for type II collagen. Briefly, the deparaffinized sections were incubated with proteinase K for 10 minutes for antigen retrieval and incubated with peroxidase blocking solution for 5 minutes and 10% goat serum solution for 30 minutes. And then the sections were incubated with rabbit polyclonal anti-collagen type II (in a 1:100 working dilution) (Thermo Scientific, Rockford, IL) for 1 hour, followed by incubation with the peroxidase-labeled polymer-conjugated second antibody (EnVision+ System-HRP (DAB), Dako, CA) for 30 minutes. The sections were then incubated with 3,3'-diaminobenzidine (DAB) for 5 minutes to develop color. All procedures were performed at room temperature. Stained tissue sections were observed under a light microscope.

4.3.8 Real-time PCR

The expression of genes for cartilage ECM by chondrocytes in the cell/scaffold constructs ($n = 3$) was analyzed using real-time polymerase chain reaction (real-time PCR). After culture for 8 weeks, each cell/scaffold construct was rinsed with PBS buffer, immersed in 1 ml Sepasol-RNA I Super G solution (Nacalai Tesque, Inc.) and frozen at -80 °C. The frozen constructs were crushed into powder by an electric crusher and transferred back into the Sepasol solution to isolate the RNA from the cells. The RNA was converted to cDNA by MuLV reverse transcriptase (Applied Biosystems, USA). Real-time PCR was used to amplify hypoxanthine guanine phosphoribosyl transferase 1 (Hprt1), glyceraldehyde-3-phosphate dehydrogenase (Gapdh), type I collagen (Col1a2), type II collagen (Col2a1) and aggrecan (Acan). The reactions were performed with 0.2 μl cDNA, 18 mM forward / reverse primers, 5 mM PCR probe and qPCR Master Mix (Eurogentec, Seraing, Belgium) in duplicate. The reactions were run for 40 cycles using a 7500 Real-Time PCR System (Applied Belgium). The expression levels of Hprt1 were used as endogenous controls and the gene expression levels relative to Gapdh were calculated using a comparative Ct method.[31] The primer and probe sequences were as follows: Hprt1: forward primer 5′-TGGCGTCCCAGTGAAATCA-3′, reverse primer, 5′-AGCAGCTGGCCACAGAACA-3′, probe,

5′-CAGTGACATGATCCAATG-3′; Gapdh, forward primer, 5′-GCATCGTGGAGGGACTTATGA -3′, reverse primer, 5′-GGGCCATCCACAGTCTTCTG-3′, probe, 5′-CACTGTCCACGCC ATCACTGCCA-3′; Col1a2, forward primer, 5′-TGGCAAAGACGGTCG CAT-3′, reverse primer, 5′-CCTTGGGTCTGAGAGAAGTTGGT-3′, probe, 5′-GTAACCACCAC CACTTG-3′;[32] Col2a1, forward primer, 5′-AAGAAACACATCTGGTTTGGAGAAA-3′, reverse primer, 5′-TGGGAGCCAGGTTGTCATC-3′, probe, 5′-CAACGGTGGCTTCCACTTCAGCTATG G-3′ [32]; Acan, forward primer, 5′-CCAACGAAACCTATGACGTGTACT-3′, reverse primer, 5′-GCACTCGTTGGCTGCCTC-3′, probe, 5′-ATGTTGCATAGAAGACCTCGCCCTCCAT-3′ [32].

4.3.9 Statistical analysis

One-way analysis of variance (ANOVA) was used to evaluate the experimental values of the groups of scaffolds prepared using different fractions of ice particulates or of the groups of scaffolds prepared using different concentrations of gelatin. Student-t test was used to compare two groups of data. Statistical differences were considered significant if $p<0.05$.

4.4 Results

4.4.1 Pore structure of gelatin scaffolds

Porous gelatin scaffolds prepared using different ratios of ice particulates (G20, G25, G30, G40 and G50) and different concentrations of gelatin aqueous solution (2%G, 4%G, 6%G and 8%G) are shown in Fig. 4.2a. The scaffolds prepared with ice particulates had round macropores that mirrored the ice particulates used as porogen. The scaffolds prepared with ≥70% ice particulates (G20, G25, G30, 2%G, 4%G, 6%G and 8%G) had open-pore structure with the macropores interconnected by micropores on their walls. Compared with these scaffolds, the scaffolds prepared with low ratio of ice particulates (G40 and G50) had sparse, less interconnected macropores and thick walls. Analysis of scaffold pore size (Table 4.1) showed that the size of macropores of these scaffolds was all similar to that of ice particulates while the size of micropores decreased with the decrease of ice particulate ratio (G20>G25>G30>G40>G50) and the increase of gelatin concentration (2%G>4%G>6%G>8%G). The control group, however, had heterogeneous structure with lamellar walls of different directions and the pores were less interconnected due these closed lamellar walls.

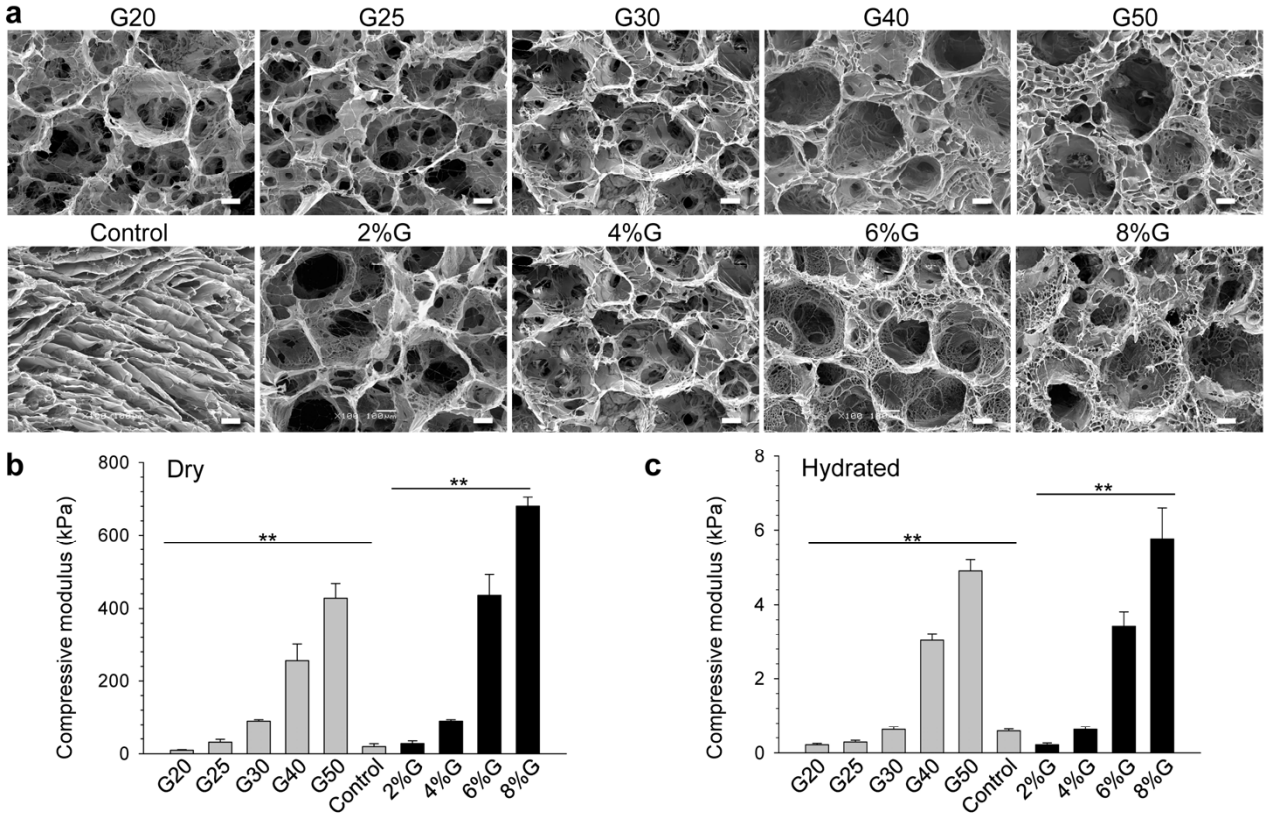

Fig. 4.2. Pore structure and mechanical property of crosslinked gelatin scaffolds. a, SEM images of the cross sections of gelatin porous scaffolds. G20, G25, G30, G40 and G50 represent scaffolds which were prepared with 4 (wt/v)% gelatin aqueous solution and the mixing ratio of the volume of gelatin solution to the weight of ice particulates at 20/80, 25/75, 30/70, 40/60 and 50/50, respectively. 2%G, 4%G, 6%G and 8%G represent scaffolds which were prepared with a fixed mixing ratio at 30/70 and gelatin concentration of 2, 4, 6 and 8 (wt/v)%, respectively. The control group was prepared with 4 (wt/v)% gelatin aqueous solution without ice particulates. Scale bar = 100 μm. Compressive modulus of dry (b) or hydrated (c) gelatin scaffolds. High ratio of gelatin solution or high concentration of gelatin could significantly increase the compressive modulus of the scaffolds (**, $p<0.001$ by ANOVA). Data represent mean ± SD (n=4).

Table 4.1. Pore size (macropores and micropores) of the gelatin scaffolds. Data represent mean ±SD.

Samples	G20	G25	G30	G40	G50
Macropores (μm)	462±65	478±49	453±75	464±68	460±63
Micropores (μm)	155±66	120±48	102±34	60±45	47±28
Samples	Control	2%G	4%G	6%G	8%G
Macropores (μm)	334±256	484±65	453±75	463±43	475±56
Micropores (μm)	-	173±87	102±34	62±36	58±46

4.4.2 Mechanical property of gelatin scaffolds

The compressive modulus of gelatin scaffolds were measured in both dry state and wet state (Fig. 4.2b, c). The compressive modulus of gelatin scaffolds increased with the ratio of gelatin solution and the concentration of gelatin used in scaffold preparation, both in the dry state and the wet state. Using high ratio of gelatin solution and high concentration of gelatin could significantly increase the compressive modulus of gelatin scaffolds (ANOVA, $p<0.001$). The compressive modulus of control gelatin scaffold measured in different directions of compression showed a great variation (Table 4.2). However, a typical gelatin scaffold prepared using ice particulates (G30) had similar compressive modulus measured in different directions of compression.

Table 4.2. Compressive modulus (kPa) of control scaffolds and G30 scaffolds measured using different directions of compression (X, Y or Z). Data represent mean ± SD (n=4).

Direction of compression	X-axis	Y-axis	Z-axis
Control	76.2±22.4	87.9±24.0	27.0±8.4
G30	89.8±3.8	87.6±3.6	92.0±8.1

4.4.3 Cell distribution in scaffolds

To visualize the distribution of chondrocytes in scaffolds, bovine chondrocytes were seeded into gelatin scaffolds and the cell/scaffold constructs after 1-day culture were fixed, sectioned and stained with DAPI (Fig. 4.3). For scaffolds prepared using ≥70% ice particulates (G20, G25, G30, 2%G, 4%G, 6%G and 8%G), chondrocytes could be seeded homogeneously throughout the whole scaffold. For scaffolds prepared using less ice particulates (G40 and G50), chondrocytes merely penetrated into the peripheral region of the scaffolds, leaving a central core with less cells. For the control scaffolds, chondrocytes were densely deposited on the surface of the scaffolds and few chondrocytes penetrated into the inner region. The gelatin scaffolds prepared with ice particulates had high seeding efficiency due to their interconnected pore structures compared to the control scaffolds (Table 4.3).

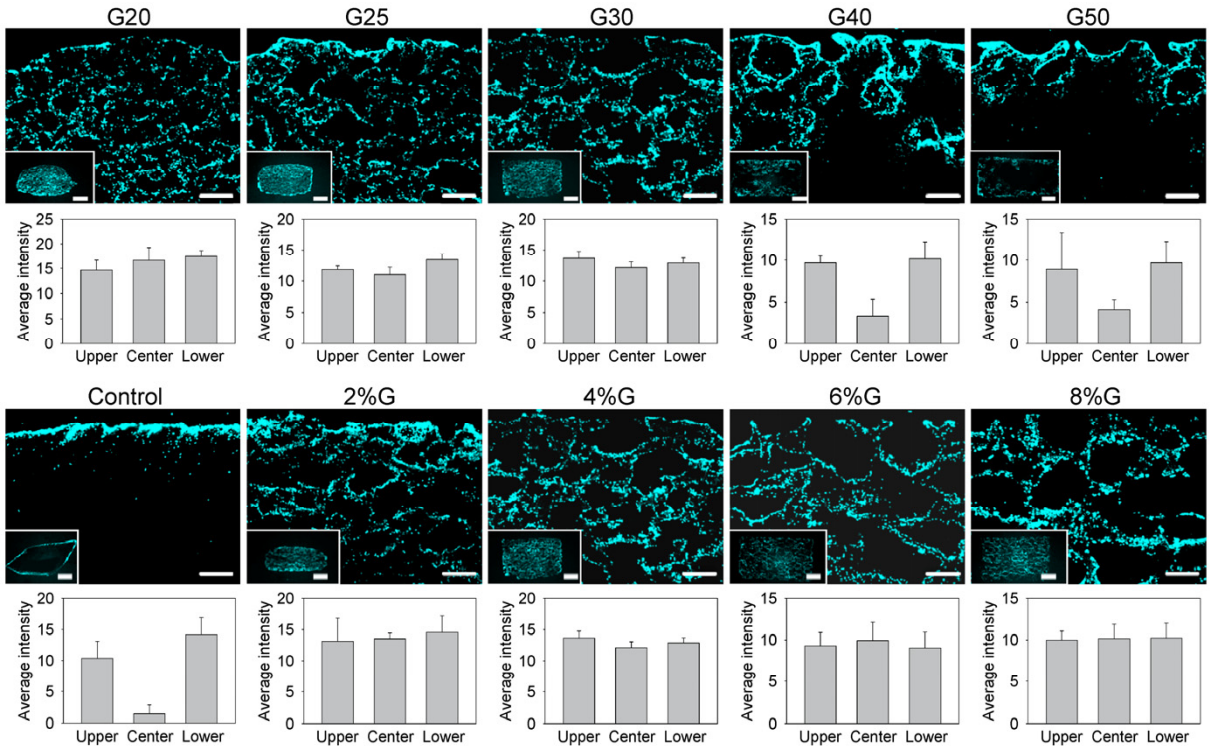

Fig. 4.3. Cell distribution in the getatin scaffolds after 1-day culture. Cell nuclei were stained by DAPI. The inserted images are the whole cross sections of scaffolds. Scale bars: 200 μm for high-magnification images; 1 mm for inserted images. The intensity of nuclei staining in three regions of interest (the upper, center and the lower zone of cross section) were analyzed.

Table 4.3. The efficiency of seeding chondrocytes (seeding efficiency) in gelatin scaffolds. Data represent mean ±SD.

Samples	G20	G25	G30	G40	G50
Seeding efficiency (%)	94.5±4.9	95.9±3.0	96.6±3.1	97.0±3.0	98.3±1.2
Samples	Control	2%G	4%G	6%G	8%G
Seeding efficiency (%)	68.3±5.2	93.8±4.7	96.6±3.1	97.8±2.1	98.5±1.2

4.4.4 Cellular contraction of scaffolds

Gelatin scaffolds underwent cellular contraction during the 8-week *in vitro* culture. After 8 weeks, all the cell/scaffold constructs except the control group remained the round-disk shape (Fig. 4.4a). The mechanical strength of these scaffolds affected the final diameter of the cell/scaffold constructs (Fig.4.4b). Soft scaffolds prepared using high fraction of ice particulates (G20) or low concentration of gelatin (2%G) exhibited the most contraction. Stiff scaffolds such as G50 and 6%G had much less contraction and the 8%G scaffolds kept their original size. The control samples contracted into irregular-shaped blocks although their diameters remained larger than the soft scaffolds prepared using ice particulates.

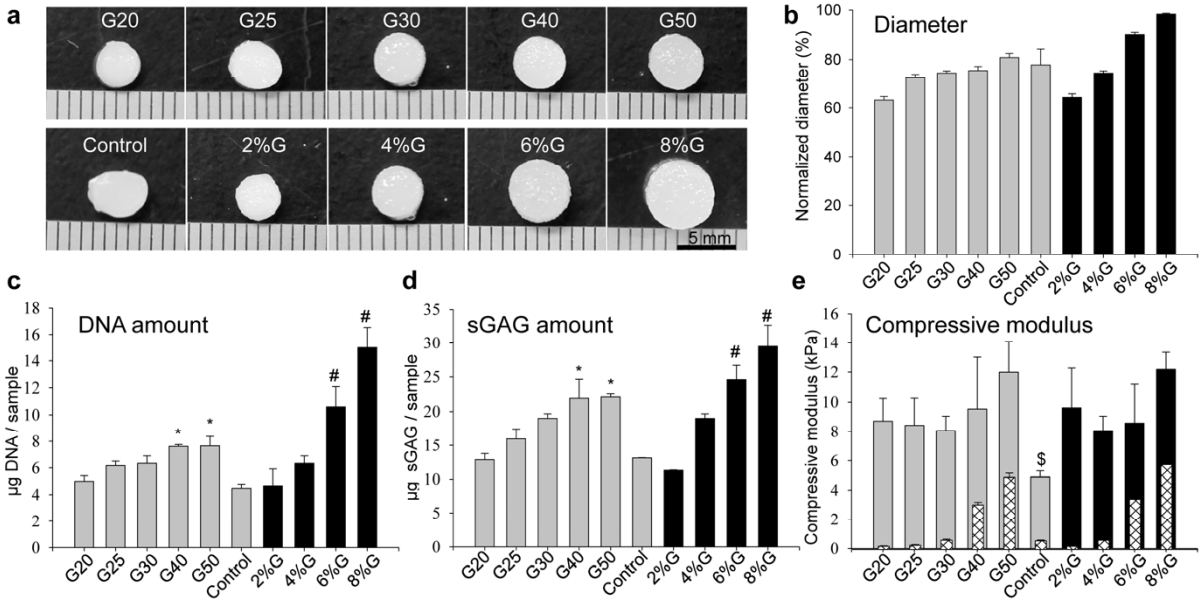

Fig. 4.4. Gross appearance (a) and diameter (b) of the cell/scaffold constructs after 8-week culture. The diameter was normalized to the initial diameter of scaffold disks. Data represent mean ± SD (n=4). Quantification of DNA amount (c) and sGAG amount (d) in the cell/scaffold constructs after 8-week culture. Compressive modulus of the cell/scaffold constructs after 8-week culture (e). The inserted narrow columns represent the compressive modulus of hydrated scaffolds before cell culture. *, $p<0.05$ compared with G20, G25, G30 and Control; #, $p<0.05$ compared with 2%G and 4%G; $, $p<0.05$ compared with all other groups. Data represent mean ± SD (n=4).

4.4.5 DNA, sGAG quantification and mechanical property of engineered tissue

After 8-week culture, the DNA content in stiff scaffolds was significantly higher than that in soft scaffolds and the 8%G group had 3.1 fold higher DNA content than the 2%G group (Fig. 4.4c). The synthesis of sGAG by chondrocytes in scaffolds showed the similar pattern as that of DNA content. More sGAG was produced in stiff scaffolds (Fig. 4.4d). Compressive modulus of cartilage tissue engineered from 8% scaffolds and G50 scaffolds had higher values compared with those from other scaffold groups. After cell culture all the scaffolds prepared with ice particulates showed significantly higher compressive modulus than the control gelatin scaffolds ($p<0.05$) (Fig. 4.4e).

4.4.6 Histological stainig of cartilage tissue

The formation of cartilage ECM (sGAG and type II collagen) was examined using Safranin O staining and type II collagen immunostaining (Fig. 4.5). Cartilage tissue engineered from scaffolds prepared using ≥70% ice particulates (G20, G25, G30, 2%G, 4%G, 6%G and 8%G) had homogeneous staining of sGAG and type II collagen. Cartilage tissue engineered from scaffolds prepared with less ratio of ice particulates (G40 and G50) had intense staining of sGAG and type II collagen at the periphery region of scaffolds. For the control scaffold prepared without ice particulates, however, synthesis of cartilage ECM was mainly observed on the surface of scaffolds.

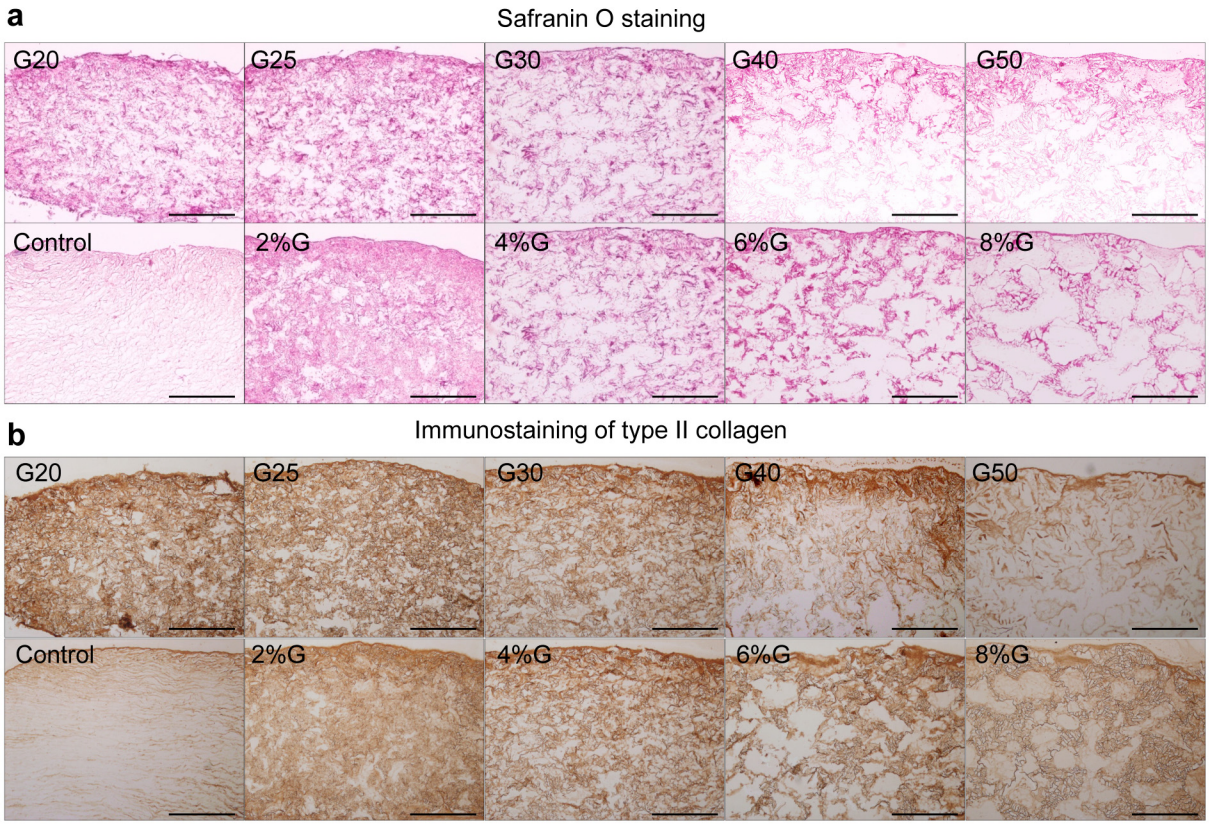

Fig. 4.5. Safranin O staining (a) and immunostaining of type II collagen (b) of the cell/scaffold constructs after 8-week culture. Scale bar = 500 μm.

4.4.7 Gene expression of cell/scaffold constructs

Cell/scaffold constructs cultured for 8 weeks were harvested for analysis of gene expression (Fig. 4.6). The expression levels of type I collagen in all scaffolds were similar except that in the G50 and control groups which was significantly higher compared with other groups. Chondrocytes in the G20, G25 and 2%G scaffolds had higher expression levels of type II collagen compared to those in other scaffold groups. The expression level of aggrecan by chondrocytes in all scaffold groups did not show a significant difference.

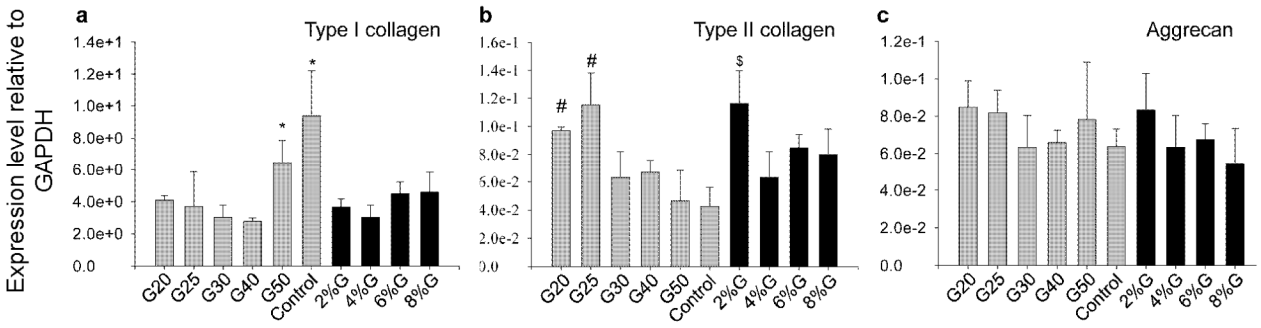

Fig. 4.6. Expression level of genes encoding type I collagen (a), type II collagen (b) and aggrecan (c) in cell/scaffold constructs after 8-week culture. *, $p<0.05$ compared with G20, G25, G30 and G40; #, $p<0.05$ compared with G30, G40, G50 and Control; $, $p<0.05$ compared with 4%G, 6%G and 8%G. Data represent mean ± SD (n=3).

4.5 Discussion

Gelatin scaffolds with open-pore structure and good mechanical property could be prepared by using ice particulates as a porogen material. Gelatin solutions were cooled at low temperature, mixed with ice particulates and freeze-dried. Freeze-drying of the gelatin solution/ice particulates mixture resulted in formation of open porous gelatin scaffolds having macropores which mirrored the ice particulate templates and micropores which mirrored the ice crystals formed during freezing process. The ratio of ice particulates higher than 70% enabled formation of well-interconnected macropores. The mechanical property of gelatin scaffolds could be improved by using high ratio of gelatin solution and high concentration of gelatin, as high amount of gelatin could form dense matrix surrounding the macropores to strengthen the scaffolds.[17, 33] Without using ice particulates, control scaffolds had heterogeneous porous structure and different compressive modulus in different directions of compressiom, showing the heterogeneity of mechanical property.

The open-pore structure of gelatin scaffolds prepared by using high ratio of ice particulates (≥70%) facilitated even cell seeding and formation of homogeneous cartilage ECM throughout the scaffolds. The pores of these scaffolds were well interconnected, which allowed penetration of chondrocytes into the full thickness of scaffolds after cell seeding and synthesis of homogeneous cartilage tissue during cell culture. Scaffolds prepared by using low ratio of ice particulates (G40 and G50) had less interconnected pore structure and therefore cells were predominantly distributed at the peripheral region of the scaffolds to form dense ECM layers at the peripehral region. Chondrocytes seeded in control scaffolds mainly adhered and synthesized ECM on scaffold surface due to the heterogeneous and less interconnected pore structure.

Chondrocytes in stiff scaffolds (G40, G50, 6%G and 8%G) had a significantly greater rate of proliferation compared with those in soft scaffolds. While soft scaffolds contracted significantly during cell culture which might limit cell proliferation,[34] stiff scaffolds could resist cellular contraction, retain their pore structure and keep pore space that could facilitate cell proliferation. It has been reported that chondrocytes react to their substrate of different stiffness and change their behaviors such as cell spreading and mitosis.[34-36] Focal adhesions of cells link the ECM with the intracellular cytoskeleton, which can transduce the force between the ECM and cytoskeleton into biochemical signals to affect cell behaviors. Stiff ECM microenvironment has been reported to activate the focal adhesion kinase, which can activate pathways to promote cell proliferation.[37, 38] Therefore the stiffness of gelatin scaffolds might have affected the cell proliferation through mechano-transductive pathways. Other factors such as the permeability of different scaffolds might also affect cell proliferation through different diffusivity of nutrients in different cell/scaffold constructs. However, these parameters were not quantified because they could change with cellular contraction and accumulation of ECM in scaffolds during cell culture. In addition, the aggrecan expression level of chondrocytes cultured in different scaffolds were similar (Fig.6c). Therefore, the stiff scaffolds which had greater number of cells should have higher production of sGAG.

Chondrocytes cultured in G50 and control scaffolds had higher expression of type I collagen. G40 and G50 were prepared from smaller ratios of ice particulates, which caused some non-interconnected pores in the scaffolds. Less cell infiltration in G40 and G50 scaffolds caused that some cells grew on the surface of scaffolds. Cells growing on the surface were similar to the 2D culture condition, which was unsuitable to maintain the chondrogenic phenotype of chondrocytes.[39] This might explain the higher expression of type I collagen by chondrocytes cultured in G50 and control scaffolds on which many cells grew on the scaffold surface.

Improved mechanical property and open-pore structure of scaffolds inhibited cellular contraction, enabled greater cell proliferation and formation of homnogeneous cartilage tissue which in turn improved the

mechanical property of engineered tissue. Inhibition of cellular contraction of scaffolds makes it possible to control the final size and shape of engineered cartilage tissue. The control scaffolds contracted into irregular-shaped blocks due to their low mechanical property and heterogeneous pore structure. Cell/scaffold constructs from control scaffolds also had much lower compressive modulus compared to other groups, due to the formation of cartilage ECM only on the scaffold surface. While the *in vitro* engineered cartilage tissue had mechanical properties lower than the natural cartilage tissue, it is expected that after implantation the more favorable *in vivo* environment could turn the *in vitro* engineered tissue into mature cartilage tissue and further improve their mechanical property.[40, 41]

4.6 Conclusions

In summary, gelatin scaffolds with open-pore structure and good mechanical property could be prepared by using ice particulates and freeze drying. The size and structure of pores and mechanical property of gelatin scaffolds could be well controlled by using different ratios of ice particulates to gelatin solution and different concentrations of gelatin. Gelatin scaffolds prepared from ≥70% ice particulates enabled homogeneous seeding of bovine articular chondrocytes throughout the scaffolds and formation of homogeneous cartilage ECM. While soft scaffolds underwent cellular contraction, stiff scaffolds resisted contraction and had significantly higher cell proliferation and synthesis of sulfated glycosaminoglycan. Compared with the gelatin scaffolds prepared without ice particulates, the gelatin scaffolds prepared with ice particulates facilitated formation of homogeneous cartilage tissue with significantly higher compressive modulus. The gelatin scaffolds with highly open-pore structure and good mechanical property can be used to improve *in vitro* tissue-engineered cartilage.

4.7 References

[1] Brenner JM, Ventura NM, Tse MY, Winterborn A, Bardana DD, Pang SC, Hurtig MB, Waldman SD. Implantation of Scaffold-Free Engineered Cartilage Constructs in a Rabbit Model for Chondral Resurfacing. Artificial Organs. 2014;38:E21-E32.
[2] Dai WD, Kawazoe N, Lin XT, Dong J, Chen GP. The influence of structural design of PLGA/collagen hybrid scaffolds in cartilage tissue engineering. Biomaterials. 2010;31:2141-52.
[3] Frenkel SR, Di Cesare PE. Scaffolds for articular cartilage repair. Annals of Biomedical Engineering. 2004;32:26-34.
[4] Zhang KX, Zhang Y, Yan SF, Gong LL, Wang J, Chen X, Cui L, Yin JB. Repair of an articular cartilage defect using adipose-derived stem cells loaded on a polyelectrolyte complex scaffold based on poly(L-glutamic acid) and chitosan. Acta Biomaterialia. 2013;9:7276-88.
[5] Chung C, Burdick JA. Engineering cartilage tissue. Advanced Drug Delivery Reviews. 2008;60:243-62.
[6] Raghunath J, Salacinski HJ, Sales KM, Butler PE, Seifalian AM. Advancing cartilage tissue engineering: the application of stem cell technology. Current Opinion in Biotechnology. 2005;16:503-9.
[7] Wang YZ, Kim UJ, Blasioli DJ, Kim HJ, Kaplan DL. In vitro cartilage tissue engineering with 3D porous aqueous-derived silk scaffolds and mesenchymal stem cells. Biomaterials. 2005;26:7082-94.
[8] Zhang YY, Yang F, Liu K, Shen H, Zhu YD, Zhang WJ, Liu W, Wang SG, Cao YL, Zhou GD. The impact of PLGA scaffold orientation on in vitro cartilage regeneration. Biomaterials. 2012;33:2926-35.
[9] Tang C, Jin CZ, Du XT, Yan C, Min BH, Xu Y, Wang LM. An Autologous Bone Marrow Mesenchymal Stem Cell-Derived Extracellular Matrix Scaffold Applied with Bone Marrow Stimulation for Cartilage

Repair. Tissue Engineering Part A. 2014;20:2455-62.
[10] Vickers SM, Squitieri LS, Spector M. Effects of cross-linking type II collagen-GAG scaffolds on chondrogenesis in vitro: Dynamic pore reduction promotes cartilage formation. Tissue Engineering. 2006;12:1345-55.
[11] Vickers SM, Gotterbarm T, Spector M. Cross-Linking Affects Cellular Condensation and Chondrogenesis in Type II Collagen-GAG Scaffolds Seeded with Bone Marrow-Derived Mesenchymal Stem Cells. Journal of Orthopaedic Research. 2010;28:1184-92.
[12] Sun HL, Zhu F, Hu Q, Krebsbach PH. Controlling stem cell-mediated bone regeneration through tailored mechanical properties of collagen scaffolds. Biomaterials. 2014;35:1176-84.
[13] Lee CR, Breinan HA, Nehrer S, Spector M. Articular cartilage chondrocytes in type I and type II collagen-GAG matrices exhibit contractile behavior in vitro. Tissue Engineering. 2000;6:555-65.
[14] Li Q, Liu TY, Zhang L, Liu Y, Zhang WJ, Liu W, Cao YL, Zhou GD. The role of bFGF in down-regulating alpha-SMA expression of chondrogenically induced BMSCs and preventing the shrinkage of BMSC engineered cartilage. Biomaterials. 2011;32:4773-81.
[15] Chen S, Nakamoto T, Kawazoe N, Chen G. Engineering multi-layered skeletal muscle tissue by using 3D microgrooved collagen scaffolds. Biomaterials. 2015;73:23-31.
[16] Mandal BB, Kundu SC. Cell proliferation and migration in silk fibroin 3D scaffolds. Biomaterials. 2009;30:2956-65.
[17] Mandal BB, Kundu SC. Non-bioengineered silk fibroin protein 3D scaffolds for potential biotechnological and tissue engineering applications. Macromolecular Bioscience. 2008;8:807-18.
[18] Chen SW, Zhang Q, Nakamoto T, Kawazoe N, Chen GP. Highly active porous scaffolds of collagen and hyaluronic acid prepared by suppression of polyion complex formation. Journal of Materials Chemistry B. 2014;2:5612-9.
[19] Zhang Q, Lu HX, Kawazoe N, Chen GP. Preparation of collagen scaffolds with controlled pore structures and improved mechanical property for cartilage tissue engineering. Journal of Bioactive and Compatible Polymers. 2013;28:426-38.
[20] Chen S, Zhang Q, Kawazoe N, Chen G. Effect of High Molecular Weight Hyaluronic Acid on Chondrocytes Cultured in Collagen/Hyaluronic Acid Porous Scaffolds. RSC Advances. 2015;5:94405-10.
[21] Cenni E, Ciapetti G, Stea S, Corradini A, Carozzi F. Biocompatibility and performance in vitro of a hemostatic gelatin sponge. Journal of Biomaterials Science-Polymer Edition. 2000;11:685-99.
[22] Ellingsworth LR, Delustro F, Brennan JE, Sawamura S, Mcpherson J. The Human Immune-Response to Reconstituted Bovine Collagen. Journal of Immunology. 1986;136:877-82.
[23] Lynn AK, Yannas IV, Bonfield W. Antigenicity and immunogenicity of collagen. Journal of Biomedical Materials Research Part B: Applied Biomaterials. 2004;71B:343-54.
[24] Sazo REG, Maenaka K, Gu WY, Wood PM, Bunge MB. Fabrication of growth factor- and extracellular matrix-loaded, gelatin-based scaffolds and their biocompatibility with Schwann cells and dorsal root ganglia. Biomaterials. 2012;33:8529-39.
[25] Niu GG, Choi JS, Wang Z, Skardal A, Giegengack M, Soker S. Heparin-modified gelatin scaffolds for human corneal endothelial cell transplantation. Biomaterials. 2014;35:4005-14.
[26] Liu Y, Cui H, Zhuang X, Wei Y, Chen X. Electrospinning of aniline pentamer-graft-gelatin/PLLA nanofibers for bone tissue engineering. Acta Biomaterialia. 2014;10:5074-80.
[27] Islam MM, Khan MA, Rahman MM. Preparation of gelatin based porous biocomposite for bone tissue engineering and evaluation of gamma irradiation effect on its properties. Mater Sci Eng C Mater Biol Appl. 2015;49:648-55.
[28] Lin H, Cheng AWM, Alexander PG, Beck AM, Tuan RS. Cartilage Tissue Engineering Application of Injectable Gelatin Hydrogel with In Situ Visible-Light-Activated Gelation Capability in Both Air and

Aqueous Solution. Tissue Engineering Part A. 2014;20:2402-11.
[29] Chang CH, Kuo TF, Lin CC, Chou CH, Chen KH, Lin FH, Liu HC. Tissue engineering-based cartilage repair with allogenous chondrocytes and gelatin-chondroitin-hyaluronan tri-copolymer scaffold: A porcine model assessed at 18, 24, and 36 weeks. Biomaterials. 2006;27:1876-88.
[30] Burgess A, Vigneron S, Brioudes E, Labbe JC, Lorca T, Castro A. Loss of human Greatwall results in G2 arrest and multiple mitotic defects due to deregulation of the cyclin B-Cdc2/PP2A balance. Proceedings of the National Academy of Sciences of the United States of America. 2010;107:12564-9.
[31] Schmittgen TD, Livak KJ. Analyzing real-time PCR data by the comparative C-T method. Nature Protocols. 2008;3:1101-8.
[32] Grad S, Gogolewski S, Alini M, Wimmer MA. Effects of simple and complex motion patterns on gene expression of chondrocytes seeded in 3D scaffolds. Tissue Engineering. 2006;12:3171-9.
[33] Wu X, Liu Y, Li X, Wen P, Zhang Y, Long Y, Wang X, Guo Y, Xing F, Gao J. Preparation of aligned porous gelatin scaffolds by unidirectional freeze-drying method. Acta Biomaterialia. 2010;6:1167-77.
[34] Haugh MG, Murphy CM, McKiernan RC, Altenbuchner C, O'Brien FJ. Crosslinking and Mechanical Properties Significantly Influence Cell Attachment, Proliferation, and Migration Within Collagen Glycosaminoglycan Scaffolds. Tissue Engineering Part A. 2011;17:1201-8.
[35] Subramanian A, Lin HY. Crosslinked chitosan: Its physical properties and the effects of matrix stiffness on chondrocyte cell morphology and proliferation. Journal of Biomedical Materials Research Part A. 2005;75A:742-53.
[36] Lee CR, Grodzinsky AJ, Spector M. The effects of cross-linking of collagen-glycosaminoglycan scaffolds on compressive stiffness, chondrocyte-mediated contraction, proliferation and biosynthesis. Biomaterials. 2001;22:3145-54.
[37] Provenzano PP, Keely PJ. Mechanical signaling through the cytoskeleton regulates cell proliferation by coordinated focal adhesion and Rho GTPase signaling. Journal of Cell Science. 2011;124:1195-205.
[38] Provenzano PP, Inman DR, Eliceiri KW, Keely PJ. Matrix density-induced mechanoregulation of breast cell phenotype, signaling and gene expression through a FAK-ERK linkage. Oncogene. 2009;28:4326-43.
[39] Benya PD, Padilla SR, Nimni ME. Independent Regulation of Collagen Types by Chondrocytes during the Loss of Differentiated Function in Culture. Cell. 1978;15:1313-21.
[40] Zhang K, Zhang Y, Yan S, Gong L, Wang J, Chen X, Cui L, Yin J. Repair of an articular cartilage defect using adipose-derived stem cells loaded on a polyelectrolyte complex scaffold based on poly(l-glutamic acid) and chitosan. Acta Biomater. 2013;9:7276-88.
[41] Zhang Q, Lu H, Kawazoe N, Chen G. Pore size effect of collagen scaffolds on cartilage regeneration. Acta Biomater. 2014;10:2005-13.

Chapter 5

Preparation of 3D microgrooved collagen scaffolds for multi-layered skeletal muscle tissue engineering

5.1 Summary

Preparation of three-dimensional (3D) micropatterned porous scaffolds remains a great challenge for engineering of highly organized tissues such as skeletal muscle tissue and cardiac tissue. Two-dimensional (2D) micropatterned surfaces with periodic features (several nanometers to less than 100 μm) are commonly used to guide the alignment of muscle myoblasts and myotubes and lead to formation of pre-patterned cell sheets. However, cell sheets from 2D patterned surfaces have limited thickness, and harvesting the cell sheets for implantation is inconvenient and can lead to less alignment of myotubes. 3D micropatterned scaffolds can promote cell alignment and muscle tissue formation. In this study, we developed a novel type of 3D porous collagen scaffolds with concave microgrooves that mimic muscle basement membrane to engineer skeletal muscle tissue. Highly aligned and multi-layered muscle bundle tissues were engineered by controlling the size of microgrooves and cell seeding concentration. Myoblasts in the engineered muscle tissue were well-aligned and had high expression of myosin heavy chain and synthesis of muscle extracellular matrix. The microgrooved collagen scaffolds could be used to engineer organized multi-layered muscle tissue for implantation to repair/restore the function of diseased tissues or be used to investigate the cell-cell interaction in 3D microscale topography.

5.2 Introduction

Skeletal muscle tissue malfunction or loss can be caused by inflammatory muscle diseases, aging of muscle and sports injuries [1-3]. In skeletal muscle tissue, muscle fibers which are surrounded by basement membrane are highly aligned and assembled into organized muscle bundles to achieve muscle functions [4, 5]. To engineer such well-organized tissue for tissue/organ repair, two-dimensional (2D) micropatterned surfaces with periodic features (several nanometer to less than 100 μm) have been fabricated by various methods, such as aligned nanofiber by electrospinning [6-8], groove/ridge micro- and nanopatterns by photolithography or spin coating [9-13], aligned extracellular matrix (ECM) molecules or cell-adhesive polymer by contact printing [14, 15]. The 2D micropatterned surfaces can guide alignment of muscle

myoblasts and myotubes from fusion of myoblasts and lead to formation of pre-patterned cell sheets [16-19]. However, cell sheets from 2D patterned surfaces have limited thickness, and harvesting the cell sheets for implantation is inconvenient and can lead to less alignment of myotubes. Three-dimensional (3D) micropatterned scaffolds that guide cell alignment and tissue formation are desirable to engineer the organized skeletal muscle tissue.

3D micropatterned porous collagen scaffolds with well controlled pore structures can be prepared via liquid dispensing and freeze-drying [20]. In this study, we used the water dispensing and freeze-drying to prepare 3D microgrooved collagen scaffolds for skeletal muscle tissue engineering (SMTE). With this method, we could use extracellular matrix (ECM) components such as collagen to prepare 3D micropatterned scaffolds for tissue engineering and the concave structure of microgrooves to mimic the tubular structure of muscle basement membrane which surrounds each muscle fiber. Muscle basement membrane is mainly composed of ECM molecules such as collagen and laminin and has a tubular shape, which promotes muscle development and myogenesis and maintains muscle integrity [21-23]. While many studies have used scaffolds of synthetic polymer and sharp-edged micropatterns for SMTE [24-30], we tried to use the 3D collagen scaffolds with large concave microgrooves (120-380 μm) to mimic the ECM environment and topographical characteristic of muscle fibers. Another advantage of the 3D micropatterned scaffolds over 2D micropatterned surfaces is that the engineered organized muscle tissue in 3D scaffolds can be directly implanted for tissue repair. By culturing rat L6 skeletal myoblasts in the 3D microgrooved collagen scaffolds we developed multi-layered muscle bundle tissue in which myoblasts aligned and formed myotubes. The formation of aligned muscle bundles from L6 myoblasts was dependent on the size of microgrooves and cell seeding concentration. The 3D structural micropatterns have potential to repair organized tissues or organs which is hard to achieve via traditional methods or be used to investigate cell-cell interaction in 3D microscale topography [26, 31-33].

5.3 Materials and methods

5.3.1 Scaffold preparation

Perfluoroalkoxy film (PFA film, Universal Co., Ltd) was wrapped on a copper plate which was cooled by liquid nitrogen. Dispensing nozzle of a jet dispenser (MJET-3-CTR, Musashi Engineering Inc.) which was controlled by a SHOT mini 200α (Musashi Engineering Inc.) moved back and forth over the PFA film-wrapped copper plate and ejected water droplets that sequentially fell onto the cooled plate. The water droplets were immediately frozen and formed continuous frozen ice lines (Fig. 5.1a,b). CAD programs were used to control the movement of dispensing nozzle which enabled formation of aligned frozen ice lines on the plate. The width of frozen ice lines was controlled by the pressure (0.001MPa) that pumped water out of the nozzle and different types of nozzles (32-35G). The temperature of the copper plate bearing frozen ice lines was balanced to -5 °C, and the plate was covered with a silicon frame (thickness: 500 μm). Cooled type I collagen aqueous solution (1 (wt/v)% in a mixture of ethanol and pure water (10:90 v/v, pH 3.0), -5 °C) (Nitta Gelatin Inc.) was cast onto the frozen ice lines and covered with a glass plate. The whole construct was frozen in liquid nitrogen and freeze-dried to get a 3D microgrooved scaffold. Different scaffolds (G120, G200 and G380) were prepared by using frozen lines of different widths. Scaffolds with a flat surface as a control group were prepared without using ice lines. All scaffolds were cross-linked using a solution of 50 mM 1-ethyl-3-(3-dimethyllaminopropyl)carbodiimide and 20 mM N-hydroxysuccinimide at room temperature for 12 h [34], rinsed with pure water and freeze-dried.

5.3.2 Scanning electron microscopy and porosity measurement

Scaffold samples were cut using sharp blades, fixated using carbon tape, sputter-coated with platinum and observed with a scanning electron microscope (SEM) at the acceleration voltage of 10 kV (JSM-5610, JEOL, Ltd.). The SEM images were imported in ImageJ software to analyze the widths and depths of scaffolds. 4 images of each type of samples were analyzed and at least 6 microgrooves in each image were analyzed. The porosity of different kinds of scaffolds was measured using the method as reported previously [35].

5.3.3 Cell culture in scaffolds

Rat L6 skeletal muscle myoblasts (American Type Culture Collection) were subcultured in Dulbecco's Modified Eagle's Medium (D8437, Sigma-Aldrich) supplemented with 10% fetal bovine serum and 10% horse serum and 1% penicillin / streptomycin. Microgrooved scaffolds were punched into disks (diameter: 10 mm), sterilized in 70% ethanol, rinsed in phosphate buffered saline (PBS) and covered with a glass ring (inner diameter : 10 mm) in 12-well plates. After culture medium (2 ml) was added beside each glass ring, myoblasts in cell suspension (200 µl) were seeded at 3 different concentrations on the microgrooved collagen scaffolds inside the glass rings. The cells were cultured for 2 days followed by removal of glass rings. And then the samples were cultured in fusion medium (FM) (D8437 + 2% horse serum + 1% penicillin / streptomycin) for another 5 or 12 days. For SEM observation, cell-seeded samples were fixed with 2.5% glutaraldehyde in PBS for 2 hours, rinsed in pure water, freeze-dried and observed as mentioned above.

5.3.4 Staining of engineered tissue

After 7 or 14 days of culture, cell-scaffold samples were fixed using 4% paraformaldehyde (30 min, room temperature(RT)), rinsed in PBS, and incubated in 0.2% Triton X-100 (10 min, RT). For staining of F-actin, Alexa Fluor 488 Phalloidin (Life Technologies) was diluted in PBS (1:40) and incubated with the samples for 40 min. For staining of myosin heavy chain (MHC), the samples were blocked in 1% BSA for 20 min, incubated in 1% BSA-diluted MF20 (Developmental Studies Hybridoma Bank) (1:300) overnight at 4 ºC, followed by rinsing in PBS and incubation in 1% BSA-diluted Goat anti-Mouse IgG Secondary Antibody (Life Technologies) (1:500) for 1 h at RT. For double staining of F-actin and MHC, the samples were incubated in diluted MF20 and Goat anti-Mouse IgG Secondary Antibody followed by incubation in Alexa Fluor® 594 Phalloidin (Life Technologies) at the same conditions described above. Finally cell nuclei were stained using PBS-diluted Cellstain-DAPI Solution (Dojindo)(1:500, 10 min, RT). Samples were rinsed in PBS and imaged using a fluorescence microscope (Olympus) or a confocal microscope (Zeiss LSM 510 Meta).

For Hematoxylin and Eosin (HE) staining and laminin immunostaining, cell-scaffold samples were fixated in 10% neutral buffered saline, dehydrated in ethanol series and embedded in paraffin. 8 µm-thick tissue sections were sectioned from the paraffin-embedded samples and used for HE staining and laminin immunostaining (Laminin α-4 (H-194), Santa Cruz Biotechnology, Inc.).

5.3.5 Analysis of cell alignment

To check cell nuclei alignment within cell bundles, confocal images of DAPI-stained nuclei were

imported in ImageJ software to analyze the angles between the major axis of nuclei and the central axis of cell bundle [36]. 4 images of each type of samples were analyzed and at least 60 nuclei in each image were analyzed.

5.3.6 Real-time PCR

Total RNA of cell-scaffold constructs after 7 or 14 d of culture was extracted by using RNeasy Plus mini kit (Qiagen). Extracted RNA (1.0 μg) was used as a first strand reaction that included random hexamer primers and murine leukaemia virus reverse transcriptase (Applied Biosystems). Real-time PCR was amplified for glyceraldehydes-3-phosphate dehydrogenase (GAPDH, TaqMan Assay ID: Rn99999916_S1), myogenin (myog, TaqMan Assay ID: Rn00567418_m1) [37], MHC class I polypeptide-related sequence B (Micb, TaqMan Assay ID: Rn01764378_m1). The reaction was performed with 10 ng of c-DNA, 90 nM PCR primers, 25 nM PCR probe and TaqMan universal PCR master mix (Applied Biosystems). The expression levels of target genes relative to that of GAPDH were calculated using a comparative Ct method. The primers and probes were obtained from Applied Biosystems.

5.3.7 Statistical analysis

One-way analysis of variance (ANOVA) was used to evaluate the myogenic gene expression levels of cells cultured in different scaffolds. Student-t test was used to compare two groups of data. Statistical differences were considered significant if $p<0.05$.

5.4 Results and discussion

5.4.1 Preparation of microgrooved collagen scaffolds

To control the pore structure of 3D microgrooved scaffolds, parallel lines of frozen ice were prepared by dispensing pure water onto a copper plate which was cooled by liquid nitrogen and served as a template to prepare the microgrooved scaffolds (Fig. 5.1a,b). A hydrophobic polyfluoroalkoxy film on the copper plate was used to deposit frozen lines so that these lines had a nearly semicircular shape in cross-section. Type I collagen was chosen to prepare the scaffolds because it can promote the proliferation of skeletal muscle cells [38]. By controlling the width of frozen ice lines, scaffolds with different width of microgrooves were prepared (120 ± 15, 200 ± 18 and 380 ± 22 μm, named as G120, G200 and G380, respectively) as shown in Fig. 1c. The micropatterned scaffolds had aligned concave microgrooves that exhibited a semicircular shape in cross-section, which was inherited from the frozen ice line replicates. The depth of the microgrooves of scaffolds in Z direction was 65 ± 8 μm for G120, 107 ± 11 μm for G200 and 188 ± 15 μm for G380. Scaffolds with a flat surface as a control group (Flat) were prepared without using frozen ice lines. These scaffolds had similar porosity (Table 5.1) as determined from the same concentration of collagen used for scaffold preparation.

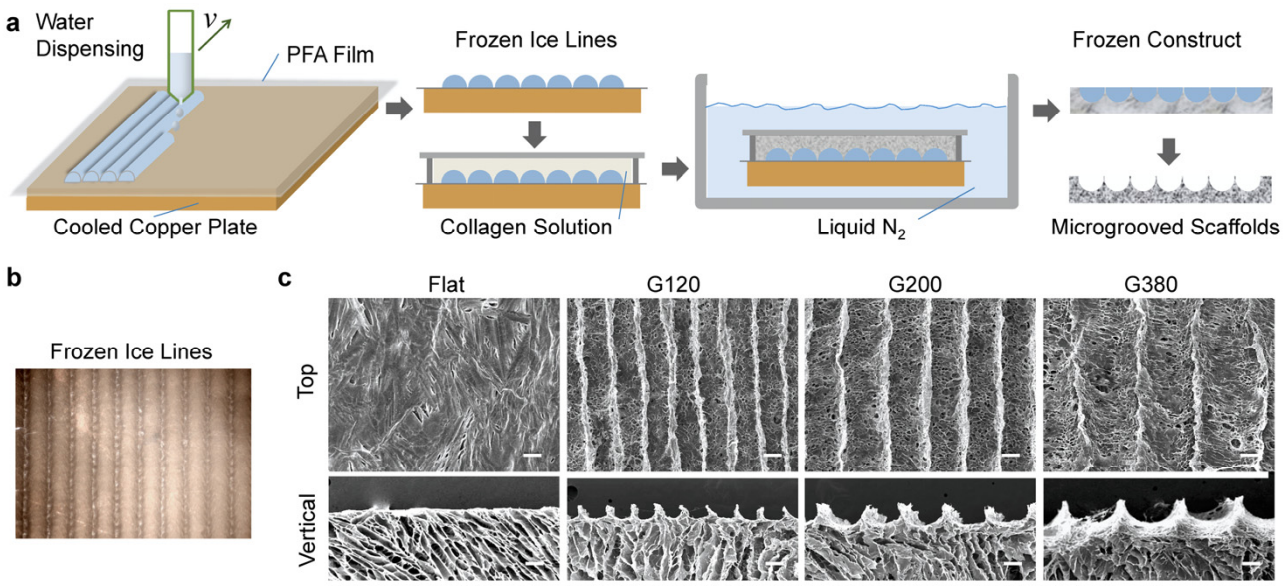

Fig. 5.1. Preparation of microgrooved collagen scaffolds. (a) A schematic for the preparation of microgrooved collagen scaffolds. (b) Image of frozen ice lines prepared from water dispensing. (c) SEM images of different microgrooved collagen scaffolds. Flat: control collagen scaffolds with a flat surface; G120, G200, G380: collagen scaffolds with mean microgroove widths of 120, 200, 380 μm, respectively. Upper images show the top view and lower images show the vertical cross-sectional view of different scaffolds. Scale bar = 100 μm.

Table 5.1. Porosity of different types of scaffolds (mean ± standard deviation, N = 3).

Scaffold	Flat	G120	G200	G380
Porosity (%)	97.2 ± 0.6	97.6 ± 1.1	98.2 ± 0.8	97.3 ± 0.5

5.4.2 Effects of seeding concentration on formation of cellular bundles

To study the potential of the microgrooved collagen scaffolds for SMTE, rat L6 skeletal myoblasts were firstly seeded at different seeding concentrations onto the G200 scaffolds. After cell seeding at an intermediate concentration (2.0×10^6 cells/ml), L6 myoblasts settled down and adhered in microgrooved scaffolds after 24 h, with the majority of myoblasts settled on the lower part of microgrooves (Fig. 5.2a). Myoblasts in the microgrooves subsequently contracted into multi-cellular strips after 48 h, and further contracted into multi-cellular bundles in microgrooves after 72 h. L6 myoblasts seeded at a low seeding concentration (0.4×10^6 cells/ml) remained homogeneously distributed in microgrooved scaffolds and did not form cell bundles or myotubes after culture for 7 d (Fig. 5.2b). L6 myoblasts seeded at an intermediate (2.0×10^6 cells/ml) or high concentration (4.0×10^6 cells/ml) formed aligned cell bundles in microgrooves and fused into some myotubes within cell bundles. The results suggested that the formation of cell bundles was dependent on seeding concentration of myoblasts. Myoblasts seeded at a high concentration would enable cell-cell interaction that led cells in each microgroove to contract together into cellular bundles and fuse into myotubes. However, if the cell seeding concentration was too high (1.2×10^7/ml), the cells would readily overgrow in the microgrooves and on the ridges, forming sheet-like structure that delaminated from the microgrooves after 72 hours.

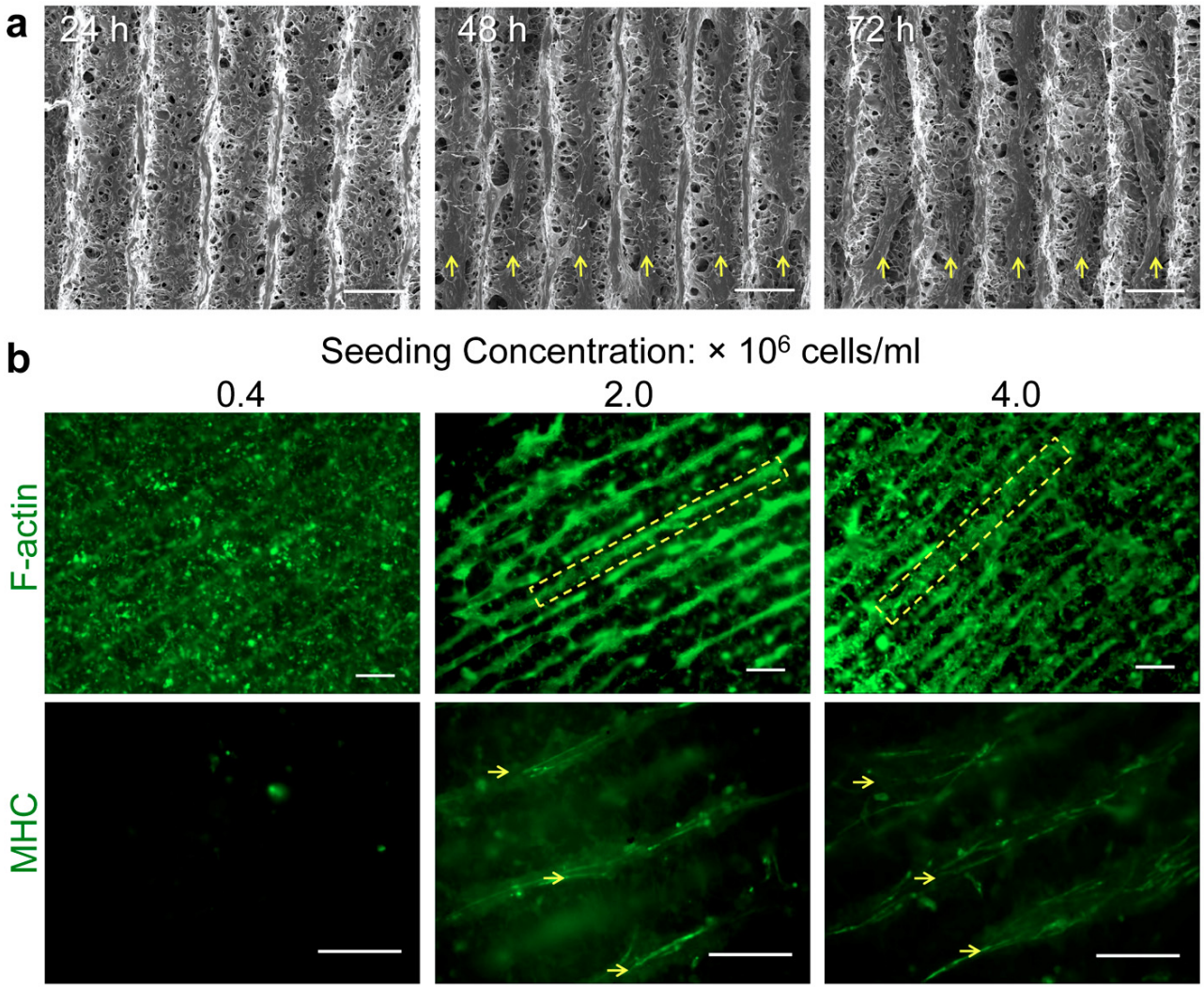

Fig. 5.2. Formation of cell bundles in microgrooved scaffolds. (a) SEM images of cell-seeded scaffolds (G200, seeding concentration: 2.0×10^6/ml) after 24 h, 48 h and 72 h culture. Arrows mark cell bundles formed in the microgrooves. (b) Cell bundle formation in scaffolds (G200) seeded with different concentrations of myoblasts (0.4, 2.0, 4.0×10^6/ml) after 7 d culture. Myoblasts were visualized using F-actin staining; myotube formation was shown using MHC staining. Dashed squares mark cell bundle in the microgrooves and arrows mark myotubes in microgrooves. Scale bar = 200 μm.

5.4.3 Effects of microgroove widths on formation of cellular bundles

L6 skeletal myoblasts were seeded onto the microgrooved scaffolds with different width of microgrooves (G120, G200, G380 and Flat control) at the intermediate concentration (2.0×10^6 cells/ml). F-actin staining of myoblasts cultured in the microgrooved scaffolds for 7 d showed that the scaffolds could guide formation of cell bundles in microgrooves (Fig. 5.3a). Scaffolds with wide microgrooves (G200 and G380) enabled formation of discrete, parallel cell bundles during 14 d culture. Scaffolds with narrow microgrooves (G120) resulted in formation of some cell bundles in microgrooves and mostly cellular flakes covering most of the area of scaffolds. Myoblasts cultured on flat scaffolds showed some aggregation into clusters and no cell bundle formation. Staining of myosin heavy chain (MHC) showed that well-aligned myotubes formed within cell bundles in G200 and G380, while in G120 some myotubes were aligned in

microgrooves and other myotubes possibly in cellular flakes had random orientation (Fig. 5.3b). On flat scaffolds most of myotubes formed in cell aggregates and had random orientation. These results indicated that the formation and alignment of cell bundles in microgrooved scaffolds were dependent on the size of microgrooves.

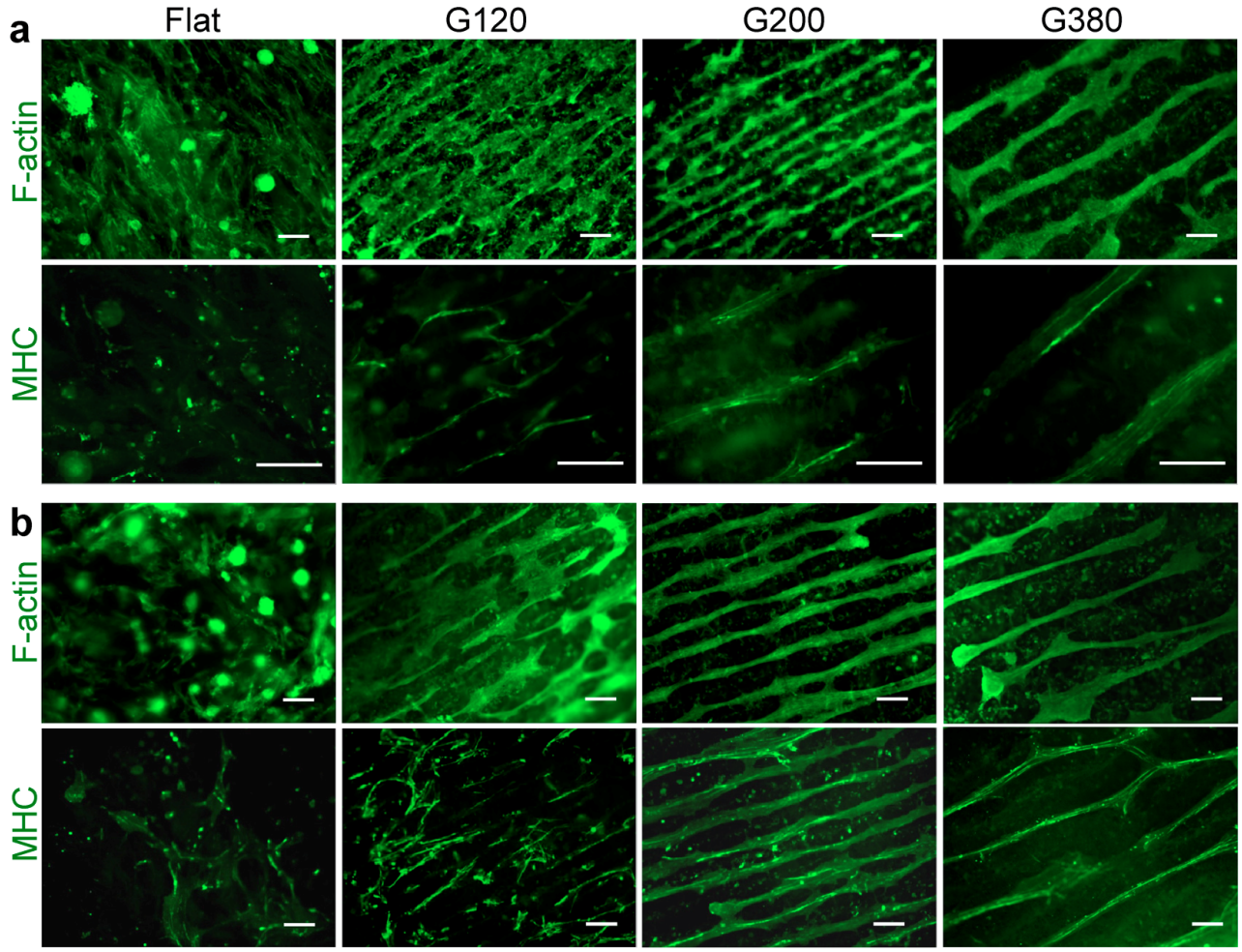

Fig. 5.3. Myotube formation in different microgrooved scaffolds after culture for 7 (a) and 14 d (b) (seeding concentration: 2.0×10^6 cells/ml). Myoblasts were visualized using F-actin staining; myotube formation was shown using MHC staining. Scale bar = 200 μm.

5.4.4 Multi-layered skeletal muscle bundles

The confocal laser scanning microscopy (CLSM) images of cross-sections of cell bundles (XZ plane) showed that the cell bundles changed from flat bundles at day 7 to circular bundles at day 14 (Fig. 5.4a), indicating cellular contraction in cell bundles from day 7 to day 14. CLSM images of cell bundles (G200 and G380, day 14) at different depths in z direction showed that cell bundles had a thickness of 116 ± 14 μm (G200) or 120 ± 40 μm (G380) (Fig. 5.4b). Multi-cellular bundle could be engineered using microgrooved scaffolds.

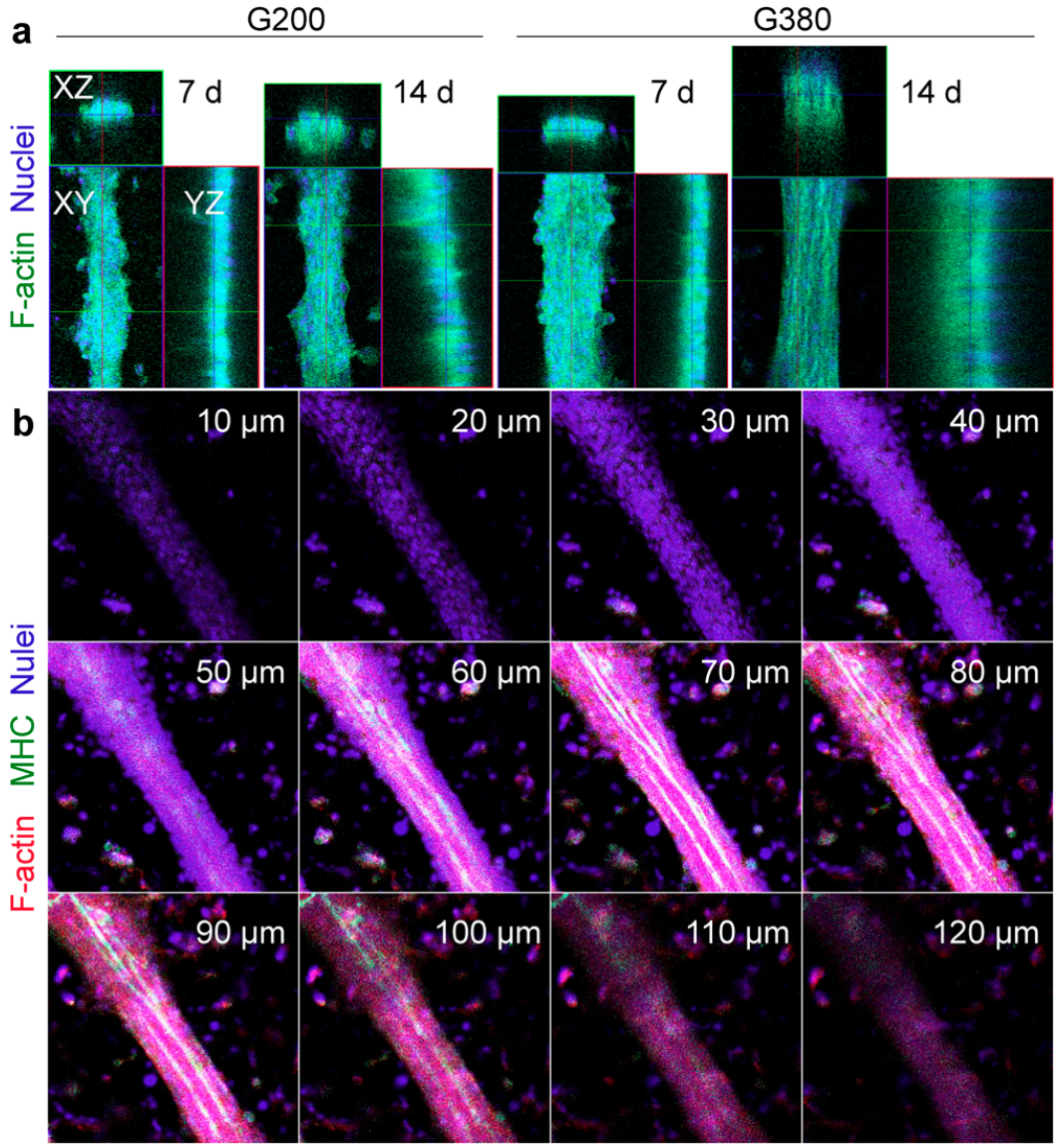

Fig. 5.4. Multi-layered skeletal muscle bundles (seeding concentration: 2.0×10^6 cells/ml). (a) z-stack CLSM images (XZ, XY and YZ planes) of cell bundle that formed in G200 and G380 scaffolds after 7 d and 14 d culture. Samples were stained for F-actin and nuclei. (b) Optical sections of stained cell bundle in different z depths as shown in the images (10-120 μm). Samples were stained for F-actin, MHC and nuclei.

5.4.5 Cell alignment in engineered muscle bundles

To check the cell alignment within each cell bundles, cell nuclei and F-actin were stained and visualized using CLSM. Analysis of cell nucleus alignment angle (Fig. 5.5a,b) and F-actin alignment (Fig. 5.5c) of myoblasts showed that the long axis of cell nuclei and F-actin were well aligned in the direction of microgrooves in G200 and G380. G120 scaffolds also guided the alignment of cell nuclei and F-actin but showed less satisfactory results compared with G200 or G380.

Many studies used groove/ridge micro- and nanopatterns with small periodic features (<100 μm) to guide the alignment of cells in monolayer [17, 18, 39-41]. It has been difficult to guide the formation of well-aligned cell bundles for SMTE in a 3D environment. Our results suggested that concave microgrooves with large sizes (200-380 μm) could guide the contraction of cell populations of multilayers to form cell bundles with well-aligned cells. For these scaffolds (G200 and G380), each microgroove had enough space

to hold seeded cells and facilitated subsequent contraction of cells in each microgroove leading to formation of well-aligned cell bundles. For scaffolds with small width microgrooves (G120), however, the seeded cells overfilled the limited space of each microgroove and overgrew on the scaffold which led to formation of cellular flakes and less organized cell bundles.

The 3D microgrooved scaffolds had some advantages over 2D patterned surfaces or cell-sheet technology. 2D patterned surfaces or cell-sheet technology can enable formation of a thin layer of aligned muscle tissue, but harvest of the tissue usually leads to formation of unorganized tissue due to cellular contraction and loss of anisotropic morphology [42]. In addition, thin layers of aligned muscle tissue need to be stacked layer by layer to form thick, anisotropic muscle tissues, which is tedious and difficult [42, 43]. In contrast, our microgrooved scaffolds can enable thick, well aligned muscle tissue with simple manipulation.

Microgrooved hydrogels have been used to enable the formation of aligned myotubes. Cells cultured in the microgrooved hydrogels show high alignment during a short culture period while cells become less aligned after 8 days culture [36]. However, the concave microgrooves (semicircular shape in cross-section) in this study enabled myoblasts to settle down, proliferate and differentiate along the central axis of each microgrooves, leading to the formation of well-aligned muscle bundle even after 14 days culture. The high cellular alignment in our microgrooved scaffolds might attribute to the concave microgroove together with the porous structures of the scaffolds.

5.4.6 Myogenic gene expressions of cells in muscle bundles

The expression levels of two myogenesis-related genes, myogenin and myosin heavy chain (MHC), were quantified by using real-time PCR (Fig. 5.5d). For all scaffold samples, the expression levels of both genes decreased a little from day 7 to day 14, although not statistically significant. While microgrooved scaffolds guided the alignment of myoblasts, there was no significant difference of myogenic gene expression levels among different microgrooved scaffolds. Similar gene expression levels of the cells cultured in the scaffolds should be due to the same fusion medium used in the cell culture, which was considered as the primary factor that determined cell differentiation. When being cultured in the micropatterned scaffolds, cells formed bundle structures with good cell-cell interaction. After cell-cell interaction reached a base level, the differentiation of myoblasts should be determined by culture medium, other than the micropattern structures. These results were in agreement of previous studies which showed that different macro-channels or micro-scale topography did not affect the differentiation of either primary or C2C12 myoblasts [17, 39, 44].

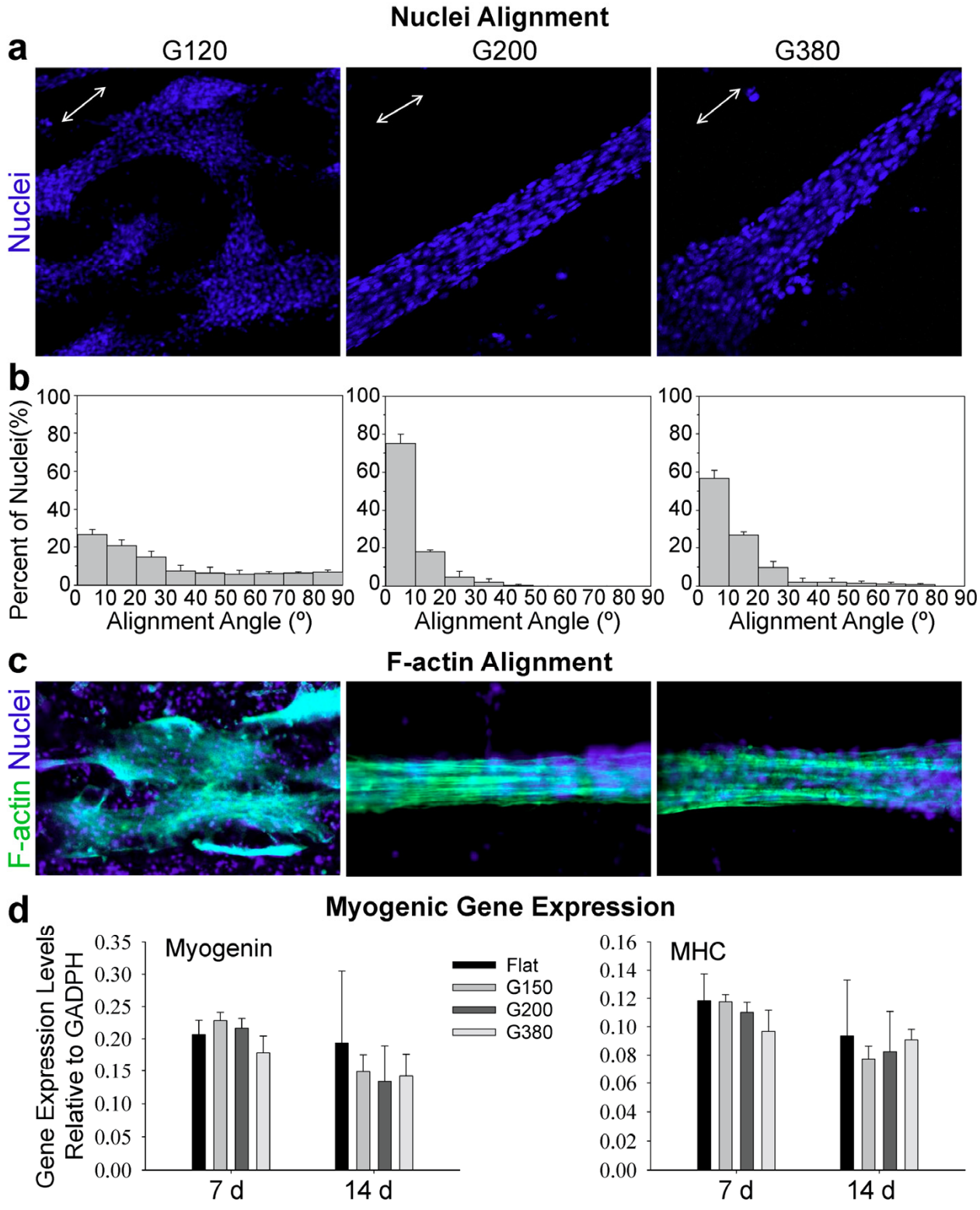

Fig. 5.5. Cell alignment within cell bundles in different microgrooved scaffolds (G120, G200 and G380) and expression of myogenic genes. (a) CLSM images of cell nuclei. (b) distribution of nuclei alignment angle. (c) F-actin staining of myoblasts with counterstained nuclei. a-c, samples were cultured for 14 d. (d) Expression of genes encoding myogenin and MHC class I polypeptide-related sequence B (MHC). No significant difference ($p > 0.05$) in expression levels of either gene among different scaffolds after 7 or 14 d of cell culture. Seeding concentration: 2.0×10^6 cells/ml.

5.4.7 Formation of organized multi-layered muscle tissue

Culture of myoblasts in G200 (seeding concentration: 4.0×10^6 cells/ml) for 2 weeks resulted in formation of organized multi-layered muscle tissue. HE staining and F-actin staining of engineered muscle tissue showed that the tissue filled the microgrooved scaffolds and cells within the tissue were highly aligned along the longitudinal direction (Fig. 6a-c). Immunostaining of MHC and laminin showed that cells had high expression of MHC and synthesis of muscle ECM in the microgrooved collagen scaffolds (Fig. 5.6d-f).

Cell culture systems using hydrogels without micropattern structures have also reported to generate multi-layered muscle bundle tissues [45-47]. However, the systems usually lead to outer region with densely packed cells and an acellular core [47, 48]. Engineering muscle tissue by 3D microgrooved porous scaffolds provided an alternative for muscle tissue engineering. The live/dead staining of the engineered tissues in our porous scaffolds showed that the cells within the tissues had a high viability and no necrosis of central core (Fig. 5.7), possibly due to the ease of oxygen diffusion and nutrient transfer in the porous structures. Myoblasts after 2-week culture aligned and had high expression of myosin heavy chain, which is closely related to the contractile function of myotube bundles [49]. Myoblasts after 4-week culture had even higher expression of myosin heavy chain (Fig. 5.8). The micropatterned porous scaffolds could regenerate well-aligned, highly differentiated and viable muscle bundles. Therefore, the 3D microgrooved collagen scaffolds may be used to engineer well-organized multi-layered muscle tissue that can be directly implanted for repairing diseased skeletal muscle or cardiac tissue.

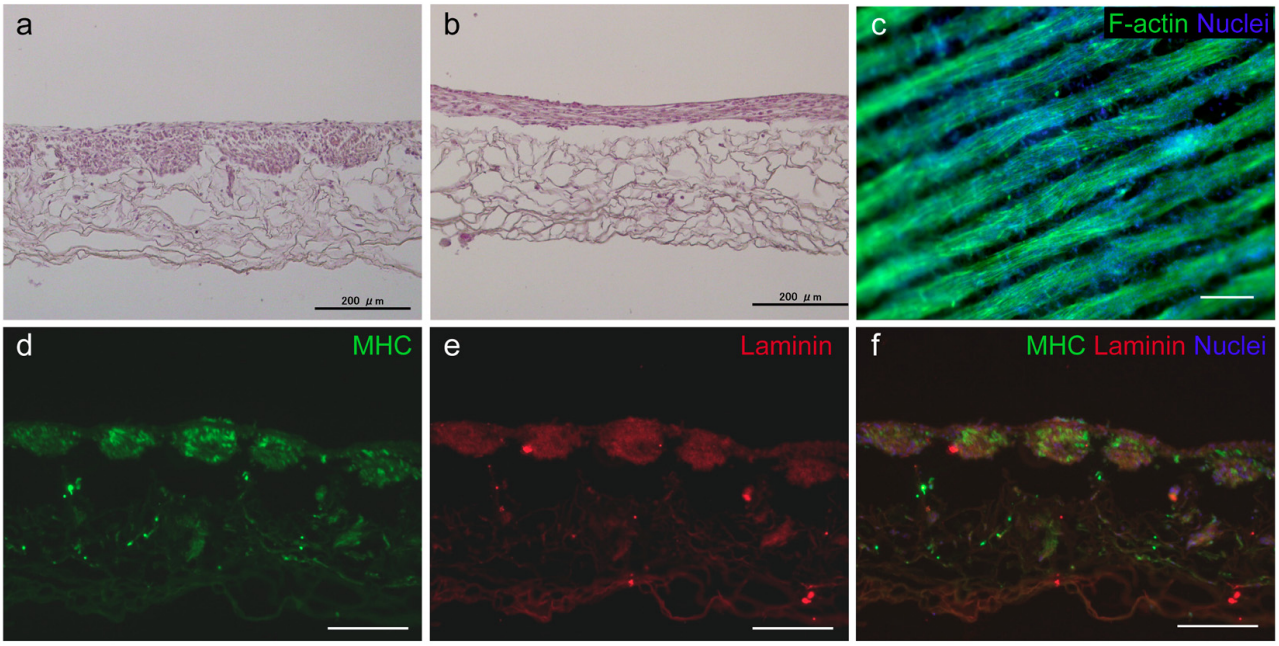

Fig. 5.6. Formation of organized multi-layered muscle tissue. Myoblasts were seeded at the concentration of 4.0×10^6 cells/ml into G200 scaffolds and cultured for 2 weeks. HE staining of (a) transversal cross-sections and (b) longitudinal cross-sections of engineered muscle tissue. (c) F-actin staining of the tissue. (d-f) MHC, laminin immunostaining and merged images of engineered muscle tissue. Cell nuclei were stained with DAPI. Scale bar = 200 μm.

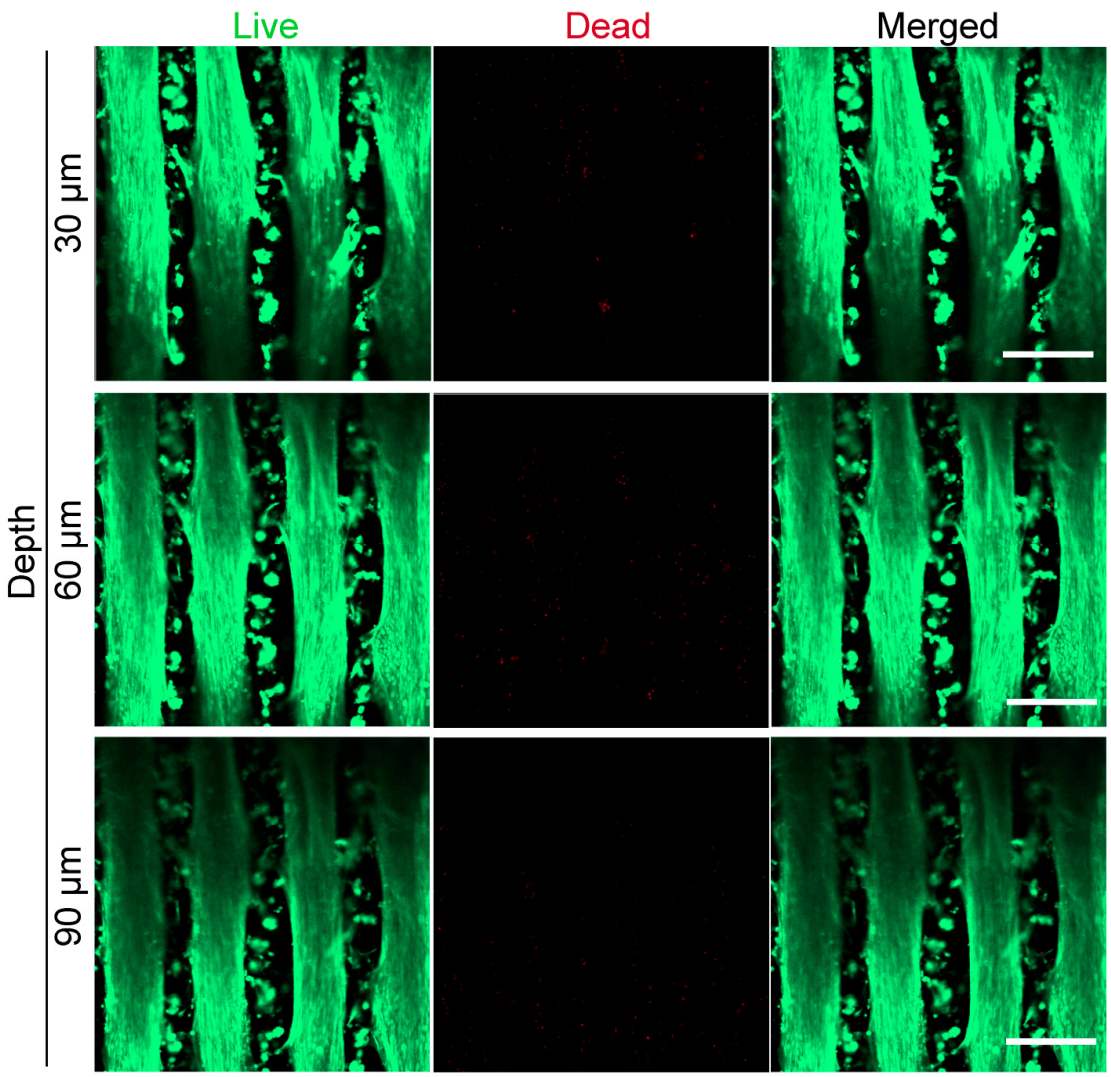

Fig. 5.7. Live/dead staining of cells in muscle bundle tissue after 2-week culture. Confocal images were scanned at different depths (30, 60, 90 um from the top) of engineered tissue. Green: live cells; red: dead cells. Myoblasts were seeded at the concentration of 4.0×10^6 cells/ml into G200 scaffolds and cultured for 2 weeks. Scale bar = 200 µm.

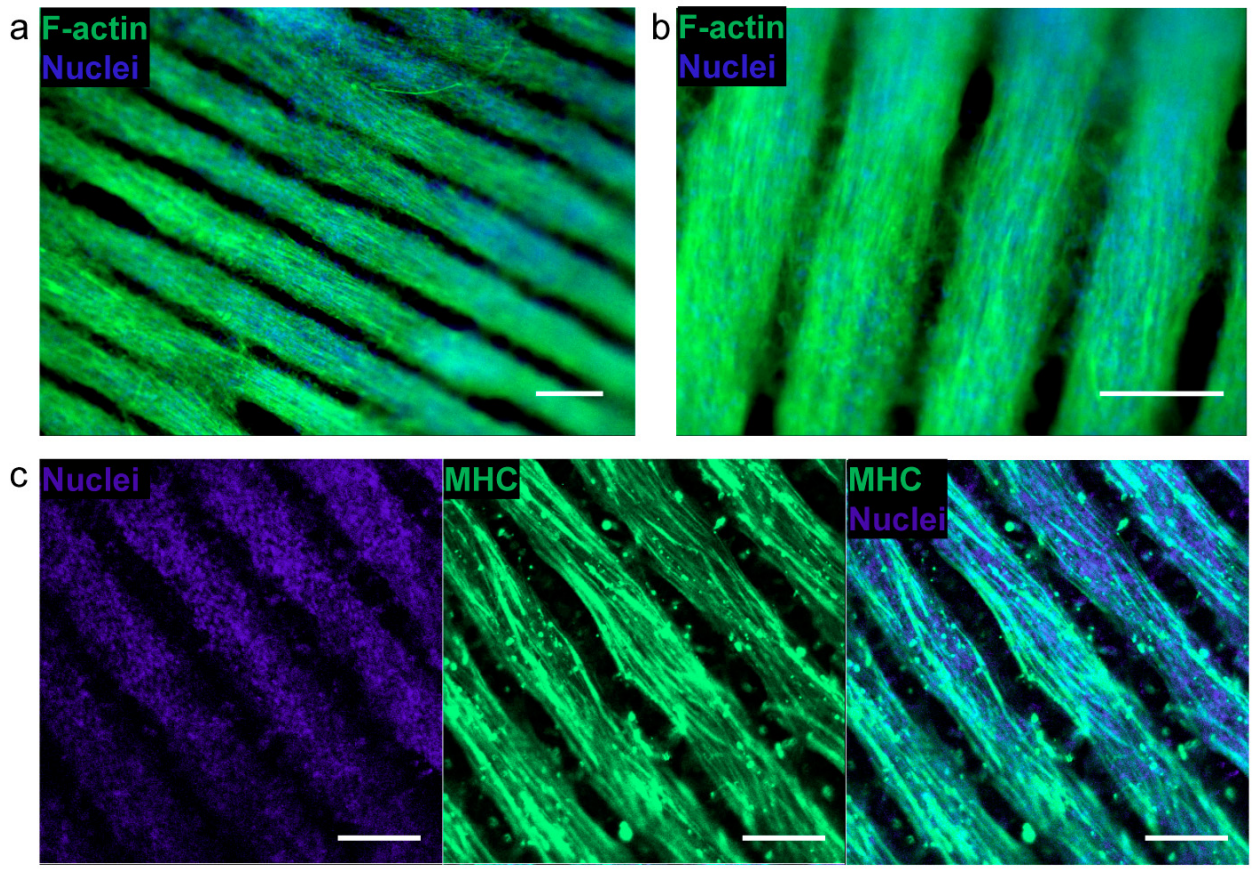

Fig. 5.8. Maintenance of highly organized and differentiated muscle bundle tissue after long-term culture. Myoblasts were seeded at the concentration of 4.0×10^6 cells/ml into G200 scaffolds and cultured for 4 weeks. (a-b) F-actin/DAPI staining of the tissue. (c) DAPI staining of nuclei , MHC immunostaining and merged images of engineered muscle tissue. Scale bar = 200 μm.

5.5 Conclusions

In summary, 3D collagen scaffolds with concave microgrooves that mimic muscle basement membrane were prepared using liquid dispensing and freeze-drying. By culturing L6 myoblasts in the microgrooved scaffolds, highly aligned and multi-layered muscle bundle tissues were engineered by controlling the size of microgrooves and cell seeding concentration. Myoblasts in the engineered muscle tissue were well-aligned and had high expression of myosin heavy chain and synthesis of muscle extracellular matrix. The microgrooved scaffolds of different groove sizes did not affect the expression levels of myogenic genes. The organized multi-layered muscle tissue engineered from microgrooved collagen scaffolds may be used for implantation to repair or restore the function of diseased muscles.

5.6 References

[1] Friedebo.G, Groher W. Sprains and Other Sports-Injuries of Muscles and Tendons. Zeitschrift Fur Orthopadie Und Ihre Grenzgebiete. 1972;110:647-53.
[2] Moller P, Bergstrom J, Furst P, Hellstrom K. Effect of Aging on Energy-Rich Phosphagens in Human Skeletal-Muscles. Clinical Science. 1980;58:553-5.
[3] Tournadre A, Dubost JJ, Soubrier M. Treatment of inflammatory muscle disease in adults. Joint Bone

Spine. 2010;77:390-4.
[4] Campbell KP, Stull JT. Skeletal muscle basement membrane-sarcolemma-cytoskeleton interaction minireview series. Journal of Biological Chemistry. 2003;278:12599-600.
[5] Sanes JR. The basement membrane/basal lamina of skeletal muscle. Journal of Biological Chemistry. 2003;278:12601-4.
[6] Ayaz HGS, Perets A, Ayaz H, Gilroy KD, Govindaraj M, Brookstein D, Lelkes PI. Textile-templated electrospun anisotropic scaffolds for regenerative cardiac tissue engineering. Biomaterials. 2014;35:8540-52.
[7] Choi JS, Lee SJ, Christ GJ, Atala A, Yoo JJ. The influence of electrospun aligned poly(epsilon-caprolactone)/collagen nanofiber meshes on the formation of self-aligned skeletal muscle myotubes. Biomaterials. 2008;29:2899-906.
[8] Cooper A, Jana S, Bhattarai N, Zhang MQ. Aligned chitosan-based nanofibers for enhanced myogenesis. Journal of Materials Chemistry. 2010;20:8904-11.
[9] Clark P, Coles D, Peckham M. Preferential adhesion to and survival on patterned laminin organizes myogenesis in vitro. Experimental Cell Research. 1997;230:275-83.
[10] Clark P, Dunn GA, Knibbs A, Peckham M. Alignment of myoblasts on ultrafine gratings inhibits fusion in vitro. International Journal of Biochemistry & Cell Biology. 2002;34:816-25.
[11] Salick MR, Napiwocki BN, Sha J, Knight GT, Chindhy SA, Kamp TJ, Ashton RS, Crone WC. Micropattern width dependent sarcomere development in human ESC-derived cardiomyocytes. Biomaterials. 2014;35:4454-64.
[12] Shi XT, Fujie T, Saito A, Takeoka S, Hou Y, Shu YW, Chen MW, Wu HK, Khademhosseini A. Periosteum-Mimetic Structures Made from Freestanding Microgrooved Nanosheets. Advanced Materials. 2014;26:3290-96.
[13] Zorlutuna P, Annabi N, Camci-Unal G, Nikkhah M, Cha JM, Nichol JW, Manbachi A, Bae HJ, Chen SC, Khademhosseini A. Microfabricated Biomaterials for Engineering 3D Tissues. Advanced Materials. 2012;24:1782-804.
[14] Fujie T, Ahadian S, Liu H, Chang HX, Ostrovidov S, Wu HK, Bae H, Nakajima K, Kaji H, Khademhosseini A. Engineered Nanomembranes for Directing Cellular Organization Toward Flexible Biodevices. Nano Letters. 2013;13:3185-92.
[15] Nakamoto T, Wang XL, Kawazoe NP, Chen G. Influence of micropattern width on differentiation of human mesenchymal stem cells to vascular smooth muscle cells. Colloids and Surfaces B-Biointerfaces. 2014;122:316-23.
[16] Evans DJR, Britland S, Wigmore PM. Differential response of fetal and neonatal myoblasts to topographical guidance cues in vitro. Development Genes and Evolution. 1999;209:438-42.
[17] Huang NF, Lee RJ, Li S. Engineering of aligned skeletal muscle by micropatterning. American Journal of Translational Research. 2010;2:43-55.
[18] Lam MT, Sim S, Zhu XY, Takayama S. The effect of continuous wavy micropatterns on silicone substrates on the alignment of skeletal muscle myoblasts and myotubes. Biomaterials. 2006;27:4340-7.
[19] Takahashi H, Shimizu T, Nakayama M, Yamato M, Okano T. The use of anisotropic cell sheets to control orientation during the self-organization of 3D muscle tissue. Biomaterials. 2013;34:7372-80.
[20] Oh HH, Ko YG, Lu HX, Kawazoe N, Chen GP. Preparation of Porous Collagen Scaffolds with Micropatterned Structures. Advanced Materials. 2012;24:4311-16.
[21] Caldwell CJ, Mattey DL, Weller RO. Role of the Basement-Membrane in the Regeneration of Skeletal-Muscle. Neuropathology and Applied Neurobiology. 1990;16:225-38.
[22] Caldwell CJ, Weller RO. The Role of the Basement-Membrane in Regeneration of Skeletal-Muscle. Neuropathology and Applied Neurobiology. 1987;13:492-3.
[23] Hurd SA, Bhatti NM, Walker AM, Kasukonis BM, Wolchok JC. Development of a biological scaffold

engineered using the extracellular matrix secreted by skeletal muscle cells. Biomaterials. 2015;49:9-17.
[24] Jiang XY, Takayama S, Qian XP, Ostuni E, Wu HK, Bowden N, LeDuc P, Ingber DE, Whitesides GM. Controlling mammalian cell spreading and cytoskeletal arrangement with conveniently fabricated continuous wavy features on poly(dimethylsiloxane). Langmuir. 2002;18:3273-80.
[25] Kolewe ME, Park H, Gray C, Ye XF, Langer R, Freed LE. 3D Structural Patterns in Scalable, Elastomeric Scaffolds Guide Engineered Tissue Architecture. Advanced Materials. 2013;25:4459-65.
[26] Li GC, Zhao XY, Zhao WX, Zhang LZ, Wang CP, Jiang MR, Gu XS, Yang YM. Porous chitosan scaffolds with surface micropatterning and inner porosity and their effects on Schwann cells. Biomaterials. 2014;35:8503-13.
[27] Patz TM, Doraiswamy A, Narayan RJ, Modi R, Chrisey DB. Two-dimensional differential adherence and alignment of C2C12 myoblasts. Materials Science and Engineering B-Solid State Materials for Advanced Technology. 2005;123:242-7.
[28] Ramon-Azcon J, Ahadian S, Estili M, Liang XB, Ostrovidov S, Kaji H, Shiku H, Ramalingam M, Nakajima K, Sakka Y, Khademhosseini A, Matsue T. Dielectrophoretically Aligned Carbon Nanotubes to Control Electrical and Mechanical Properties of Hydrogels to Fabricate Contractile Muscle Myofibers. Advanced Materials. 2013;25:4028-34.
[29] Shen JY, Chan-Park MBE, Feng ZO, V C, Feng ZW. UV-embossed microchannel in biocompatible polymeric film: Application to control of cell shape and orientation of muscle cells. Journal of Biomedical Materials Research Part B-Applied Biomaterials. 2006;77B:423-30.
[30] Ye XF, Lu L, Kolewe ME, Hearon K, Fischer KM, Coppeta J, Freed LE. Scalable Units for Building Cardiac Tissue. Advanced Materials. 2014;26:7202-8.
[31] Guillame-Gentil O, Semenov O, Roca AS, Groth T, Zahn R, Voros J, Zenobi-Wong M. Engineering the Extracellular Environment: Strategies for Building 2D and 3D Cellular Structures. Advanced Materials. 2010;22:5443-62.
[32] Kurland NE, Dey T, Kundu SC, Yadavalli VK. Precise Patterning of Silk Microstructures Using Photolithography. Advanced Materials. 2013;25:6207-12.
[33] Yao X, Peng R, Ding JD. Cell-Material Interactions Revealed Via Material Techniques of Surface Patterning. Advanced Materials. 2013;25:5257-86.
[34] Chen SW, Zhang Q, Nakamoto T, Kawazoe N, Chen GP. Highly active porous scaffolds of collagen and hyaluronic acid prepared by suppression of polyion complex formation. Journal of Materials Chemistry B. 2014;2:5612-9.
[35] Zhang Q, Lu HX, Kawazoe N, Chen GP. Pore size effect of collagen scaffolds on cartilage regeneration. Acta Biomaterialia. 2014;10:2005-13.
[36] Hosseini V, Ahadian S, Ostrovidov S, Camci-Unal G, Chen S, Kaji H, Ramalingam M, Khademhosseini A. Engineered Contractile Skeletal Muscle Tissue on a Microgrooved Methacrylated Gelatin Substrate. Tissue Engineering Part A. 2012;18:2453-65.
[37] Flynn JM, Meadows E, Fiorotto M, Klein WH. Myogenin Regulates Exercise Capacity and Skeletal Muscle Metabolism in the Adult Mouse. Plos One. 2010;5.
[38] Macfelda K, Kapeller B, Wilbacher I, Losert UM. Behavior of cardiomyocytes and skeletal muscle cells on different extracellular matrix components - Relevance for cardiac tissue engineering. Artificial Organs. 2007;31:4-12.
[39] Charest JL, Garcia AJ, King WP. Myoblast alignment and differentiation on cell culture substrates with microscale topography and model chemistries. Biomaterials. 2007;28:2202-10.
[40] Yang HS, Ieronimakis N, Tsui JH, Kim HN, Suh KY, Reyes M, Kim DH. Nanopatterned muscle cell patches for enhanced myogenesis and dystrophin expression In a mouse model of muscular dystrophy. Biomaterials. 2014;35:1478-86.

[41] Fujie T, Shi X, Ostrovidov S, Liang X, Nakajima K, Chen Y, Wu H, Khademhosseini A. Spatial coordination of cell orientation directed by nanoribbon sheets. Biomaterials. 2015;53:86-94.
[42] Jiao A, Trosper NE, Yang HS, Kim J, Tsui JH, Frankel SD, Murry CE, Kim DH. Thermoresponsive Nanofabricated Substratum for the Engineering of Three-Dimensional Tissues with Layer-by-Layer Architectural Control. Acs Nano. 2014;8:4430-9.
[43] Sasagawa T, Shimizu T, Sekiya S, Haraguchi Y, Yamato M, Sawa Y, Okano T. Design of prevascularized three-dimensional cell-dense tissues using a cell sheet stacking manipulation technology. Biomaterials. 2010;31:1646-54.
[44] Hume SL, Hoyt SM, Walker JS, Sridhar BV, Ashley JF, Bowman CN, Bryant SJ. Alignment of multi-layered muscle cells within three-dimensional hydrogel macrochannels. Acta Biomaterialia. 2012;8:2193-202.
[45] VanDusen KW, Syverud BC, Williams ML, Lee JD, Larkin LM. Engineered Skeletal Muscle Units for Repair of Volumetric Muscle Loss in the Tibialis Anterior Muscle of a Rat. Tissue Engineering Part A. 2014;20:2920-30.
[46] Juhas M, Engelmayr GC, Fontanella AN, Palmer GM, Bursac N. Biomimetic engineered muscle with capacity for vascular integration and functional maturation in vivo. Proceedings of the National Academy of Sciences of the United States of America. 2014;111:5508-13.
[47] Hinds S, Bian WN, Dennis RG, Bursac N. The role of extracellular matrix composition in structure and function of bioengineered skeletal muscle. Biomaterials. 2011;32:3575-83.
[48] Juhas M, Bursac N. Roles of adherent myogenic cells and dynamic culture in engineered muscle function and maintenance of satellite cells. Biomaterials. 2014;35:9438-46.
[49] Harridge SDR, Bottinelli R, Canepari M, Pellegrino MA, Reggiani C, Esbjornsson M, Saltin B. Whole-muscle and single-fibre contractile properties and myosin heavy chain isoforms in humans. Pflugers Archiv-European Journal of Physiology. 1996;432:913-20.

Chapter 6

Biomimetic assembly of HUVECs and muscle cells in the microgrooved collagen scaffolds

6.1 Summary

Porous polymer scaffolds can be used to engineer 3D tissues for tissue repair. However, conventional scaffolds are not compatible for regeneration of anisotropic tissues such as muscle and nerve which have well aligned cells, blood vessels and extracellular matrix of ordered structure. Micropatterned porous scaffolds with anisotropic microstructure are desirable for recapitulation of tissue anisotropy. We developed microgrooved collagen porous scaffolds with parallel and concave microgrooves by using ice template and freeze-drying to coculture skeletal muscle myoblasts and vascular endothelial cells. When the cells are seeded at a proper ratio and concentration, the unique microstructure of the scaffolds triggers spontaneous assembly of the cells into vascularized and well ordered muscle tissue which mimic normal muscle tissue organization.

6.2 Introduction

Living tissues can be engineered by culturing cells in polymer scaffolds to repair or restore the function of diseased tissues. Engineering three-dimensional (3D) thick tissues and maintaining their viability *in vivo* necessitates the vascularization of engineered tissues.[1-3] Vascularization of engineered tissue can enable the delivery of nutrients and oxygen and removal of waste matter from living tissues. On the other hand, many types of tissues such as skeletal muscle and limb bones have well ordered tissue structure and vasculature to maintain the viability of these tissues.[4, 5] Engineering vascularized 3D tissues with well ordered structure remains a challenge in tissue engineering. In this study, microgrooved collagen scaffolds with parallel, concave microgrooves are fabricated to coculture skeletal muscle myoblasts and vascular endothelial cells. When the cells are seeded at a proper ratio and concentration, the unique microstructure of microgrooved scaffolds trigger spontaneous assembly of the cells into vascularized, well ordered muscle tissue which mimic the normal muscle tissue organization.

Many approaches have been used to engineer vascularized tissues, such as the use of 2D micropatterned surfaces, microfabricated conduits in hydrogel and 3D porous scaffolds.[3, 6] Although 2D micropaterned surfaces could guide the assembly of vascular endothelial cells and muscle cells into ordered cell sheets, they are not suitable to engineer thick tissues.[7, 8] Microfabricated conduits in hydrogel could be used to obtain

endothelialized network but complicated perfusion bioreactors are required for the cell culture.[9, 10] 3D porous scaffolds with incorporation of vascularization-promoting growth factors or coculture of endothelial cells and cells of target tissue can be used to engineer vascularized 3D tissue, but these scaffolds cannot guide the formation of highly ordered tissues such as muscle.[11, 12]

In this study, we used 3D microgrooved collagen scaffolds to engineer vascularized muscle tissue with highly ordered tissue organization. The 3D microgrooved structure of porous scaffolds can provide physical cues to guide the controlled assembly of human umbilical vascular endothelial cells (HUVECs) and L6 rat skeletal myoblasts into ordered tissue. Collagen as the major component of extracellular matrix can provide biological cues to regulate the cell migration, proliferation and vessel morphogenesis of vascular endothelial cells.[13, 14] Microgrooved collagen scaffold, flat collagen membrane and open porous collagen scaffold were used to study the effects of scaffold architecture on the cell assembly. The ratio of endothelial cells in cocultures and the concentration of seeded cells in microgrooved scaffolds were varied to study their effects on vascularization of engineered muscle tissue.

6.3 Experiments

6.3.1 Preparation of microgrooved collagen scaffolds

Microgrooved collagen scaffolds were prepared from ice line template and 1 wt.% collagen solution (solvent: 10% ethanol). Ice line template was prepared by dispensing pure water onto a hydrophobic PFA film-wrapped copper plate that was cooled by liquid nitrogen. Water droplets were dispensed from a moving nozzle of a liquid dispenser (MJET-3-CTR, Musashi Engineering Inc.), forming frozen ice lines on the copper plate. The size of the droplets and hence the width of ice lines were controlled by the pumping pressure (0.001 MPa) and type of nozzle (34G). The movement of nozzle was controlled by CAD programs. Ice line template was balanced at -5 ºC for 20 min and covered with cooled collagen solution in a silicon mold (thickness: 500 μm). The construct were cooled in liquid nitrogen for 10 min and freeze-dried for 24 h.

6.3.2 Preparation of flat collagen membrane and open-pore collagen scaffolds

Flat collagen membrane were prepared by freezing the collagen solution in a silicon frame mold (thickness: 500 μm) in the liquid nitrogen for 10 min and freeze-drying. Open-pore collagen scaffolds were prepared by freezing the collagen solution in the silicon mold (thickness: 3 mm) at -80 ºC and freeze-drying. All of the scaffolds were crosslinked (8h, RT) by using 50 mM 1-ethyl-(dimethylaminopropyl) carbodiimide dissolved in 80:20 ethanol/water solvent and freeze-dried before cell culture. The skin layer of open-pore collagen scaffolds was cut away before cell culture.

6.3.3 Scanning electron microscopy

The collagen scaffolds were cut with a sharp blade and fixed with carbon tape and coated with platinum. Coated samples were observed at an acceleration voltage of 10 kV by using a scanning electron microscope (JSM-5610, JEOL).

6.3.4 Culture of myoblasts and HUVECs in scaffolds

L6 skeletal myoblasts (ATCC® CRL-1458™) were subcultured in growth medium (Dulbecco's Modified Eagle Medium (D8437) supplemented with 10% fetal bovine serum and 10% horse serum). HUVECs (C2519A, Lonza) were subcultured in EGM2 medium. The two types of cells were harvested and mixed to prepare cell suspensions for cell seeding. The ratio of myoblasts to HUVECs varied from 1:0, 3:1 to 1:1 and the total seeding concentration varied from 1×10^6, 4×10^6 to 6×10^6 cells/ml. All scaffolds were punched and cut into circular shape (diameter = 10 mm; thickness = 500 μm) and sterilized before cell seeding. Each scaffold was put in one well of 12-well plate and confined in a glass ring (inner diameter=10 mm). 2 ml of culture medium (1:1 growth medium/EGM2) was added in each well and 200 μl of cell suspension was dropped into the scaffolds. Seeded scaffolds were cultured in 1:1 growth medium/EGM2 for 48 hours and 1:1 differentiation medium/EGM2 for 2 weeks. The differentiation medium were D8437 supplemented with 2% horse serum.

6.3.5 Immunostaining of cocultured cells

Seeded scaffolds were harvested at different incubation time and fixated by using 4% paraformaldehyde (20 min, room temperature (RT)). Samples were rinsed in phosphate buffered saline (PBS), permeabilized in 0.2 % Triton X-100 (1 h, RT) and blocked in 1% bovine serum albumin (BSA) (30 min, RT) on a rocker.[15] Primary antibody were diluted in 1% BSA and incubated with the samples overnight at 4 ºC. The samples were rinsed in PBS and incubated with secondary antibody (1 h, RT). F-actin were stained by using Alexa Fluor 488 Phalloidin or Alexa Fluor 594 Phalloidin (Thermo Fisher Scientific). Cell nuclei were stained with Cellstain-DAPI Solution (Dojindo) (10 min, RT). Samples were incubated in antibody and dye solutions on a rocker. The primary antibodies were Monoclonal Mouse Anti-Human CD31 antibody (Clone JC70A, Dako) (1:40 dilution) and MF20 (Developmental Studies Hybridoma Bank) (1:300 dilution). The secondary antibody was Goat anti-Mouse IgG Secondary Antibody (Life Technologies) (1:500 dilution).

6.4 Results and discussion

6.4.1 Microstructure of collagen scaffolds

3D microgrooved collagen scaffolds were prepared by using liquid dispensing and freeze-drying method. A moving nozzle of a dispenser ejected water droplets onto a polyfluoroalkoxy (PFA) film-wrapped copper plate cooled by liquid nitrogen. The rapid freezing of the ejected droplets on the plate resulted in formation of ice lines. The hydrophobic PFA film resulted in the semicylindrical shape of ice lines. The size of water droplets and hence the width of ice lines on the copper plate were controlled by the air pressure that pumped water out of the nozzle (0.001 MPa) and the size of nozzle (34G). Parallel ice lines were prepared by controlling the movement of the dispensing nozzle with CAD programs. These parallel ice lines were covered with cooled collagen solution in silicon mold and freeze-dried to get microgrooved scaffolds. Flat collagen membranes (Flat) and open porous collagen scaffolds were also prepared for cell culture.

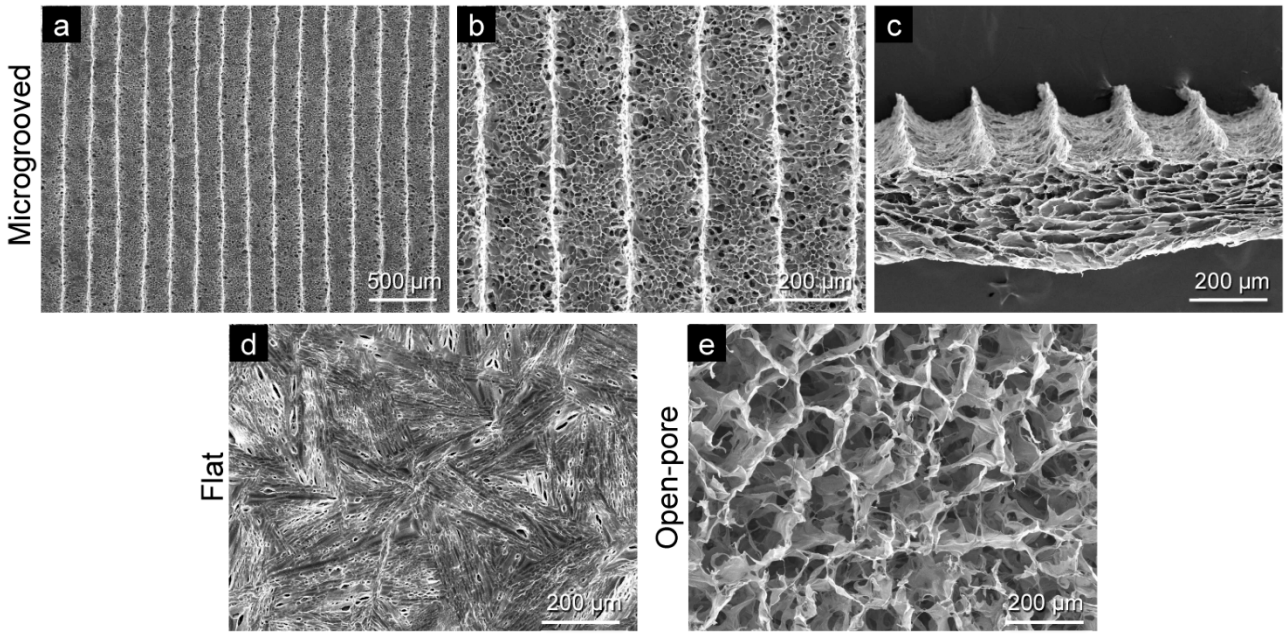

Fig. 6.1. The microstructure of (a-c) microgrooved scaffolds (G200), (d) flat collagen membrane (Flat) and (e) open-porous collagen scaffolds (Open-pore). a, b, d, e: surface view; c: vertical cross sectional view.

Collagen scaffolds with different structures were used for coculture of myoblasts and HUVECs to study the effects of scaffold structure on cell assembly. Microgrooved collagen scaffolds with the average microgroove width of 200 µm (G200) were used for the coculture because previous work showed G200 enabled more ordered muscle tissue formation than narrower (120 µm) or wider microgrooves (380 µm).[16] G200 microgrooved scaffolds had parallel microgrooves (width: 205 ± 12 µm; height: 103 ± 8 µm) with concave structure in vertical cross section which mirrored the ice line template used to prepare the scaffolds (Fig. 6.1a-c). Flat collagen membranes had a flat and dense surface, which was resulted from the rapid freezing of collagen solution (Fig. 6.1d). Open-pore collagen scaffolds had a porous morphology with uncontrolled structure (Fig. 6.1e).

6.4.2 The effect of scaffold structure on cell assembly

The cell assembly of myoblasts and HUVECs were studied after culturing the two types of cells in these 3 types of scaffolds for 12 h, 24 h or 48 h (Fig. 6.2). After 12 h incubation, myoblasts and HUVECs homogenously adhered on the 3 types of collagen scaffolds. After 24 h incubation, HUVECs aggregated into individual cellular islands surrounded by myoblasts. After 48 h incubation, the HUVEC islands remained in Flat and Open-pore scaffolds. However, myoblasts contracted in the microgrooves and formed cell bundle tissue in which the HUVEC islands fused into tubule-like structure along the microgrooves.

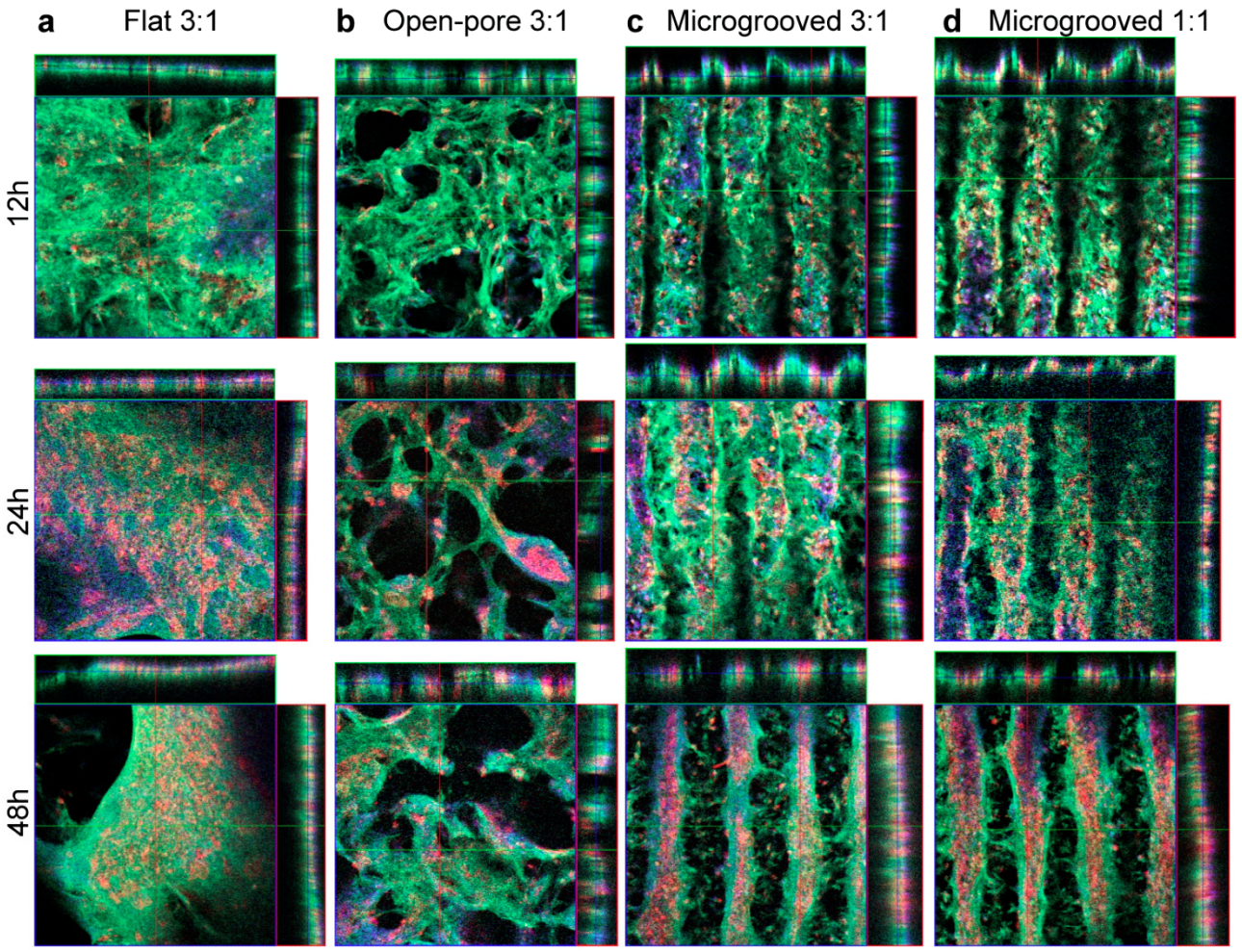

Fig. 6.2. The assembly of myoblasts and HUVECs in flat collagen membrane (Flat), open porous collagen scaffolds (Open-pore) and microgrooved collagen scaffolds (G200). Myoblasts and HUVECs at the ratio of 3:1 (a-c) or 1:1 (d) were seeded in 3 types of scaffolds, with a fixed total seeding concentration (4×10^6 myoblasts and HUVECs). Confocal microscopic images of XY, YZ and XZ planes of seeded constructs were obtained after the constructs were cultured for 12 h, 24 h or 48 h. Cells were stained with F-actin (green) and nuclei (blue); HUVECs were stained using anti-hCD31 antibody (red).

6.4.3 The effect of HUVEC ratio and seeding concentration on cell assembly

The effect of seeding ratios and total seeding concentrations of myoblasts and HUVECs on cell assembly in microgrooved scaffolds were shown in Fig. 6.3. With a proper seeding concentration (4×10^6 cells/ml), monoculture (1:0) and cocultures (3:1 and 1:1) in microgrooved collagen scaffolds all formed well-aligned muscle bundle tissue. However, the ratios of myoblasts and HUVECs affected the formation of tubule-like structure (Fig. 6.3a and Fig. S6.1). A low ratio of HUVECs in the coculture (3:1) resulted in formation of intermittent tubule-like structure from HUVECs and some small HUVEC aggregates that were not fused to the tubule-like structure. A high ratio of HUVECs in the coculture (1:1) resulted in formation of continuous tubule-like structure from HUVECs and the majority of HUVECs were fused to the tubule-like structure. The assembly of myoblasts and HUVECs were also affected by the total cell seeding concentrations. With a fixed ratio of myoblasts and HUVECs (1:1), the cocultures from an intermediate seeding concentration (4×10^6 cells/ml) formed muscle bundle tissue with aligned HUVEC tubules. A low

seeding concentration (1 × 10^6 cells/ml) resulted in formation of cellular spheroids in the microgrooved scaffolds, while a high seeding concentration (6 × 10^6 cells/ml) resulted in formation of HUVEC sheet covering the underlying muscle bundle tissue.

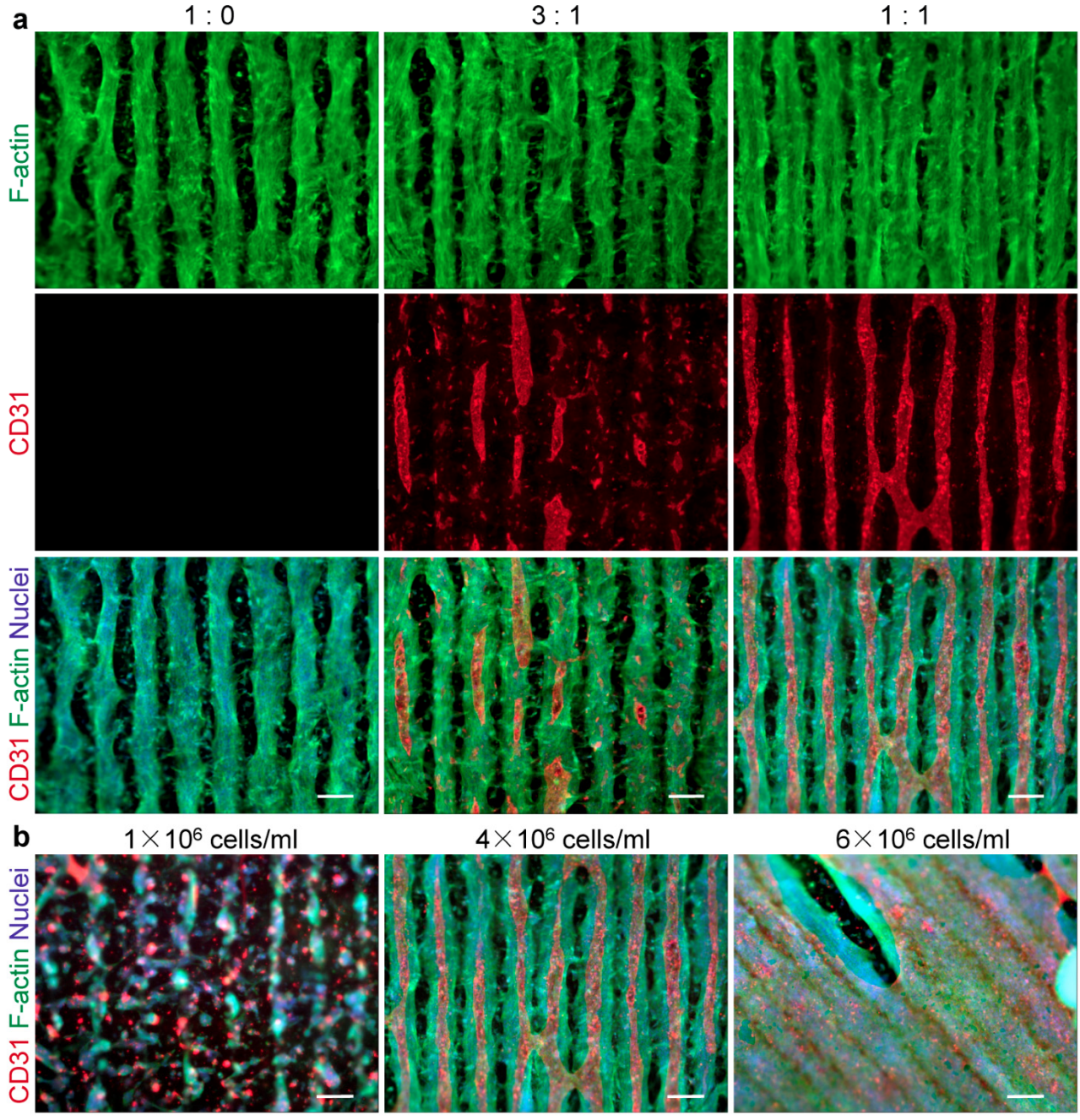

Fig. 6.3. The assembly of myoblasts and HUVECs seeded at (a) different ratios (1:0, 3:1 or 1:1, total seeding concentration=4 × 10^6 cells/ml) or (b) different total seeding concentrations (1 × 10^6, 4 × 10^6, or 6 × 10^6 cells/ml; ratio=1:1) in microgrooved scaffolds after 1-week culture. Cells were stained with F-actin (green) and nuclei (blue); HUVECs were stained using anti-hCD31 antibody (red). Scale bar = 200 μm.

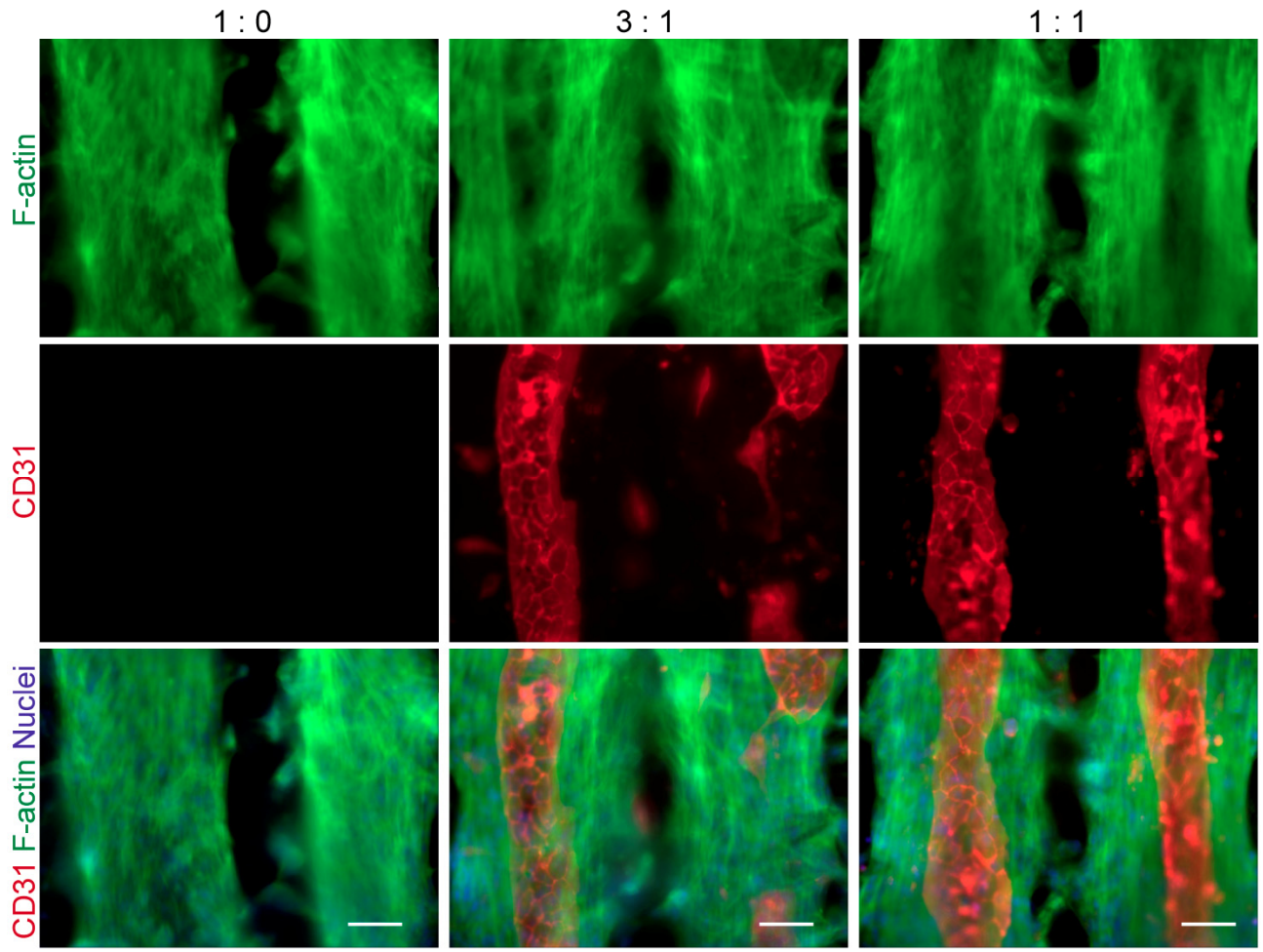

Fig. S6.1. The assembly of myoblasts and HUVECs seeded at (a) different ratio (1:0, 3:1 or 1:1, total cell seeding concentration=4×10^6 cells/ml) in the microgrooved scaffolds after 1 week culture. Cells were stained with F-actin (green) and nuclei (blue); HUVECs were stained using anti-hCD31 antibody (red). Scale bar = 50 μm.

6.4.4 Formation of vascularized and well-ordered muscle

Vascularized and well-ordered muscle tissue could be engineered by coculturing myoblasts and HUVECs in the microgrooved scaffolds (Fig. 6.4). Confocal microscopic images of cocultures in the microgrooved scaffolds showed that HUVECs assembled into tubule-like structure that was incorporated within the aligned muscle bundle tissue from myoblasts (Fig. S6.2). While seeding a low ratio of HUVECs (3:1) resulted in intermittent tubules, seeding a high ratio of HUVECs (1:1) resulted in continuous tubules from HUVECs. By coculturing the cells in a medium of low serum level (2% serum; differentiation medium:EGM2=1:1) for 2 weeks, myoblasts fused into muscle bundle tissue that showed a high expression of myosin heavy chain (MHC) proteins (Figure 6.4b), which indicated the maturation of myotubes within the tissue. In addition, the muscle cells within the tissue were highly aligned as shown by the immunostaining of the MHC and F-actin.

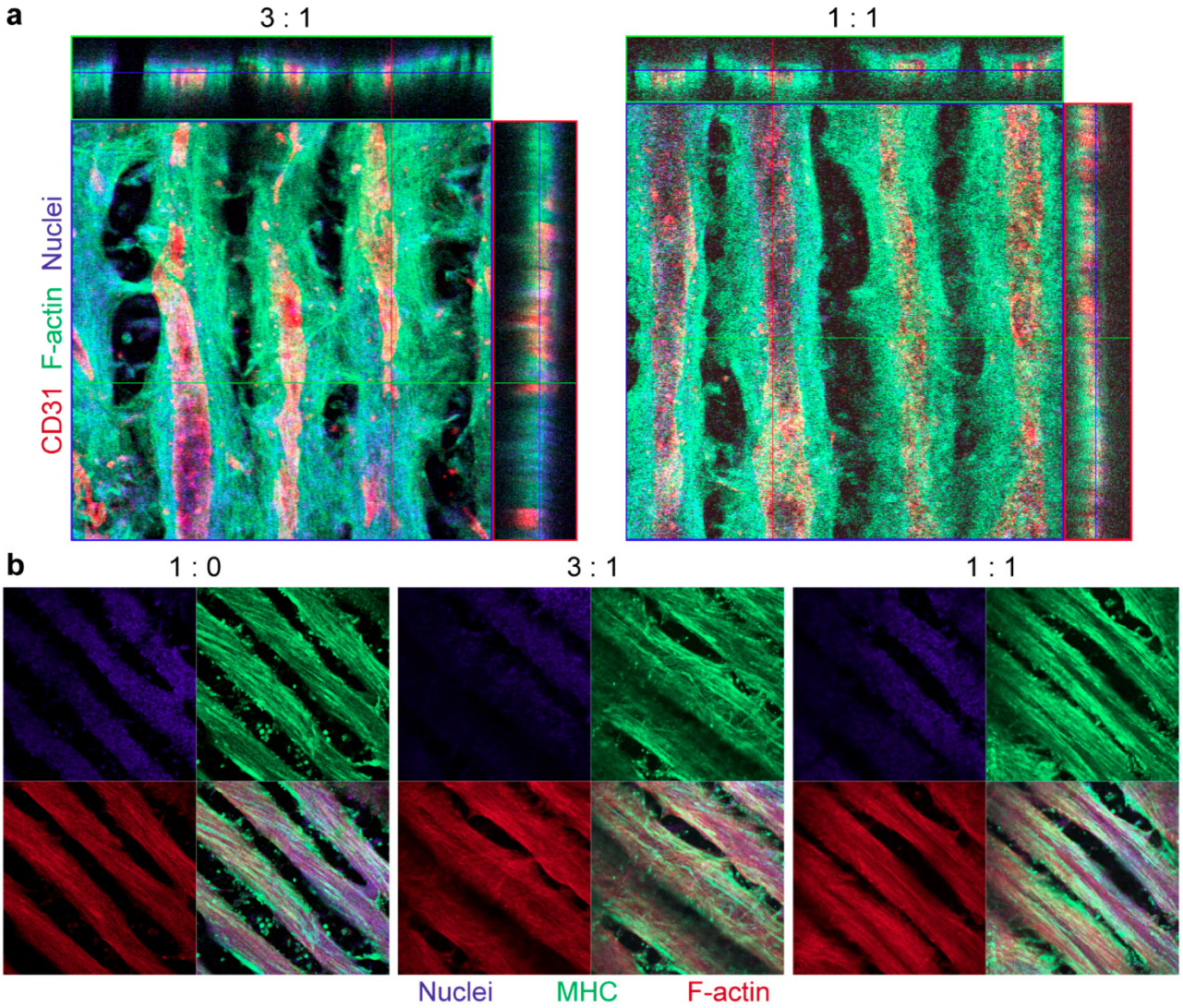

Fig. 6.4. The formation of vascularized, well-ordered muscle bundle tissue within microgrooved scaffolds after 2-week culture. (a) Confocal microscopic images of XY, YZ and XZ planes of seeded constructs showing the cell assembly in scaffolds (seeding ratio=3:1 or 1:1). Cells were stained with F-actin (green) and nuclei (blue); HUVECs were stained using anti-hCD31 antibody (red). (b) The maturation of myotubes in the well ordered muscle bundle tissue. Myosin heavy chain protein (MHC) was stained in green and F-actin were stained in red. Cell nuclei were stained in blue.

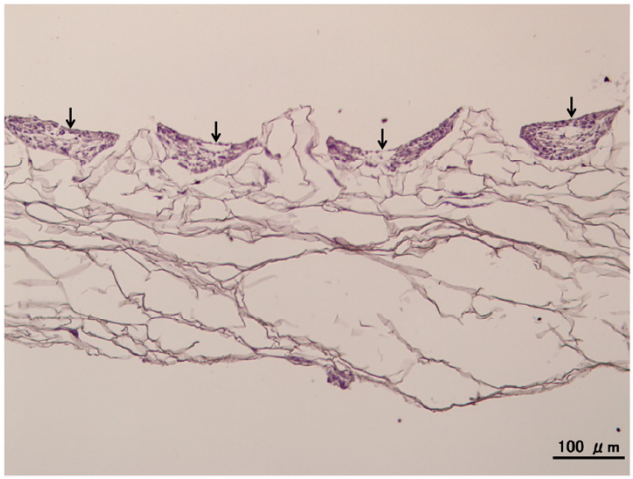

Figure S6.2. HE staining of tubule-like structure assembled from coculture of HUVECs and myoblasts in the microgrooved scaffolds after 2-week culture. Seeding ratio=1:1, total cell seeding concentration = 4×10^6 cells/ml.

Based on the results we proposed a mechanism for the assembly of myoblasts and HUVECs in the microgrooved scaffolds (Fig. 6.5). A homogenous mixture of myoblasts and HUVECs were seeded and adhered the scaffolds. Subsequently the cells proliferated and migrated and HUVECs formed cellular islands surrounded by myoblasts. With the contraction of myoblasts within the microgrooves, myoblasts formed cell bundle tissue in which the HUVEC islands fused into tubular-like structure. Further culturing the assembled cells in the microgrooved scaffolds led to formation of vascularized muscle tissue with ordered structure. Vascular endothelial cells are polar cells that have the apical surface that exclude adhesion to extracellular matrix (ECM) proteins and the basal surface that adhered on the underlying basement membrane proteins.[17] The polar vascular endothelial cells can assemble into capillary-like networks within ECM matrix such as collagen gels.[18] Endothelial cells were also found to form individual cell aggregates when cultured with cells of another type.[5] In this study, the aggregation of HUVEC into islands might be that HUVECs migrated together to exclude the surrounding myoblasts or the ECM synthesized by myoblasts. Scaffold architecture affected the subsequent assembly of the cells. Unlike the Flat collagen membranes or the Open-pore collagen scaffolds which retained the HUVEC islands during the coculture (Fig. 6.2a,b; 24h-48h), microgrooved collagen scaffolds triggered the contraction of myoblasts to the central axis of concave microgrooves, causing fusion of HUVEC islands into tubule-like structure and formation of vascularized muscle bundle tissue.

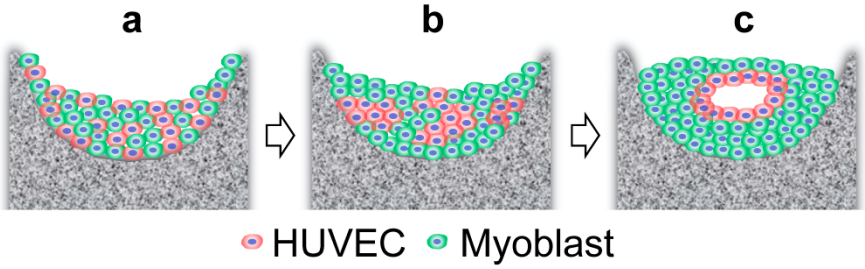

Fig. 6.5. The proposed mechanism for the assembly of myoblasts and HUVECs within the microgrooved scaffolds. (a) A homogenous mixture of myoblasts and HUVECs were seeded in microgrooved scaffolds. (b)

Cells proliferated and HUVECs assembled into cellular islands surrounded by myoblasts. (c) The contraction of myoblasts within the microgrooves led to the formation of cell bundle with tubule-like structure.

Apart from the scaffold architecture, the seeding ratio of HUVECs and the total seeding concentration also affected the assembly of the two types of cells. Seeding myoblasts and HUVECs at the ratio of 3:1 or 1:1 did not affect the formation of muscle bundle tissue when compared with the monoculture (1:0). A low ratio of HUVECs in the coculture (3:1) resulted in intermittent tubule-like structure from HUVECs and some small HUVEC aggregates not incorporated into the tubules. The reason might be that less HUVECs in the coculture had smaller frequency of encountering each other and fusing together.[19] A high ratio of HUVECs in the coculture, however, resulted in formation of continuous tubule-like structure and the majority of HUVECs were incorporated within the tubules. A proper seeding concentration was required to form muscle bundle tissue with HUVEC tubules. The two types of cells seeded at a low concentration (1×10^6 cells/ml) formed cellular spheroids rather than cell bundles in the scaffolds, which is in agreement of our previous study and other studies.[16, 20] Cells seeded at a high concentration (6×10^6 cells/ml) would form a layer of HUVEC covering the muscle bundle tissue, which could be resulted from the encountering of HUVECs in neighboring microgrooves and adhesion of these cells into a layer above the muscle cells to reestablish the polar HUVEC environment.[19, 21]

Coculturing vascular endothelial cells and target tissue cells has been used to engineer vascularized tissues. Endothelial cells have been cocultured with other types of cells such as muscle cells or fibroblasts in 2D polymer substrates, hydrogel or porous scaffolds to engineer vascularized tissue, but these materials lack the topography that guide the formation of well-organized tissues such as muscle.[22-25] The assembly of HUVECs within myoblast sheets into capillary networks also lack the organization of skeletal muscle.[26] Recently, thermo-responsive micropatterns were used to generate anisotropic myoblast sheets to guide the assembly of endothelial cells, but the multiple steps of harvesting and stacking the cell sheets was tedious.[5] With proper seeding ratio and seeding concentration in microgrooved collagen scaffolds, vascular endothelial cells and muscle cells could spontaneously assemble into well-aligned vascularized muscle bundle tissue. To the best of our knowledge, this is the first work reporting the spontaneous assembly of cocultured cells into well-ordered vascularized tissue by using micropatterned scaffolds.

6.5 Conclusion

In summary, microgrooved collagen scaffolds with parallel, concave microgroove patterns have been fabricated to coculture muscle cells and vascular endothelial cells. Myoblasts and HUVECs in the microgrooved scaffolds spontaneously assembled into well-ordered vascularized muscle bundle tissue. The seeding ratio of HUVECs and the total seeding concentration of HUVECs and myoblasts affected the cell assembly in the microgrooved scaffolds. Culturing different types of cells in the microgrooved collagen scaffolds could be a useful tool to engineer vascularized tissue of highly ordered structure, or to study the cell-cell interaction or cell-material interaction within a 3D micropatterned material or to obtain an *in vitro* angiogenesis model.

6.6 References

[1] Cassell OCS, Hofer SOP, Morrison WA, Knight KR. Vascularisation of tissue-engineered grafts: the regulation of angiogenesis in reconstructive surgery and in disease states. British Journal of Plastic Surgery.

2002;55:603-10.
[2] Verseijden F, Posthumus-van Sluijs SJ, Farrell E, van Neck JW, Hovius SER, Hofer SOP, van Osch GJVM. Prevascular Structures Promote Vascularization in Engineered Human Adipose Tissue Constructs Upon Implantation. Cell Transplantation. 2010;19:1007-20.
[3] Kaully T, Kaufman-Francis K, Lesman A, Levenberg S. Vascularization-The Conduit to Viable Engineered Tissues. Tissue Engineering Part B-Reviews. 2009;15:159-69.
[4] van der Schaft DWJ, van Spreeuwel ACC, van Assen HC, Baaijens FPT. Mechanoregulation of Vascularization in Aligned Tissue-Engineered Muscle: A Role for Vascular Endothelial Growth Factor. Tissue Engineering Part A. 2011;17:2857-65.
[5] Takahashi H, Shimizu T, Nakayama M, Yamato M, Okano T. Anisotropic Cellular Network Formation in Engineered Muscle Tissue through the Self-Organization of Neurons and Endothelial Cells. Advanced Healthcare Materials. 2015;4.
[6] Wang MO, Vorwald CE, Dreher ML, Mott EJ, Cheng MH, Cinar A, Mehdizadeh H, Somo S, Dean D, Brey EM, Fisher JP. Evaluating 3D-Printed Biomaterials as Scaffolds for Vascularized Bone Tissue Engineering. Advanced Materials. 2015;27:138-44.
[7] Li J, Zhang K, Wu J, Liao Y, Yang P, Huang N. Co-culture of endothelial cells and patterned smooth muscle cells on titanium: construction with high density of endothelial cells and low density of smooth muscle cells. Biochem Biophys Res Commun. 2015;456:555-61.
[8] Li JG, Li GC, Zhang K, Liao YZ, Yang P, Maitz MF, Huang N. Co-culture of vascular endothelial cells and smooth muscle cells by hyaluronic acid micro-pattern on titanium surface. Applied Surface Science. 2013;273:24-31.
[9] Cerino G, Gaudiello E, Grussenmeyer T, Melly L, Massai D, Banfi A, Martin I, Eckstein F, Grapow M, Marsano A. Three dimensional multi-cellular muscle-like tissue engineering in perfusion-based bioreactors. Biotechnol Bioeng. 2015.
[10] Tocchio A, Tamplenizza M, Martello F, Gerges I, Rossi E, Argentiere S, Rodighiero S, Zhao WW, Milani P, Lenardi C. Versatile fabrication of vascularizable scaffolds for large tissue engineering in bioreactor. Biomaterials. 2015;45:124-31.
[11] Fuchs S, Ghanaati S, Orth C, Barbeck M, Kolbe M, Hofmann A, Eblenkamp M, Gomes M, Reis RL, Kirkpatrick CJ. Contribution of outgrowth endothelial cells from human peripheral blood on in vivo vascularization of bone tissue engineered constructs based on starch polycaprolactone scaffolds. Biomaterials. 2009;30:526-34.
[12] Levenberg S, Rouwkema J, Macdonald M, Garfein ES, Kohane DS, Darland DC, Marini R, van Blitterswijk CA, Mulligan RC, D'Amore PA, Langer R. Engineering vascularized skeletal muscle tissue. Nature Biotechnology. 2005;23:879-84.
[13] Whelan MC, Senger DR. Collagen I initiates endothelial cell morphogenesis by inducing actin polymerization through suppression of cyclic AMP and protein kinase A. Journal of Biological Chemistry. 2003;278:327-34.
[14] Delvos U, Gajdusek C, Sage H, Harker LA, Schwartz SM. Interactions of Vascular Wall Cells with Collagen Gels. Laboratory Investigation. 1982;46:61-72.
[15] Juhas M, Bursac N. Roles of adherent myogenic cells and dynamic culture in engineered muscle function and maintenance of satellite cells. Biomaterials. 2014;35:9438-46.
[16] Chen S, Nakamoto T, Kawazoe N, Chen G. Engineering multi-layered skeletal muscle tissue by using 3D microgrooved collagen scaffolds. Biomaterials. 2015;73:23-31.
[17] Kramer RH. Extracellular-Matrix Interactions with the Apical Surface of Vascular Endothelial-Cells. Journal of Cell Science. 1985;76:1-16.
[18] Montesano R, Orci L, Vassalli P. In vitro rapid organization of endothelial cells into capillary-like

networks is promoted by collagen matrices. J Cell Biol. 1983;97:1648-52.
[19] Nagamori E, Ngo TX, Takezawa Y, Saito A, Sawa Y, Shimizu T, Okano T, Taya M, Kino-oka M. Network formation through active migration of human vascular endothelial cells in a multilayered skeletal myoblast sheet. Biomaterials. 2013;34:662-8.
[20] Hsu SH, Ho TT, Huang NC, Yao CL, Peng LH, Dai NT. Substrate-dependent modulation of 3D spheroid morphology self-assembled in mesenchymal stem cell-endothelial progenitor cell coculture. Biomaterials. 2014;35:7295-307.
[21] Gholobova D, Decroix L, Van Muylder V, Desender L, Gerard M, Carpentier G, Vandenburgh H, Thorrez L. Endothelial Network Formation Within Human Tissue-Engineered Skeletal Muscle. Tissue Eng Part A. 2015;21:2548-58.
[22] Chen XF, Aledia AS, Popson SA, Him L, Hughes CCW, George SC. Rapid Anastomosis of Endothelial Progenitor Cell-Derived Vessels with Host Vasculature Is Promoted by a High Density of Cotransplanted Fibroblasts. Tissue Engineering Part A. 2010;16:585-94.
[23] Caspi O, Lesman A, Basevitch Y, Gepstein A, Arbel G, Huber I, Habib M, Gepstein L, Levenberg S. Tissue engineering of vascularized cardiac muscle from human embryonic stem cells. Circulation Research. 2007;100:263-72.
[24] Chen XF, Aledia AS, Ghajar CM, Griffith CK, Putnam AJ, Hughes CCW, George SC. Prevascularization of a Fibrin-Based Tissue Construct Accelerates the Formation of Functional Anastomosis with Host Vasculature. Tissue Engineering Part A. 2009;15:1363-71.
[25] Wang JL, Yang MY, Zhu Y, Wang L, Tomsia AP, Mao CB. Phage Nanofibers Induce Vascularized Osteogenesis in 3D Printed Bone Scaffolds. Advanced Materials. 2014;26:4961-6.
[26] Sasagawa T, Shimizu T, Sekiya S, Haraguchi Y, Yamato M, Sawa Y, Okano T. Design of prevascularized three-dimensional cell-dense tissues using a cell sheet stacking manipulation technology. Biomaterials. 2010;31:1646-54.

Chapter 7

Concluding remarks and future prospects

7.1 Concluding remarks

This thesis summarizes the development of natural polymer scaffolds with controlled microstructure to engineer cartilage and skeletal muscle, and study the effect of scaffold properties (composition, biophysical cues) that affect cell-cell and cell-material interactions in 3D culture.

Low molecular weight salts were used to suppress polyion complex(PIC) formation in collagen/hyaluronic acid(HA) suspensions during scaffold preparation. PIC formation was found to be dependent on the ionic strength of the suspension. The suppression of PIC formation resulted in collagen/HA scaffolds with homogeneous pore structure and remarkably enhanced mechanical property. Collagen/HA scaffolds prepared under suppression of PIC formation promoted proliferation of dermal fibroblasts and upregulated the expression of genes encoding EGF, VEGF and IGF-1.

Homogeneous collagen/HA scaffolds with well-controlled and interconnected pore structure were prepared to study the effect of high molecular HA on chondrocyte behavior. Collagen/HA scaffolds were prepared by suppression of PIC formation between collagen and HA and using ice particulates as porogen. The pore structure and mechanical property of collagen/HA scaffolds and collagen scaffolds could be well controlled. High molecular weight HA in collagen/HA scaffolds inhibited the cellular proliferation, synthesis of sulfated glycosaminoglycan (sGAG) and cartilage ECM, compared with the results of collagen scaffolds. The results should provide additional information on the effects of HA in porous scaffolds on the chondrocyte behavior in 3D culture.

Gelatin porous scaffolds with homogeneous and open pores were developed to engineer cartilage tissue *in vitro*. Gelatin scaffolds were prepared by using ice particulates and freeze-drying. The pore structure and mechanical property of gelatin scaffolds could be well controlled by using different ratios of ice particulates to gelatin solution and different concentrations of gelatin. Gelatin scaffolds prepared from ≥ 70% ice particulates enabled homogeneous seeding of bovine articular chondrocytes throughout the scaffolds and formation of homogeneous cartilage ECM. While soft scaffolds underwent cellular contraction, stiff scaffolds resisted cellular contraction and had significantly higher cell proliferation and synthesis of sulfated glycosaminoglycan. Compared with the gelatin scaffolds prepared without ice particulates, the gelatin

scaffolds prepared with ice particulates facilitated formation of homogeneous cartilage tissue with significantly higher compressive modulus. The gelatin scaffolds with highly open-pore structure and good mechanical property can be used to promote chondrocyte functions for *in vitro* tissue-engineered cartilage.

3D porous collagen scaffolds with anisotropic and concave microgrooves were developed to engineer skeletal muscle tissue. Highly aligned and multi-layered muscle bundle tissues were engineered by controlling the size of microgrooves and cell seeding concentration. Myoblasts in the engineered muscle tissue were well-aligned and had high expression of myosin heavy chain and synthesis of muscle extracellular matrix. The microgrooved collagen scaffolds could be used to engineer organized multi-layered muscle tissue for implantation to repair/restore the function of diseased tissues.

Microgrooved collagen scaffolds with anisotropic microgrooves, non-patterned collagen scaffolds and flat collagen scaffolds were prepared to coculture of skeletal muscle myoblasts and vascular endothelial cells. When the two types of cells were seeded at a proper ratio and concentration, the unique microstructure of microgrooved scaffolds triggered the spontaneous assembly of cells into vascularized anisotropic muscle tissue that mimicked the normal muscle tissue organization.

In conclusion, natural polymer scaffolds with homogeneous, open-pore structure can be used to engineer homogeneous tissues. Natural polymer scaffolds with anisotropic micropatterned structure can guide cell alignment to engineer anisotropic tissues. Natural polymer scaffolds with controlled microstructures can be used to study the effects of composition and biophysical cues (stiffness, topography) on cell-cell and cell-material interactions in 3D material environment.

7.2 Future prospects

The study described in this thesis was focused on the design of scaffold microstructures for tissue engineering and investigation of cell behaviors in the 3D material environment. The cell types used to study the potential of the scaffolds for tissue engineering were limited to differentiated cells such as articular chondrocytes and progenitor cells such as skeletal myoblasts. However, some cell types such as chondrocytes have limited cell number and harvesting a great number of these cells for tissue engineering is difficult. In the future work, stem cells can be subcultured and differentiated to get a specific type of cells, which can be combined with the natural polymer porous scaffolds to engineer a specific type of tissue. For example, mesenchymal stem cells can be cultured in the gelatin scaffolds with homogeneous and open-pore structure and differentiated into chondrocytes for cartilage tissue engineering. Skeletal muscle stem cells (satellite cells) can be subcultured and differentiated in microgrooved collagen scaffolds to engineer skeletal muscle tissue.

The natural polymer porous scaffolds were used to culture cells *in vitro* to engineer cartilage tissue and skeletal muscle. However, the *in vitro* cell culture conditions are different from the *in vivo* environment. To further validate the feasibility of these scaffolds for tissue engineering applications, the engineered tissues such as cartilage and skeletal muscle need to be implanted into large-animal models to check the maturation and function of engineered tissues and the integration of the engineered tissues with native tissues.

The scaffold fabrication methods of this study (the use of homogeneous polymer solution by suppression of polyion complex and the use of sacrificial templates such as ice particulates and micropatterned ice lines) can be used to prepare polymer scaffolds to engineer other types of tissues with homogeneous structure (such as liver) or with anisotropic structure (such as cardiac muscle and nerve). Co-culture of vascular endothelial cells and the cells of target tissue in the polymer scaffolds with controlled

microstructures can enable vascularization of engineered tissues, which is vital for engineering of large and thick living tissues and maintaining their viability *in vivo*.

The fabrication techniques can also be used to prepare polymer scaffolds for implantation in animal models to study material-tissue interactions such as foreign body response. Many studies reported that the pore structure of synthetic polymer based scaffolds affect the foreign body response to the implanted scaffolds. Natural polymer scaffolds with controlled and open-pore microstructure can be used to study tissue response, which can guide the design of biomaterial for long-term tissue regeneration or the surface microstructure of medical implants.

The polymer scaffolds with controlled microstructure can also be combined with drug carriers and implanted to achieve controlled release of drug for tissue regeneration or other therapeutic applications. Drug carriers such as polymer micro- or nano-particles can encapsulate drug and be incorporated into the scaffolds. The controlled microstructure of polymer scaffolds may enable the reproducible, controlled and sustainable drug delivery.

List of publications

1. Shangwu Chen, Qin Zhang, Tomoko Nakamoto, Naoki Kawazoe, Guoping Chen.
   Highly active porous scaffolds of collagen and hyaluronic acid prepared by suppression of polyion complex formation.
   Journal of Material Chemistry B 2014,2:5612-5619.

2. Shangwu Chen, Tomoko Nakamoto, Naoki Kawazoe, Guoping Chen.
   Engineering multi-layered skeletal muscle tissue by using 3D microgrooved collagen scaffolds.
   Biomaterials 2015,73:23-31.

3. Shangwu Chen, Qin Zhang, Naoki Kawazoe, Guoping Chen.
   Effect of High Molecular Weight Hyaluronic Acid on Chondrocytes Cultured in Collagen/Hyaluronic Acid Porous Scaffolds.
   RSC Advances 2015,5:94405-94410.

4. Shangwu Chen, Qin Zhang, Tomoko Nakamoto, Naoki Kawazoe, Guoping Chen.
   Gelatin Scaffolds with Controlled Pore Structure and Mechanical Property for Cartilage Tissue Engineering.
   Tissue Engineering, January 2016, ahead of print. doi:10.1089/ten.tec.2015.0281.

5. Shangwu Chen, Naoki Kawazoe, Guoping Chen.
   Microgrooved Collagen Scaffold Triggered Biomimetic Assembly of HUVECs and Muscle Cells.
   Submitted.

6. Himansu Sekhar Nanda, Shangwu Chen, Qin Zhang, Naoki Kawazoe, Guoping Chen.
   Collagen scaffolds with controlled insulin release and controlled pore structure for cartilage tissue engineering.
   Biomed Research International 2014,2014:623805.

7. Himansu Sekhar Nanda, Tomoko Nakamoto, Shangwu Chen, Rong Cai, Naoki Kawazoe, Guoping Chen.
   Collagen microgel-assisted dexamethasone release from PLLA-collagen hybrid scaffolds of controlled pore structure for osteogenic differentiation of mesenchymal stem cells.
   Journal of Biomaterials Science. Polymer edition 2014,25:1374-1386.

8. Himansu Sekhar Nanda, Naoki Kawazoe, Qin Zhang, Shangwu Chen, Guoping Chen.
   Preparation of collagen porous scaffolds with controlled and sustained release of bioactive insulin.
   Journal of Bioactive and Compatible Polymers: Biomedical Applications 2014,29: 95-109.

9. Qin Zhang, Tomoko Nakamoto, Shangwu Chen, Naoki Kawazoe, Kaili Lin, Jiang Chang, Guoping Chen.
   Collagen/Wollastonite nanowire hybrid scaffolds promoting osteogenic differentiation and angiogenic factor expression of mesenchymal stem cells.
   Journal of Nanoscience and Nanotechnology 2014,14:3221-3227.

Acknowledgements

This PhD thesis was accomplished with the supervision of my supervisor Professor Guoping Chen. During my PhD study, Professor Chen has devoted to supervising my research from selecting research topics and suggesting solutions of problems encountered in my experiments and revising research papers and thesis. His expertise, innovation, passion and seriousness in scientific research have deeply affected me and greatly encouraged me during my PhD study. In addition, Professor Chen has always been generous in offering tips on effective communication and building interpersonal relationships. His advice in scientific research and life will continue guiding me in my future career and life. It is my great honor to be able to do research in Professor Chen's group. Therefore, I am taking this opportunity to give my sincere great gratitude to him.

Special thanks also go to Dr. Naoki Kawazoe for his warm support and encouragement during my 5 years of research in NIMS. His immense knowledge, professional skill, and modest character have deeply impressed me. It is my great pleasure to work and learn from him.

I really appreciate the valuable suggestion and assistance from Dr. Hongxu Lu, Dr. Qin Zhang, and Mrs. Harue Nagata, Mrs. Kobayashi and Mrs. Tateno. Dr. Lu and Dr. Qin Zhang has always been supporting me in my research and daily life. Mrs. Harue Nagata, Mrs. Kobayashi and Mrs. Tateno has helped me a lot for the procedures of university enrollment and daily life in Tsukuba. And I would like to give my thanks to current members in Tissue Regeneration Materials Unit and former members in Polymeric Biomaterials Group for their teaching of experiments and cooperation in managing of our lab. They are Dr. Ida Dulinska, Dr. Tomoko Nakamoto, Dr. Jasmine Lee, Dr. Hwan Hee Oh, Dr. Koki Hagiwara, Dr. Himansu Nandasekhar, Dr. Hongli Mao, Dr. Cai Rong, Dr. Jianming Yang, Professor Gang Wu, Mr. Yuichi Hirayama, Mr. Radyum Ikono, Mr. Xinlong Wang, Mr. Jingchao Li, Mr. Xiaomeng Li, Ms. Jing Zhang, Ms. Ying Chen, Ms. Jiahui Ng and Ms. Nur Rofiqoh Eviana Putri.

Beside my supervisor, I would like to give my sincere thanks to the rest of my thesis committee, Professor Yukio Nagasaki, Professor Kazushi Miki, Professor Seiya Tsujimura and Professor Tetsushi Taguchi, for their insightful comments, encouragement and kind suggestions during my PhD defense and my presentations in NIMS student seminars.

I would like to give my most sincere thanks to my parents and all my friends who have been supporting me during my PhD study.

This work was performed at Tissue Regeneration Materials Unit, International Center for Materials Nanoarchitectonics (MANA), National Institute for Materials Science and Graduate School of Pure and Applied Science of University of Tsukuba. I appreciate the financial support from NIMS (Junior Research Assistantship) during my 5-year research in NIMS.